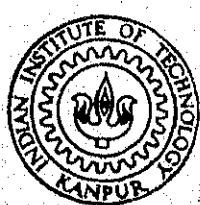


DIGITAL SIMULATION OF TRANSIENTS OF THE STEAM GENERATOR OF 600 MWe PRESSURIZED WATER NUCLEAR REACTOR

By

M. JAGAN MOHAN RAO

ME
1981
M
RAO
DIGI



**DEPARTMENT OF MECHANICAL ENGINEERING
INDIAN INSTITUTE OF TECHNOLOGY, KANPUR**

JULY, 1981

**DIGITAL SIMULATION OF TRANSIENTS OF THE STEAM
GENERATOR OF 600 MWe PRESSURIZED
WATER NUCLEAR REACTOR**

A Thesis Submitted
in Partial Fulfilment of the Requirements
for the Degree of
MASTER OF TECHNOLOGY

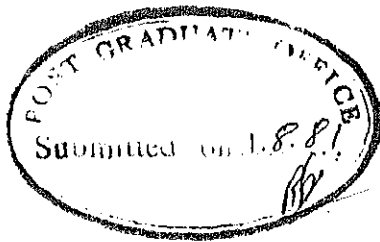
By
M. JAGAN MOHAN RAO

to the

DEPARTMENT OF MECHANICAL ENGINEERING
INDIAN INSTITUTE OF TECHNOLOGY, KANPUR
JULY, 1981

ME-1981-M-RAO-DIG

I.I.T. KANPUR
CENTRAL LIBRARY
Reg. No. A 66825
T SEP 1981



CERTIFICATE

This is to certify that the thesis entitled "Digital Simulation of the Transients of Steam Generator of 600 MWe Pressurized Water Nuclear Reactor" by Shri M. Jagan Mohan Rao is a record of work carried out under my supervision and has not been submitted elsewhere for a degree.

K. Sri Ram

Professor and Head
Nuclear Engineering and Technology Programme
Indian Institute of Technology
Kanpur

POST GRADUATE OFFICE
This thesis has been approved
for the award of the Degree of
Master of Technology (M.Tech.)
in accordance with the
regulations of the Indian
Institute of Technology, Kanpur
Dated:

ACKNOWLEDGEMENT

I wish to express my gratitude and indebtedness to Professor K. Sri Ram for his invaluable guidance, constant encouragement, and prompt discussion throughout this investigation.

I am grateful to Dr. D.P. Rao for giving useful suggestions in the course of this work.

I express my sincere thanks to Miss Deepa for her help in correcting the manuscript. I am also thankful to Mr. Chalapathi Rao and Mr. Ramulu for their help in proof reading.

I would like to thank Mr. J.P. Gupta for his excellent typing skill and Mr. Srivastava for his neat tracings.

Finally I would like to thank all my friends who have made my stay at IIT pleasant.

MANDAVILLI JAGAN MOHAN RAO

LIST OF FIGURES

	<u>Page</u>	
FIGURE 2.1	A schematic of an integral economizer U-tube steam generator	8
FIGURE 2.2	Simulation model of steam generator	12
FIGURE 3.1	Flow chart of the program calculating the steady state values	29
FIGURE 3.2	Flow chart of the program simulating the transients	31
FIGURE 3.3	Flow chart of the subroutine Soluc	33
FIGURE	Internal energy of primary fluid was increased by 5 %. The effect of this perturbation on	
FIGURE 5.1(a)	Total heat transfer rate	58
FIGURE 5.1(b)	Temperature of the secondary exit	58
FIGURE 5.1(c)	Pressure of the secondary exit	59
FIGURE 5.1(d)	Quality of the secondary exit	59
FIGURE 5.1(e)	Temperature of the secondary exit	60
FIGURE 5.1(f)	Mass flow rate of the secondary exit	60
	Mass flow rate was increased by 5 % at the entrance of the primary circuit. Effect of this on	
FIGURE 5.2(a)	Quality of the secondary exit	61
FIGURE 5.2(b)	Mass flow rate of the secondary exit	61
FIGURE 5.2(c)	Pressure of the secondary exit	62

	<u>Page</u>
FIGURE 5.2(d) Temperature of the secondary exit	62
FIGURE 5.2(e) Mass flow rate of the primary exit	63
FIGURE 5.2(f) Temperature of the primary exit	63
FIGURE 5.2(g) Internal energy of the primary exit	64
FIGURE 5.2(h) Pressure of the primary exit	64
Internal energy of the secondary liquid was increased by 15 % at the inlet. Effect of this perturbation on	
FIGURE 5.3(a) Pressure at the secondary exit	65
FIGURE 5.3(b) Temperature at the secondary exit	65
FIGURE 5.3(c) Quality at the secondary exit	66
FIGURE 5.3(d) Internal energy at the secondary exit	66
FIGURE 5.3(e) Total heat transfer rate from primary to secondary circuit	67
FIGURE 5.3(f) Mass flow rate at the secondary exit	67
FIGURE 5.3(g) Temperature at the primary exit	68
FIGURE 5.3(h) Pressure at the primary exit	68
Mass flow rate of the secondary liquid was increased by 20 % at the inlet. Effect of this perturbation on	
FIGURE 5.4(a) Mass flow rate at the secondary exit	69

	<u>Page</u>
FIGURE 5.4(b) Quality at the secondary exit	69
FIGURE 5.4(c) Pressure at the secondary exit	70
FIGURE 5.4(d) Temperature at the secondary exit	70
FIGURE 5.4(e) Temperature at the primary exit	71
FIGURE 5.4(f) Mass flow rate at the primary exit	71

NOMENCLATURE

A	-	Cross sectional area for flow, ft ²
A _T	-	Heat transfer area, ft ²
C _P	-	Specific heat at constant pressure, Btu/lbm
D _e	-	Equivalent diameter, ft
d	-	Spacing of the tubes, inch.
d _e	-	External diameter of the tubes of primary circuit, inch.
d _i	-	Internal diameter of the tubes of primary circuit, inch.
e	-	Energy per unit mass, Btu/lbm
F _K	-	Frictional force, lbf
f	-	Friction coefficient
G	-	Mass flux, lbm/ft ² -hr
g	-	Acceleration due to gravity, ft/sec ²
g _c	-	Conversion ratio, lbm-ft/lbf-sec ²
H	-	Specific enthalpy, Btu/lbm
H _{fg}	-	Latent heat of vaporization, Btu/lbm
H _{in}	-	Enthalpy at the inlet of the generator, Btu/lbm
h	-	Mechanical equivalent of heat, J = 778 lbf-ft/Btu
k	-	Thermal Conductivity, Btu/hr-ft-°F
L _{ev}	-	Length of the evaporator, ft

L_{PA}	-	Length of the preheater, ft
P_m	-	Wetted perimeter, ft
P	-	Pressure, Psi
ΔP	-	Pressure drop, Psi
Q	-	Rate of heat transfer, Btu/hr
\dot{q}	-	Heat flux, Btu/hr-ft ²
T	-	Temperature, °F
T_p	-	Temperature of the wall of the tube, °F
ΔT_{sat}	-	$T_p - T_{Sat}$, °F
u	-	Internal energy, Btu/lbm
U	-	Total internal energy, Btu/lbm
v	-	Velocity, ft/hr
v	-	Specific volume, ft ³ /lbm
w	-	Mass flow rate, lbm/hr
x, X	-	Quality of vapour
X_{tt}	-	Lockhart and Martinelli's parameter
Z	-	Direction of flow
ΔZ	-	Height of each control volume, ft.
α	-	Void fraction
μ	-	Viscosity, lbf/hr-ft
ρ	-	Density, lbm/ft ³
σ	-	Surface tension, lbf/ft

- ϕ_{10}^2 - Multiplicator for calculating frictional pressure drop in two-phase flow
- γ - Empirical constant used in Thom's correlation for calculating the void-fraction

Superscript:

- - Refers to the value at the middle of a control volume.

Subscript:

- e - Refers to the exit
- ev - Evaporator
- f - Saturated liquid condition
- g - Saturated vapour condition
- i - Inlet condition
- iso - Refers to isothermal condition
- j - Refers to junction
- l - Saturated liquid
- P - Refers to primary circuit
- PA - Refers to preheater
- S - Refers to secondary circuit
- Sat - Saturation condition
- v - Saturated vapour condition
- c.v. - Control volume.

\circ, i - Outlet wall condition of the control volume, i

Dimensionless Groups:

Nu - Nusselt Number = $h \cdot D_e / k$

Pr - Prandtl Number = $\mu \cdot C_p / k$

Re - Reynolds Number = $G \cdot D / \mu$.

CONTENTS

	<u>Page</u>
ACKNOWLEDGEMENT	iii
LIST OF FIGURES	iv
NOMENCLATURE	vii
CONTENTS	xii
ABSTRACT	xiv
 <u>CHAPTER I</u>	
1.1	Introduction
1.2	Review of Previous Models
1.3	Present Work
 <u>CHAPTER II</u>	
2.1	Description of the System
2.2	Different Components of the Model
I EUTSG	9
2.3	Model of the Steam Generator
 <u>CHAPTER III</u>	
3.1	Mathematical Model
3.1.1	Fundamental Conservation equations
3.1.2	Final system of equations for transient simulation
3.2	Relationship between Junction Variables and Control Volume Variables and corresponding Derivatives among them
3.3	Functional relations that are assumed

	<u>Page</u>
3.4 Solution of System of equations	19
3.4.1 Scheme suggested by porschning	19
3.4.2 Scheme derived in ref.[9]	19
3.4.3 Derivation of present scheme used	21
3.5 Description of Various Matrices of Equation (3.20)	22
3.5.1 Matrix F	22
3.5.2 Derivatives of \dot{S}_i , \dot{U}_i , \dot{W}_i	22
3.5.3 Derivatives of pressure and temperature with respect to independent variables density and internal energy	24
3.5.4 Elements of matrix 'A'	25
3.6 Method of Calculation	26
3.7 Flow Chart	28
 CHAPTER IV	
4.1 Modifications made in the Steady State Simulation	34
4.2 Modifications made in the Transient Simulation	36
 CHAPTER V	
5.1 Results and Discussion	49

	<u>Page</u>
5.1.1 Steady state values	49
5.1.2 Transient values	49
5.1.3 Comparison of results with previous results	53
5.1.4 Conclusions	56
5.1.5 Further scope	57
References	72
Appendix I	74
Appendix II	75
Appendix III	79

ABSTRACT

A digital computer code was developed by Kar [1] to simulate the transient behaviour of a steam generator typically used in Pressurized Water reactor type of Nuclear Power Plants. The present work is an extension to the above thesis.

The three fundamental time dependent equations of conservation of mass, energy and momentum were converted into a set of linear algebraic equations using finite difference method, from which an explicit numerical scheme was formulated.

On the primary side single phase flow and forced convection heat transfer were assumed and on the secondary side the possibility of the existence of different flow regimes was assumed and the heat transfer in these regimes was calculated using appropriate correlations.

Some important modifications were made and the numerical instabilities in the program were corrected. Program was studied for disturbances in flow and internal energy of varying step increments. Suitable time step was found. Some ranges for the step increments were fixed. Comparison of the results was made with the two previous works and the results are in agreement.

CHAPTER I

1.1 INTRODUCTION

With the increasing trend in the studies of safety measures of nuclear reactor behaviour, it becomes necessary to simulate the behaviour of various components of the reactor. Dynamic analysis is an essential part of system design for nuclear power plants. Simulation studies provide information needed to assess plant maneuvering capability, control strategies and tolerance to malfunctions.

One of the important components of the nuclear reactor system is the steam generator, which serves as heat transfer link between the coolant, which flows through the primary side and the secondary fluid, which provides power for the turbine.

It is quite difficult to model a large system via state variable methods, because of the fact, that the overall system has to be broken into various sub-systems, and then the individual systems have to be modelled separately. The overall system is then constructed by coupling the sub-system models. The steam generator presents to a complex modelling problem, as it involves sub-cooled and boiling heat transfer on the secondary side.

Dynamic modelling is particularly important when system design with new features are contemplated. It is not possible to assess the performance of the new system design with the previous experience.

Though a great deal of care is taken to ensure public safety in nuclear power plant, there is always a finite probability that a system may fail and lead to an undesirable situation. An equipment may fail due to some disturbed condition. The transient analysis helps us in studying the degree of danger that may occur during such failure, and hence gives guidelines for proper instrumentation to prevent such accidents. In case of steam generator, large number of possibilities which can lead to an accident can be enumerated. There is always a possibility for a pipe to be ruptured in the primary or secondary circuit. Such a rupture in primary circuit can reduce the flow rate and in some cases lead to a very severe accident called loss of coolant accident (LOCA). In this situation coolant at very high pressure will be exposed to low pressure system. This coolant which is radioactive can be hazardous to human life. Partial or complete failure of one of the valves or pump can also create lot of problems, as it can lead to an accident called loss of flow accident (LOFA). All such disturbances will effect the pressure and temperature of primary fluid. Similarly a reduced flow in the feed water pipe will effect the steam output, and hence the power

output of whole plant, as it will upset the operation of the turbine. In order to ensure that the heat exchanger can accommodate certain deviation from steady state operation and to ensure safe operation if there is an accident, the transient analysis of steam generator is a must

1.2 REVIEW OF PREVIOUS MODELS

In the literature there are no simplified models available for simulating steam generator excepting the complicated models of the Reactor thermal hydraulic computer codes such as RELAP-4 [2] and FLASH [3] etc. Recently, a mathematical model was developed by Arwood and Kerlin [4] to simulate the U-tube steam generator. This paper used linearized equations to predict the behaviour around a steady state operating point. The detailed heat transfer regimes were also not considered explicitly. Hoeld [5] developed a nonlinear transient model for the calculation of the dynamic behaviour of a vertical natural circulation U-tube Steam Generator (UTSG). But modern power plants use IEUTSG which is an improved version of UTSG and has higher heat transfer coefficient. Pinto [7] has developed a model for steady state simulation of the IEUTSG and Silva [6] developed a model for simulating transients of an IEUTSG. The above two models take various flow regimes into account. The second one by Silva [6] follows an implicit numerical technique for finding the dynamic behaviour of the steam

generator. Similar work with some modifications was simultaneously done by two people recently. One was done by Silva [9] using implicit method and the other one was done by Kar [1] using explicit method. In Kar's work there are some numerical instabilities, around 0.4 seconds.

1.3 PRESENT WORK

The present work is an extension of the work done by Kar [1] for his M.Tech. thesis.

It consists of developing a model to simulate the transient behaviour of an Integral Economizer U-tube Steam Generator (IEUTSG) utilised in 600 MWe Pressurized Water Reactor. To give an accurate representation of steam generator due considerations have been given to two phase flow and heat transfer.

As fundamental equations, the well known conservation equations for mass, energy and momentum and Fourier's heat conduction equation, all of them given in the form of partial differential equations have been chosen. Additional approximate equations for the thermodynamic properties of water and steam, for a two phase correlation, for one and two phase friction coefficients and heat conduction equations have been established.

For steady state values, the model and computer code developed by Pinto [7] have been used.

Some important modifications have been made in the program developed by Kar [1], for the study of transients of a heat exchanger (IEUTSG). The instabilities in the scheme have been eliminated. Program was run for various possible accidents and some important conclusions have been drawn. Varying the amount of perturbation, feasible ranges of perturbations, below which the program can be used, have been established. By running the program at various time steps a suitable (economical) time step has been found. The final results were verified with those of [1] and [9].

In the second chapter a brief discription of the model IEUTSG design and it's functioning have been given. Simulation model of the steam generator as well as schematic representation of steam generator are also given.

In the third chapter the mathematical model, different functional relationships that were assumed, formulation of system of equations and it's solution and the method of calculation are given.

In the fourth chapter the important modifications that were done for the present work have been presented in details. Later, the importance and effect of all the modifications are discussed.

In the fifth chapter the final results have been discussed and some important conclusions have been drawn.

In Appendix I the steady state simulation done by Pinto [6] has been given.

In Appendix II have been given, brief description of various subroutines that were used for transient simulation.

CHAPTER II

2.1 DESCRIPTION OF THE SYSTEM

A schematic of the Integral Economizer U-Tube Steam Generator (IEUTSG) is shown in Fig. (2.1).

This is a natural circulation steam generator with integral feed water pre-heating which produces dry and saturated steam. The steam generator, consistant with previous designs, is a vertical shell and U-tube heat exchanger. The 48500 sq.foot surface area tube bundle provides the boundary between the primary and secondary flow paths. Incorporated in the tube bundle are multiple tube supports and anti-vibration bars in the cold leg side. The entire tube bundle is enclosed by a wrapper to provide controlled distribution of recirculated water. The feed water inlet nozzle is installed in the lower shell where the steam outlet nozzle is located in the elliptical head. The upper internals of the steam generator consists of moisture separator and associated support structure.

The model IEUTSG steam generator produces dry saturated steam by transfer of heat from the reactor coolant water to a steam water mixture on the secondary side.

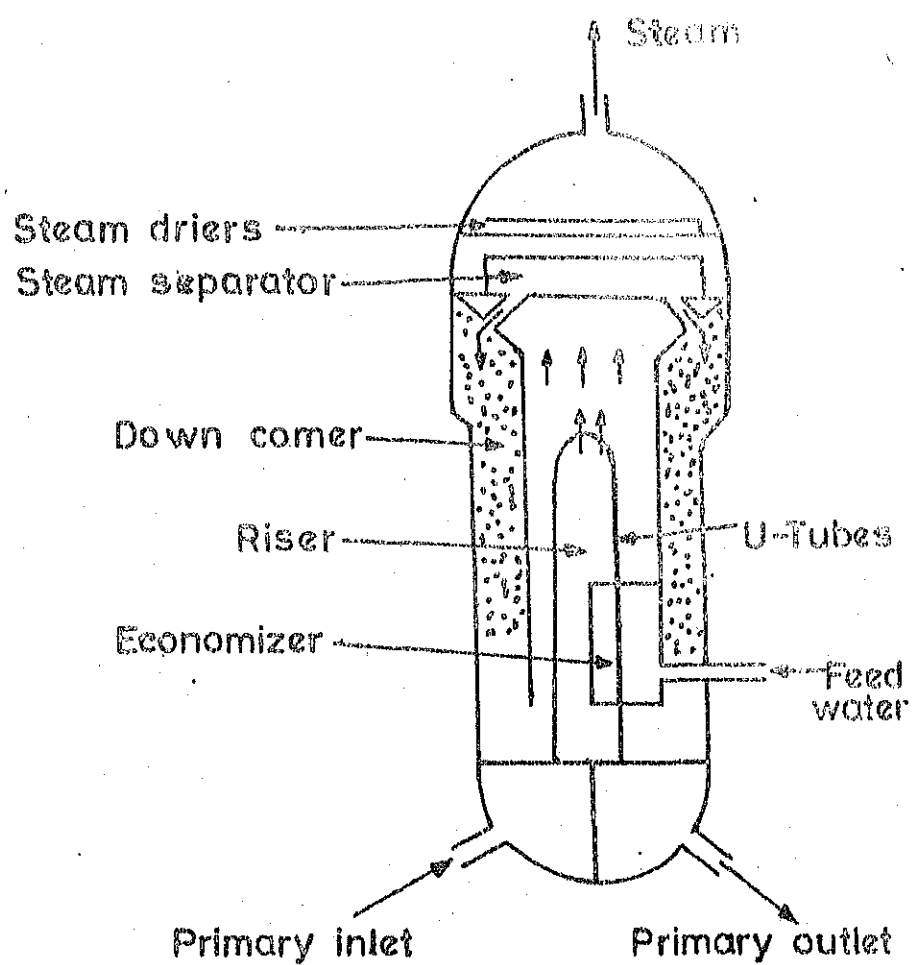


Fig.2.1 A schematic of an integral Economizer
U-tube steam generator (IEUT)

2.2 DIFFERENT COMPONENTS OF THE MODEL IEUTSG

(A) Primary Side :

The hot primary fluid coming from the reactor enters the IEUTSG at the inlet nozzle and flows into the primary inlet plenum. The fluid then enters the upward portion (hot leg) of the U-tube, where it begins to lose heat through the tube walls of the secondary fluid. The primary flow continues into the downward side (cold leg) and into the economizer section.

(B) Tube Metal Walls :

The tube metal walls separate the primary and secondary fluids. Heat is transferred from the primary to the secondary fluid through the tube walls at a rate determined by the overall heat transfer coefficient and temperature difference between primary and secondary circuits. The overall heat transfer coefficient is dependent upon the tube metal conductance and the film heat transfer coefficients at the inner and outer surfaces of the tube.

(C) Secondary Side :

Just above the bottom plenum there is an economizer. This is nothing but a closed container covering portion of the cold legs and separate them from the rest of the secondary side. Feed water enters the integral economizer section,

where baffles direct the flow upward across the tubes (counter flow relative to the primary liquid in the cold leg). This brings the cold feed water into a region where heat is transferred with the cooler primary liquid. The baffles in this section promote turbulence and therefore increase the film heat transfer coefficient of the secondary liquid.

The feed water mixes with recirculating water to form a slightly subcooled mixture that is forced upward around the tubes of the hot leg section. The temperature of this mixture increases as it takes heat from the primary liquid until the boiling point is reached and steam is formed. The steam water mixture continues flowing upward part of the economizer section. The steam water mixture enters the separators where the saturated liquid is separated from the steam and returns to the downcomer while the steam is collected in the upper part of the steam generator shell.

The IEUTSG design is a modification of the U-tube recirculation type steam generator (UTSG) used in many operating PWR. In order to increase the heat transfer effectiveness of the system a change in the design was made. The IEUTSG is same as standard UTSG excepting that in the UTSG the whole feed water is introduced into the downcomer and there is no preheating (economizer) section. As the recirculation ratio is very high, the circulated water that enters the heated section from downcomer is near the saturation

temperature. Hence there is very small temperature difference between the primary liquid in cold legs of the tubes and the secondary water, in a UTSG. This will lead to a very poor heat transfer rate at the cold leg section. By introducing colder feed water directly in this region the IEUTSG design reduces the temperature of secondary fluid and hence increases the temperature difference. This in turn, will increase the heat transfer from primary to secondary liquid.

2.3 MODEL OF THE STEAM GENERATOR [6]

The steam generator model used in the present study is shown in Fig. (2.1). The steam generator is represented in two sections, preheater (economizer) and an evaporator. In reality, the steam generators of the PWR reactors have U-tube geometry. The present model simplifies it to parallel tube geometry but retains all the significant factors such as the total heat transfer area, total amount of heat transferred, preheater etc. Lack of detailed data about the internals of the steam generator such as the pressure drop due to baffles, quality of steam at the outlet of the generator before the steam separates etc. is circumvented by the pressure balance and heat balance equations as described in the later sections.

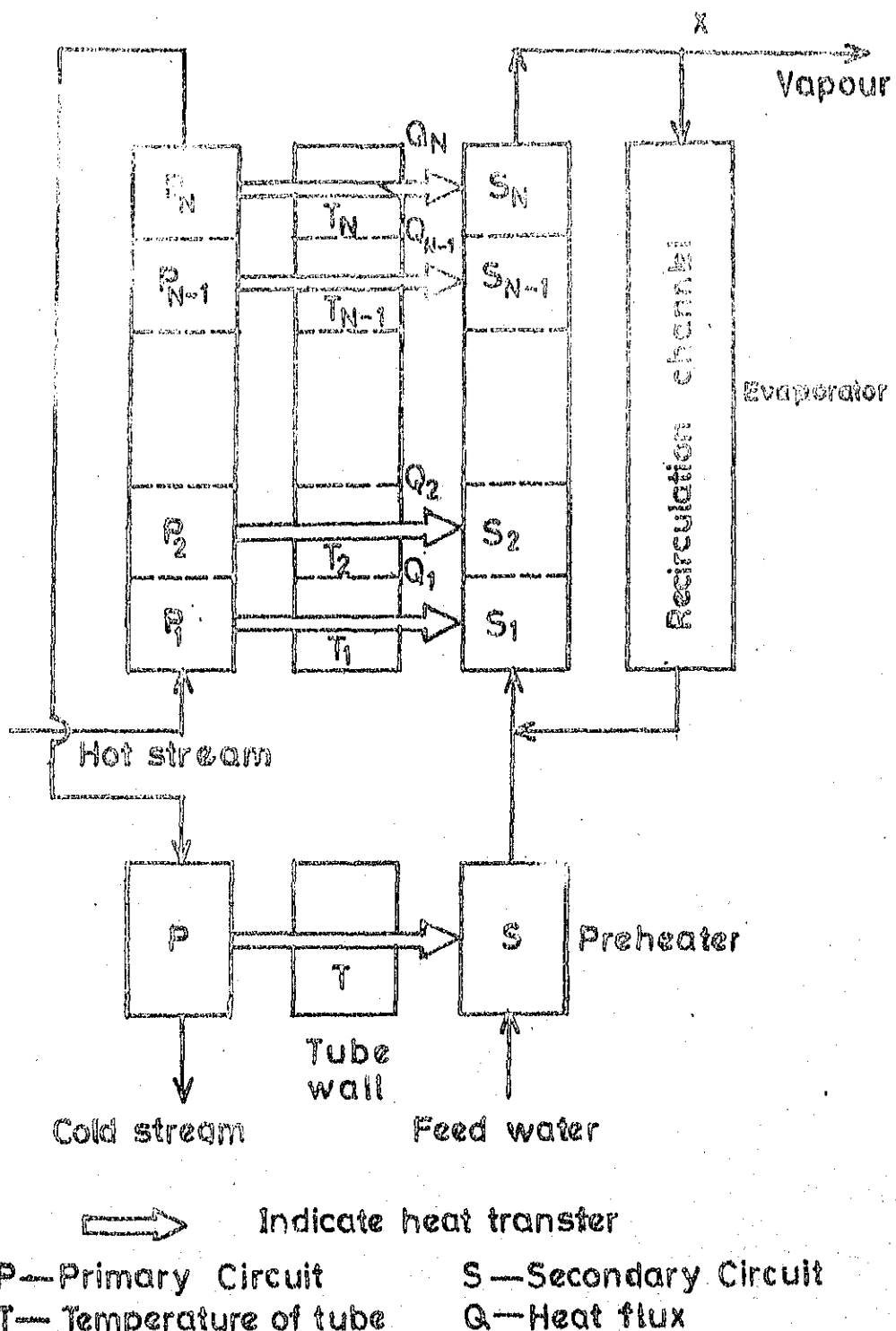


Fig.2.2 Simulation model of steam generator

As indicated in fig. (2.2) the coolant from the reactor outlet enters the primary side of the generator as a hot stream in the evaporator section and leaves the generator from the preheater section as a cold stream to re-enter the reactor. The heatflow from the primary side is conducted through the tube walls of the steam generator and enters the secondary stream. The figure also indicates that the secondary stream leaves the evaporator section of generator as vapor and part of the steam is recirculated. Some make up feed water enters the preheater and mixes with the secondary stream after the preheater.

CHAPTER 3

3.1 MATHEMATICAL MODEL:

A simplified mathematical model and computer code were developed by A.C. PINTO [8] for the steady state analysis of a steam generator utilized in a 600 Mwe pressurized water reactor nuclear power plants. As a reference to present work the reprint of the above paper is included as Appendix 1.

3.1.1 Fundamental Conservation equations :

Some assumptions are made to derive the equations that are given in this section.

1. The flow is vertical
2. There is no transfer of work across each control volume indicated in fig. (2.2)
3. The area of flow cross section is constant
4. The effect of gravity is negligible.

Thus the three fundamental equations of mass, energy and momentum conservation become

$$\text{Mass : } A \frac{\partial \rho}{\partial t} = - \frac{\partial W}{\partial Z} \quad (3.1)$$

Where $W = \rho AV$

$$\text{Energy : } A \frac{\partial (\rho e)}{\partial t} = \ddot{q} \frac{\partial A_T}{\partial Z} - \frac{\partial (We)}{\partial Z} - \frac{\partial (PAV)}{\partial Z} \quad (3.2)$$

Where $e = u + V^2/2 + gZ$ is the energy per unit mass of the fluid.

$$\text{Momentum : } A \cdot \frac{\partial(\rho V)}{\partial t} = - A \frac{\partial P}{\partial Z} - \frac{\partial F_k}{\partial Z} - A \rho g - \frac{\partial}{\partial Z} (WV) \quad (3.3)$$

Because of the 4th assumption the term gZ in the expression of 'e' and $A \cdot g$ in equation (3.3) can be neglected.

3.1.2 Final system of equation for transient simulation

$$A \frac{\partial(\rho V)}{\partial t} = - A \frac{\partial P}{\partial Z} - \frac{\partial(WV)}{\partial Z} - \frac{\partial F_k}{\partial Z} \quad (3.4)$$

$$A \frac{\partial(\rho u)}{\partial t} = \ddot{q} \frac{\partial A_T}{\partial Z} - \frac{\partial}{\partial Z} (Wu) - PA \frac{\partial V}{\partial Z} + V \frac{\partial F_k}{\partial Z} \quad (3.5)$$

$$A \frac{\partial e}{\partial t} = - \frac{\partial W}{\partial Z} \quad (3.6)$$

3.1.3 Integration of conservation equations :

Integrating the above equations over a control volume i bounded by junctions i and i+1 with respect to Z lead to the following equations :

(a) The equation of momentum conservation gives:

$$\frac{\partial}{\partial t} \int_i^{i+1} \rho A V dz = - \int_i^{i+1} \frac{\partial(WV)}{\partial Z} dz - \int_i^{i+1} \frac{\partial F_k}{\partial Z} dz - A \int_i^{i+1} \frac{\partial P}{\partial Z} dz$$

$$+ \int_i^{i+1} \rho A V dz$$

Let us define $\bar{W}_i = \frac{1}{i+1} \int_i^{i+1} dz$

$$\int_i^{i+1} dz$$

With this definition we get

$$\Delta Z \frac{d\bar{W}_i}{dt} = -A(P_{i+1} - P_i) - [WV_{i+1} - WV_i] - \bar{F}_{Ki}$$

But $W = \rho AV$, i.e., $WV = W^2/\rho A$, and

$$\bar{F}_{Ki} = \bar{f}_i \frac{\bar{W}_i}{2AD_e \bar{\rho}_i} \Delta Z$$

So the momentum equation takes the form:

$$\bar{W}_i = \frac{A}{\Delta Z} (P_i - P_{i+1}) + \frac{1}{A \cdot \Delta Z} \left(\frac{W_i^2}{\rho_i} - \frac{W_{i+1}^2}{\rho_{i+1}} \right) - \bar{f}_i \frac{W_i}{2AD_e \bar{\rho}_i} \quad (3.7)$$

(b) The equation of energy conservation will give:

$$\frac{\partial}{\partial t} \int_i^{i+1} A \rho u \, dz = \int_i^{i+1} \dot{q} \frac{\partial A_T}{\partial Z} \, dz - \int_i^{i+1} \frac{\partial (wu)}{\partial Z} \, dz - \int_i^{i+1} PA \frac{\partial V}{\partial Z} \, dz + \int_i^{i+1} V \frac{\partial F_K}{\partial Z} \, dz$$

We now define

$$\bar{U}_i = \int_i^{i+1} A \rho u \, dz \quad \text{and} \quad \bar{Q}_i = \int_i^{i+1} \dot{q} \frac{\partial A_T}{\partial Z} \, dz$$

$$\int_i^{i+1} PA \frac{\partial V}{\partial Z} \, dz = \bar{F}_i A(V_{i+1} - V_i) = P_i \left(\frac{W_{i+1}}{\rho_{i+1}} - \frac{W_i}{\rho_i} \right)$$

$$\text{and} \quad \int_i^{i+1} V \frac{\partial F_K}{\partial Z} \, dz = \bar{V}_i \bar{F}_{K,i} = \bar{f}_i \frac{\bar{W}_i^3}{2A^2 D_e \bar{\rho}_i} \cdot \Delta Z$$

With these simplifying assumptions we get

$$\dot{\bar{U}} = \bar{Q}_i + W_i u_i - W_{i+1} u_{i+1} - \bar{P}_i \left(\frac{W_{i+1}}{\rho_{i+1}} - \frac{W_i}{\rho_i} \right) + \bar{f}_i \frac{\bar{W}_i^3}{2A^2 D_e \bar{\rho}_i} \cdot \Delta Z \quad (3.8)$$

(c) The equation of mass conservation gives:

$$\frac{\partial}{\partial t} \int_i^{i+1} \rho A \, dz = - \int_i^{i+1} \frac{\partial W}{\partial Z} \, dz$$

Let us define

$$\bar{\rho}_i = \frac{\int_i^{i+1} A \rho dz}{\int_i^{i+1} A dz}$$

With this definition we get

$$\dot{\bar{\rho}}_i = \frac{1}{A \cdot \Delta Z} (w_i - w_{i+1}) \quad (3.9)$$

Now we finally rewriting the above equations

$$\dot{\bar{\rho}}_i = \frac{1}{A \cdot \Delta Z} (w_i - w_{i+1}) \quad (3.10)$$

$$\dot{\bar{U}}_i = \bar{Q}_i + w_i u_i - w_{i+1} u_{i+1} - \bar{\rho}_i C_{22} \left(\frac{w_{i+1}}{\bar{\rho}_{i+1}} - \frac{w_i}{\bar{\rho}_i} \right) \quad (3.11)$$

$$\begin{aligned} \dot{\bar{W}}_i &= \frac{C_{21}}{\Delta Z} (P_i - P_{i+1}) - \frac{\bar{F}_i \bar{W}_i^2}{2A D_e \bar{\rho}_i} + \frac{1}{A \cdot \Delta Z} (r_i \frac{w_i^2}{\bar{\rho}_i} - r_{i+1} \frac{w_{i+1}^2}{\bar{\rho}_{i+1}}) \\ &\quad + C_{23} \frac{\bar{F}_i \bar{W}_i^3 \Delta Z}{2A^2 D_e \bar{\rho}_i^2} \end{aligned} \quad (3.12)$$

3.2 Relationship between Junction Variables and Control

Volume Variables and Corresponding Derivatives Among Them:

$$\bar{W}_i = \frac{1}{2} (w_i + w_{i+1}), \text{ i.e., } w_{i+1} = 2\bar{W}_i - w_i$$

$$\bar{U}_i = \frac{1}{2} (U_i + U_{i+1}), \text{ i.e., } U_{i+1} = 2\bar{U}_i - U_i$$

$$\dot{\bar{\rho}}_i = \frac{1}{2} (\dot{\rho}_i + \dot{\rho}_{i+1}), \text{ i.e., } \dot{\rho}_{i+1} = 2\dot{\bar{\rho}}_i - \dot{\rho}_i$$

Definition of specific internal energy

$$\bar{u}_i = \frac{\int_i^{i+1} A \rho u dz}{\int_i^{i+1} A dz} = \frac{\bar{U}_i}{A \cdot \Delta Z \bar{\rho}_i} \quad (3.13)$$

Some of the derivatives obtained from the above relations

$$\frac{\partial \bar{u}_i}{\partial \bar{U}_i} = \frac{1}{A \cdot \Delta Z \rho_i}$$

$$\frac{\partial \bar{u}_i}{\partial \rho_i} = -\frac{\bar{U}_i}{A \cdot \Delta Z \rho_i^2} = -\frac{\bar{u}_i}{\rho_i}$$

$$\frac{\partial \rho_{i+1}}{\partial \rho_i} = -2$$

$$\frac{\partial \rho_{i+1}}{\partial \rho_i} = -1$$

$$\frac{\partial u_{i+1}}{\partial \bar{u}_i} = 2$$

$$\frac{\partial u_{i+1}}{\partial u_i} = -1$$

$$\frac{\partial W_{i+1}}{\partial \bar{W}_i} = 2$$

$$\frac{\partial W_{i+1}}{\partial W_i} = -1$$

3.3 Functional Relations that are assumed

$$\bar{P}_i = f(P_i, P_{i+1})$$

$$P_i = f(u_i, \rho_i)$$

$$P_{i+1} = f(u_{i+1}, \rho_{i+1})$$

$$u_{i+1} = f(u_i, \bar{u}_i)$$

$$\bar{u}_i = f(\bar{U}_i, \bar{\rho}_i)$$

$$\rho_{i+1} = f(\rho_i, \bar{\rho}_i)$$

$$\bar{T}_i = f(\bar{u}_i, \bar{\rho}_i)$$

$$\bar{p}_i = f(\bar{u}_i, \bar{\rho}_i)$$

3.4 SOLUTION OF SYSTEM OF EQUATIONS:

The whole length of the channel is devided into different control volumes. The three conservation equations consists of three unknowns. porching [12] has given a scheme which can be utilised for solving hydraulic networks. Similar scheme was derived in ref. [9]. Porschings's scheme is very powerful for nonlinear problems. This can be used explicitely and implicitely as well. The explicit scheme is going to be used in this work.

3.4.1 Scheme suggested by porsching:

For a given initial value problem of the type

$$\dot{y} = F(t, y), \quad y(0) = y^0 \quad (3.14)$$

One can use an explicit method given below

$$[I - h dF(t^n, y^n)] \Delta y^{n+1} = hF(t^n, y^n) \quad (3.15)$$

$$\Delta y^{n+1} = y^{n+1} - y^n$$

3.4.2 Scheme derived in ref. [9]

$$[I - \theta/2 \frac{\partial F_i}{\partial Y_i}]_f^T \Delta Y_i^{T+1} = F_i^T \cdot \theta + \frac{\partial F_i}{\partial f_i} \frac{\Delta f_i^{T+1}}{y} \cdot \frac{\theta}{2} \quad (3.16)$$

where $Y_i = f(\bar{\rho}_i, \bar{u}_i, \bar{w}_i)$

$f_i = f(\rho_i, u_i, w_i)$

$\theta = \text{Time interval} = (t^{T+1} - t^T)$

Implicit scheme used for transient simulation

$$[I - \frac{\partial F_i}{\partial Y_i}]_f^T \Delta Y_i^{T+1} = F_i^T \cdot \theta + \frac{\partial F_i}{\partial f_i} \frac{\Delta f_i^{T+1}}{y} \cdot \theta/2 \quad (3.17)$$

In the matrix form it will be as follows

$$\begin{bmatrix} (1 - \theta \frac{\partial \dot{\rho}_i}{\partial \bar{\rho}_i}) & -\theta \frac{\partial \dot{\rho}_i}{\partial \bar{U}_i} & -\theta \cdot \frac{\partial \dot{\rho}_i}{\partial \bar{W}_i} \\ -\theta \cdot \frac{\partial \dot{U}_i}{\partial \bar{\rho}_i} & (1 - \theta \cdot \frac{\partial \dot{U}_i}{\partial \bar{U}_i}) & -\theta \cdot \frac{\partial \dot{U}_i}{\partial \bar{W}_i} \\ -\theta \cdot \frac{\partial \dot{W}_i}{\partial \bar{\rho}_i} & -\theta \cdot \frac{\partial \dot{W}_i}{\partial \bar{U}_i} & (1 - \theta \cdot \frac{\partial \dot{W}_i}{\partial \bar{W}_i}) \end{bmatrix} \begin{bmatrix} \Delta \dot{\rho}_i \\ \Delta \dot{u}_i \\ \Delta \dot{w}_i \end{bmatrix} = \begin{bmatrix} \dot{\rho}_i \\ \dot{u}_i \\ \dot{w}_i \end{bmatrix} \theta$$

$$+ \frac{\theta}{2} \begin{bmatrix} \frac{\partial \dot{\rho}_i}{\partial \rho_i} & \frac{\partial \dot{\rho}_i}{\partial u_i} & \frac{\partial \dot{\rho}_i}{\partial w_i} & \frac{\partial \dot{\rho}_i}{\partial T_{o,i}} \\ \frac{\partial \dot{U}_i}{\partial \rho_i} & \frac{\partial \dot{U}_i}{\partial u_i} & \frac{\partial \dot{U}_i}{\partial w_i} & \frac{\partial \dot{U}_i}{\partial T_{o,i}} \\ \frac{\partial \dot{W}_i}{\partial \rho_i} & \frac{\partial \dot{W}_i}{\partial u_i} & \frac{\partial \dot{W}_i}{\partial w_i} & \frac{\partial \dot{W}_i}{\partial T_{o,i}} \end{bmatrix} \quad (3.18)$$

3.4.3 Derivation of present scheme used:

$$[I - \frac{dF}{dy} \Big|_n \Delta t] \Delta \underline{y}^{n+1} = \underline{F}^n \Delta t \quad (3.19)$$

The given differential equation can be written as

$$\begin{aligned} \frac{dy}{dt} &= F(t, y) \\ \text{i.e., } \Delta \underline{y}^{n+1} &= \underline{F}^{n+1} \Delta t \\ &= (\underline{F}^n + \underline{F}^{n+1} - \underline{F}^n) \Delta t \\ &= (\underline{F}^n + \Delta \underline{F}^{n+1}) \Delta t \end{aligned}$$

If we approximate

$$\frac{dF}{dy} \Big|_n = \frac{\Delta F^{n+1}}{\Delta y^{n+1}}$$

$$\text{then } \Delta F^{n+1} = \frac{dF}{dy} \Big|_n \times \Delta y^{n+1}$$

So we now have

$$\begin{aligned} \Delta \underline{y}^{n+1} &= [\underline{F}^n + \frac{dF}{dy} \Big|_n \Delta \underline{y}^{n+1}] \Delta t \\ \text{i.e., } [I - \frac{dF}{dy} \Big|_n \Delta t] \Delta \underline{y}^{n+1} &= \underline{F}^n \Delta t \end{aligned}$$

The matrix representation of this equation will be

$$\begin{bmatrix} 1 - \Delta t \frac{\partial \dot{\bar{\rho}}_i}{\partial \bar{\rho}_i} & - \Delta t \frac{\partial \dot{\bar{\rho}}_i}{\partial \bar{U}_i} & - \Delta t \frac{\partial \dot{\bar{\rho}}_i}{\partial \bar{W}_i} \\ - \Delta t \frac{\partial \dot{\bar{U}}_i}{\partial \bar{\rho}_i} & 1 - \Delta t \frac{\partial \dot{\bar{U}}_i}{\partial \bar{U}_i} & - \Delta t \frac{\partial \dot{\bar{U}}_i}{\partial \bar{W}_i} \\ - \Delta t \frac{\partial \dot{\bar{W}}_i}{\partial \bar{\rho}_i} & - \Delta t \frac{\partial \dot{\bar{W}}_i}{\partial \bar{U}_i} & 1 - \Delta t \frac{\partial \dot{\bar{W}}_i}{\partial \bar{W}_i} \end{bmatrix} \begin{bmatrix} \Delta \bar{\rho}_i \\ \Delta \bar{U}_i \\ \Delta \bar{W}_i \end{bmatrix} = \begin{bmatrix} \dot{\bar{\rho}}_i \\ \dot{\bar{U}}_i \\ \dot{\bar{W}}_i \end{bmatrix} \Delta t$$

$$A \cdot X = B$$

(3.20)

$$B = F \cdot \Delta t$$

3.5 Description of various matrices of equation (3.20)

3.5.1 Matrix 'F' :

$$f_1 = \frac{1}{A \cdot \Delta Z} (w_i - w_{i+1})$$

$$f_2 = (H_{A,i} (T_{o,i} - \bar{T}_i) + w_i u_i - w_{i+1} u_{i+1} - c_{22} \bar{\rho}_i (\frac{w_{i+1}}{\rho_{i+1}} - \frac{w_i}{\rho_i}))$$

$$+ c_{23} \frac{\bar{F}_i \bar{W}_i^3 \Delta Z}{A^2 D_e \bar{\rho}_i^3}$$

$$f_3 = (\frac{c_{21}}{\Delta Z} (P_i - P_{i+1}) - \frac{\bar{F}_i \bar{W}_i^2}{2A D_e \bar{\rho}_i} + \frac{w_i^2 r_i}{A \bar{F}_i \Delta Z} - \frac{w_{i+1}^2 r_{i+1}}{A \rho_{i+1} \Delta Z})$$

3.5.2 Derivatives of $\dot{\bar{\rho}}_i$, $\dot{\bar{U}}_i$, $\dot{\bar{W}}_i$

$$\frac{\partial \dot{\bar{\rho}}_i}{\partial \bar{\rho}_i} = 0.0$$

$$\frac{\partial \dot{\rho}_i}{\partial \bar{U}_i} = 0.0$$

$$\frac{\partial \dot{\rho}_i}{\partial \bar{W}_i} = -2/A \cdot \Delta Z$$

$$\begin{aligned} \frac{\partial \dot{\bar{U}}_i}{\partial \bar{\rho}_i} &= -H_{A,i} \cdot \frac{\partial \bar{T}_i}{\partial \bar{\rho}_i} + C_{22} \bar{P}_i \left(\frac{2W_{i+1}}{\rho_{i+1}} \right) - \\ &\quad C_{22} \left(\frac{\partial \bar{P}_i}{\partial \bar{\rho}_i} \right) \left(\frac{W_{i+1}}{\rho_{i+1}} - \frac{W_i}{\rho_i} \right) + 2W_{i+1} \frac{\bar{u}_i}{\bar{\rho}_i} \\ &\quad - \frac{C_{23} \bar{f}_i \bar{W}_i^3 \Delta Z}{A^2 D_e \bar{\rho}_i^3} \end{aligned}$$

$$\begin{aligned} \frac{\partial \dot{\bar{U}}_i}{\partial \bar{U}_i} &= -H_{A,i} \left(\frac{\partial \bar{T}_i}{\partial \bar{u}_i} \cdot \frac{\partial \bar{u}_i}{\partial \bar{U}_i} \right) - W_{i+1} \left(\frac{\partial \bar{U}_{i+1}}{\partial \bar{U}_i} \cdot \frac{\partial \bar{U}_i}{\partial \bar{U}_i} \right) \\ &\quad - C_{22} \frac{\partial \bar{P}_i}{\partial \bar{u}_i} \cdot \frac{\partial \bar{u}_i}{\partial \bar{U}_i} \left(\frac{W_{i+1}}{\rho_{i+1}} - \frac{W_i}{\rho_i} \right) \end{aligned}$$

$$\begin{aligned} \frac{\partial \dot{\bar{U}}_i}{\partial \bar{W}_i} &= -u_{i+1} \frac{\partial W_{i+1}}{\partial \bar{W}_i} - C_{22} \frac{\bar{P}_i}{\rho_{i+1}} \frac{\partial W_{i+1}}{\partial \bar{W}_i} \\ &\quad + \frac{C_{23} \bar{f}_i 3\bar{W}_i^2 \Delta Z}{2A^2 D_e \bar{\rho}_i^2} \end{aligned}$$

$$\frac{\partial \dot{\bar{W}}_i}{\partial \bar{\rho}_i} = -\frac{C_{21} A}{\Delta Z} \left(\frac{\partial P_{i+1}}{\partial \bar{\rho}_i} \right) + \frac{\bar{f}_i \bar{W}_i^2}{2A D_e \bar{\rho}_i^2} + \frac{2W_{i+1}^2 r_{i+1}}{A \rho_{i+1}^2 \Delta Z}$$

$$\frac{\partial \dot{\bar{W}}_i}{\partial \bar{W}_i} = \frac{-\bar{f}_i \bar{W}_i}{A D_e \bar{\rho}_i} - \frac{4W_{i+1} r_{i+1}}{A \Delta Z \rho_{i+1}}$$

$$\frac{\partial \bar{W}_i}{\partial \bar{U}_i} = \frac{C_{21}}{\Delta Z} A \left(- \frac{\partial P_{i+1}}{\partial \bar{U}_i} \right)$$

3.5.3 Derivatives of pressure And Temperature : With respect to Independent Variables Density (ρ) and Internal Energy (u):

(i) Derivatives of pressure:

$$\begin{aligned}
 \frac{\partial \bar{P}_i}{\partial \bar{\rho}_i} &= \frac{1}{2} \left[\frac{\partial P_{i+1}}{\partial \bar{\rho}_i} + \cancel{\frac{\partial P_i}{\partial \bar{\rho}_i}} \right] \\
 &= \frac{1}{2} \left[\left(\frac{\partial P_{i+1}}{\partial u_{i+1}} \right)_p \cancel{u_{i+1}} \left(\frac{\partial u_{i+1}}{\partial \bar{U}_i} \right)_{u_i} \left(\frac{\partial \bar{U}_i}{\partial \bar{\rho}_i} \right) \bar{U}_i \right. \\
 &\quad \left. + \left(\frac{\partial P_{i+1}}{\partial \bar{\rho}_{i+1}} \right)_{u_{i+1}} \left(\frac{\partial \bar{\rho}_{i+1}}{\partial \bar{\rho}_i} \right) \rho_i \right] \\
 &= \frac{1}{2} \left[2 \left(\frac{\partial P_{i+1}}{\partial \bar{\rho}_{i+1}} \right)_{u_{i+1}} - 2 \left(\frac{\partial P_{i+1}}{\partial u_{i+1}} \right)_p \cancel{u_{i+1}} \frac{\bar{u}_i}{\bar{\rho}_i} \right] \\
 \left(\frac{\partial \bar{P}_i}{\partial \bar{\rho}_i} \right) &= \left(\frac{\partial P_{i+1}}{\partial \bar{\rho}_{i+1}} \right)_{u_{i+1}} - \frac{\bar{u}_i}{\bar{\rho}_i} \left(\frac{\partial P_{i+1}}{\partial u_{i+1}} \right)_p \cancel{u_{i+1}} \quad (3.21) \\
 \frac{\partial \bar{P}_i}{\partial \bar{U}_i} &= \frac{1}{2} \left[\left(\frac{\partial P_{i+1}}{\partial \bar{U}_i} \right) + \cancel{\frac{\partial P_i}{\partial \bar{U}_i}} \right] \\
 &= \frac{1}{2} \left[\left(\frac{\partial P_{i+1}}{\partial \bar{\rho}_{i+1}} \right)_{u_{i+1}} \cancel{\left(\frac{\partial \bar{\rho}_{i+1}}{\partial \bar{U}_i} \right)} + \left(\frac{\partial P_{i+1}}{\partial u_{i+1}} \right)_p \cancel{u_{i+1}} \left(\frac{\partial \bar{U}_i}{\partial \bar{U}_i} \right) \right] \\
 &= \frac{1}{2} \left[\left(\frac{\partial P_{i+1}}{\partial u_{i+1}} \right)_p \cancel{u_{i+1}} \left(\frac{\partial \bar{U}_i}{\partial \bar{U}_i} \right) \right] \\
 &= \frac{1}{2} \left[\left(\frac{\partial P_{i+1}}{\partial u_{i+1}} \right)_p \cdot 2 \cdot \frac{1}{A \Delta Z \bar{\rho}_i} \right]
 \end{aligned}$$

$$\frac{\partial \bar{P}_i}{\partial \bar{U}_i} = \frac{1}{A \Delta Z} \bar{\rho}_i \left(\frac{\partial P_{i+1}}{\partial u_{i+1}} \right) \quad (3.22)$$

(ii) Derivatives of Temperature:

$$\begin{aligned} \bar{T}_i &= f(\bar{u}_i, \bar{\rho}_i) \\ \left(\frac{\partial \bar{T}_i}{\partial \bar{\rho}_i} \right) &= \left(\frac{\partial \bar{T}_i}{\partial \bar{u}_i} \right) \bar{u}_i + \left(\frac{\partial \bar{T}_i}{\partial \bar{\rho}_i} \right) \bar{\rho}_i \left(\frac{\partial \bar{u}_i}{\partial \bar{\rho}_i} \right) \\ &= \left(\frac{\partial \bar{T}_i}{\partial \bar{\rho}_i} \right) \bar{u}_i + \left(\frac{\partial \bar{T}_i}{\partial \bar{\rho}_i} \right) \bar{\rho}_i \left(- \frac{\bar{u}_i}{\bar{\rho}_i} \right) \\ &= \left(\frac{\partial \bar{T}_i}{\partial \bar{\rho}_i} \right) \bar{u}_i - \left(\frac{\partial \bar{T}_i}{\partial \bar{\rho}_i} \right) \bar{\rho}_i \left(\frac{\bar{u}_i}{\bar{\rho}_i} \right) \end{aligned} \quad (3.23)$$

$$\begin{aligned} \left(\frac{\partial \bar{T}_i}{\partial \bar{U}_i} \right) &= \left(\frac{\partial \bar{T}_i}{\partial \bar{u}_i} \right) \bar{\rho}_i \left(\frac{\partial \bar{u}_i}{\partial \bar{U}_i} \right) \\ &= \left(\frac{\partial \bar{T}_i}{\partial \bar{u}_i} \right) \bar{\rho}_i \frac{1}{A \Delta Z \cdot \bar{\rho}_i} \end{aligned} \quad (3.24)$$

3.5.4 Elements of Matrix 'A':

$$a_{11} = 1.0$$

$$a_{12} = 0.0$$

$$a_{13} = \Delta T \left(\frac{2}{A \cdot \Delta Z} \right)$$

$$\begin{aligned} a_{21} &= \Delta T [H_{A,i} \left\{ \left(\frac{\partial \bar{T}_i}{\partial \bar{\rho}_i} \right) \bar{u}_i - \frac{\bar{u}_i}{\bar{\rho}_i} \left(\frac{\partial \bar{T}_i}{\partial \bar{\rho}_i} \right) \bar{\rho}_i \right\} - 2w_{i+1} \frac{\bar{u}_i}{\bar{\rho}_i} \\ &\quad - 2c_{22} \frac{\bar{\rho}_i w_{i+1}}{\bar{\rho}_{i+1}^2} + c_{23} \frac{\bar{f}_i \cdot \bar{w}_i^3 \cdot \Delta Z}{A^2 D_e \bar{\rho}_i^3}] \end{aligned}$$

$$+ c_{22} \left(\frac{w_{i+1}}{\bar{\rho}_{i+1}} - \frac{w_i}{\bar{\rho}_i} \right) \left\{ \left(\frac{\partial P_{i+1}}{\partial u_{i+1}} \right) u_{i+1} - \frac{\bar{u}_i}{\bar{\rho}_i} \left(\frac{\partial P_{i+1}}{\partial u_{i+1}} \right) \bar{\rho}_i \right\}]$$

$$\begin{aligned}
 a_{22} &= 1 - \Delta T \left[-H_{A,i} \frac{1}{A \Delta Z} \frac{\partial \bar{T}_i}{\partial \bar{u}_i} \bar{s}_i - \frac{2 \bar{W}_{i+1}}{A \Delta Z \bar{s}_i} - C_{22} \left(\frac{\bar{W}_{i+1} - \bar{W}_i}{\bar{s}_{i+1}} \right) \frac{1}{A \Delta Z \bar{s}_i} \right. \\
 &\quad \left. - \left(\frac{\bar{P}_{i+1}}{\bar{u}_{i+1}} \right) \bar{s}_{i+1} \right] \\
 a_{23} &= \Delta T \left[2 \bar{u}_{i+1} + \frac{2 C_{22} \bar{P}_i}{\bar{r}_{i+1}} - \frac{3}{2} \frac{C_{23} \bar{F}_i \bar{W}_i^2 \Delta Z}{A^2 D_e \bar{r}_i^2} \right] \\
 a_{31} &= - \Delta T \left[\frac{2 C_{21} A}{\Delta Z} \left\{ \left(\frac{\partial \bar{P}_{i+1}}{\partial \bar{u}_{i+1}} \right) \bar{u}_{i+1} + \frac{\bar{u}_i}{\bar{r}_i} \left(\frac{\partial \bar{P}_{i+1}}{\partial \bar{u}_{i+1}} \right) \bar{r}_{i+1} \right\} \right. \\
 &\quad \left. - \frac{-\bar{F}_i \bar{W}_i^2}{2 \cdot A \cdot D_e \bar{r}_i^2} - \frac{2 \bar{W}_{i+1}^2 \bar{r}_{i+1}}{A \cdot \bar{r}_{i+1}^2 \cdot \Delta Z} \right] \\
 a_{32} &= \Delta T \left[\frac{2 C_{21}}{(\Delta Z)^2 \cdot \bar{r}_i} \left(\frac{\partial \bar{P}_{i+1}}{\partial \bar{u}_{i+1}} \right) \right] \\
 a_{33} &= 1 + \Delta T \left[\frac{\bar{F}_i \bar{W}_i}{A D_e \bar{r}_i} - \frac{4 \bar{W}_{i+1} \bar{r}_{i+1}}{A \bar{r}_{i+1} \Delta Z} \right]
 \end{aligned}$$

VECTOR 'X':

$$x(1) = \Delta \bar{r}_i^T = \bar{r}_i^{T+1} - \bar{r}_i^T$$

$$x(2) = \Delta \bar{U}_i^T = \bar{U}_i^{T+1} - \bar{U}_i^T$$

$$x(3) = \Delta \bar{W}_i^T = \bar{W}_i^{T+1} - \bar{W}_i^T$$

3.6 Method of Calculation:

Steady state values have been taken as initial values for the given problem of type

$$\dot{y} = F(t, y), \quad y(0) = y_0$$

Introduce a step change in one of the given variables: u, ρ, W, P at time $t = 0$ and at the inlet.

N
1
2
3
2

Solve for the increments $\Delta \bar{\rho}_i^T$, $\Delta \bar{U}_i^T$, $\Delta \bar{W}_i^T$ at any time t^T equation (3.20) at all control volumes explicitly.

Then add these increments to values at previous time step to get the values at new time step

$$\bar{\rho}_i^{T+1} = \bar{\rho}_i^T + \Delta \bar{\rho}_i^T$$

$$\bar{U}_i^{T+1} = \bar{U}_i^T + \Delta \bar{U}_i^T$$

$$\bar{W}_i^{T+1} = \bar{W}_i^T + \Delta \bar{W}_i^T$$

Knowing the density find out the specific volume at the new time step.

Finding P, T, H, X :

Compressed water : Here isothermal flow is assumed as the temperature change from one time step to another is negligibly small

$$\text{i.e., } \left(\frac{\bar{P}_i}{\bar{\rho}_i}\right)^T = \left(\frac{\bar{P}_i}{\bar{\rho}_i}\right)^{T+1}$$

$$\text{So } \bar{P}_i^{T+1} = \left(\frac{\bar{P}_i}{\bar{\rho}_i}\right)^T \cdot \bar{\rho}_i^{T+1}$$

$$\text{Then } \bar{H}_i^{T+1} = \bar{U}_i^{T+1} + \frac{\bar{P}_i^{T+1}}{\bar{\rho}_i^{T+1}} \cdot c_{22}$$

$$\bar{x}_i^{T+1} = 0$$

Using the table of temperature as a function of pressure for compressed water temperature \bar{T}_i^{T+1} can be calculated.

Saturated water : Pressure, quality can be calculated as a function of internal energy and density

$$X = X(P)$$

$$P = P(\bar{\rho}_i, \bar{u}_i)$$

Knowing pressure corresponding saturation temperature can be calibrated from the table.

Then enthalpy is given as

$$H = H_L + X(H_V - H_L)$$

H_L , H_V saturation enthalpy of liquid

and vapor corresponding to the above pressure P .

Definition of some constants used in this chapter.

$$C_{21} = g_c \times 3600^2 \frac{\text{sec}^2}{\text{Hr}^2} \times 144 \frac{\text{in}^2}{\text{ft}^2} = 0.600444 \times 10^{11}$$

$$C_{22} = 144 \frac{\text{in}^2}{\text{ft}^2} \times 0.001285 \frac{\text{Btu}}{\text{lbf-ft}} = 0.18504$$

$$C_{23} = \frac{1}{g_c} \times \frac{\text{Hr}^2}{3600^2 \text{Sec}^2} \times 0.001285 \frac{\text{Btu}}{\text{lbf-ft}} = 0.308172 \times 10^{-11}$$

3.7 Flow Chart :

The flow charts developed for steady state simulation and transient simulation are given below.

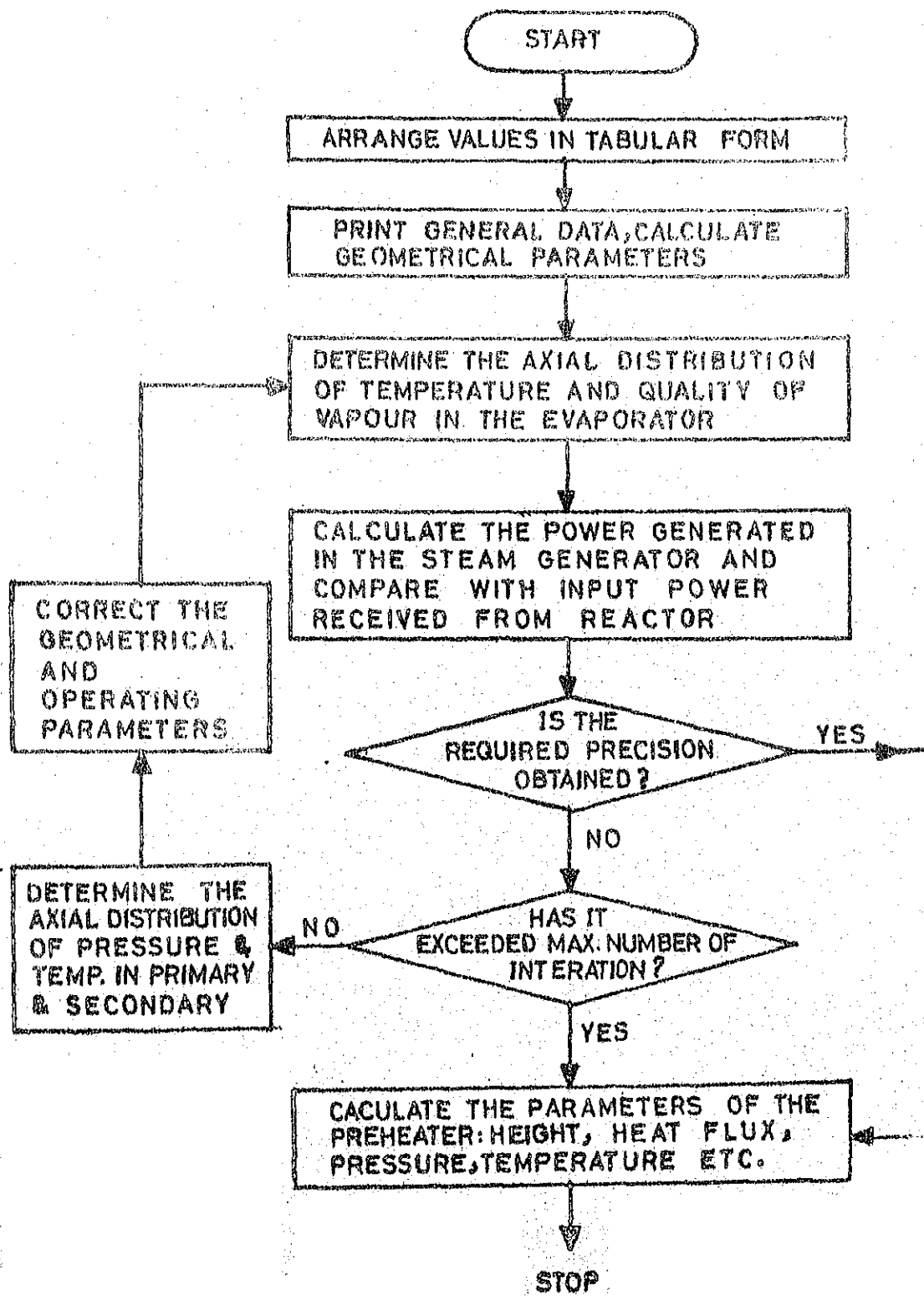
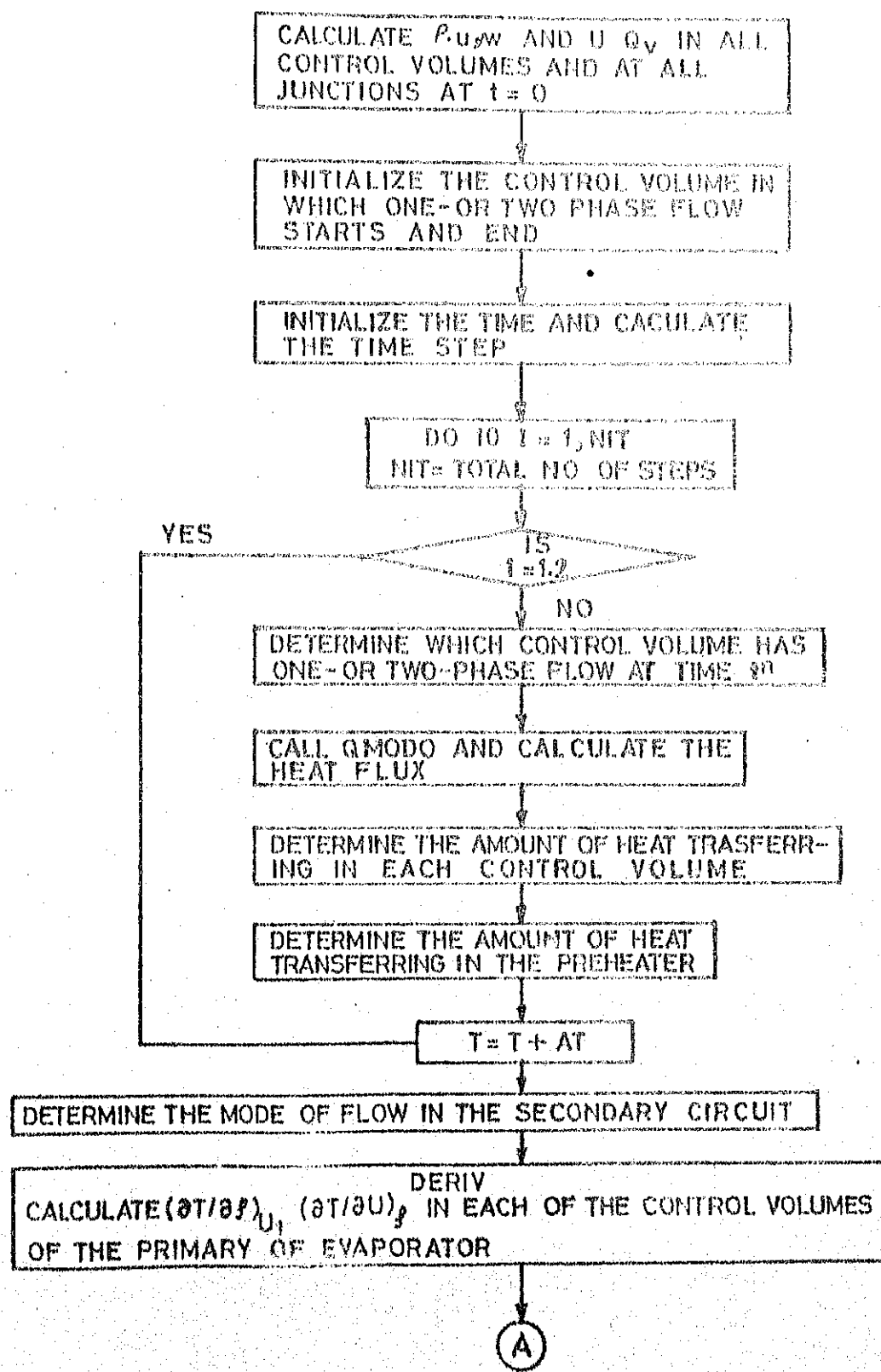


Fig.3.1 Flow chart of the computer programme calculating the study state values



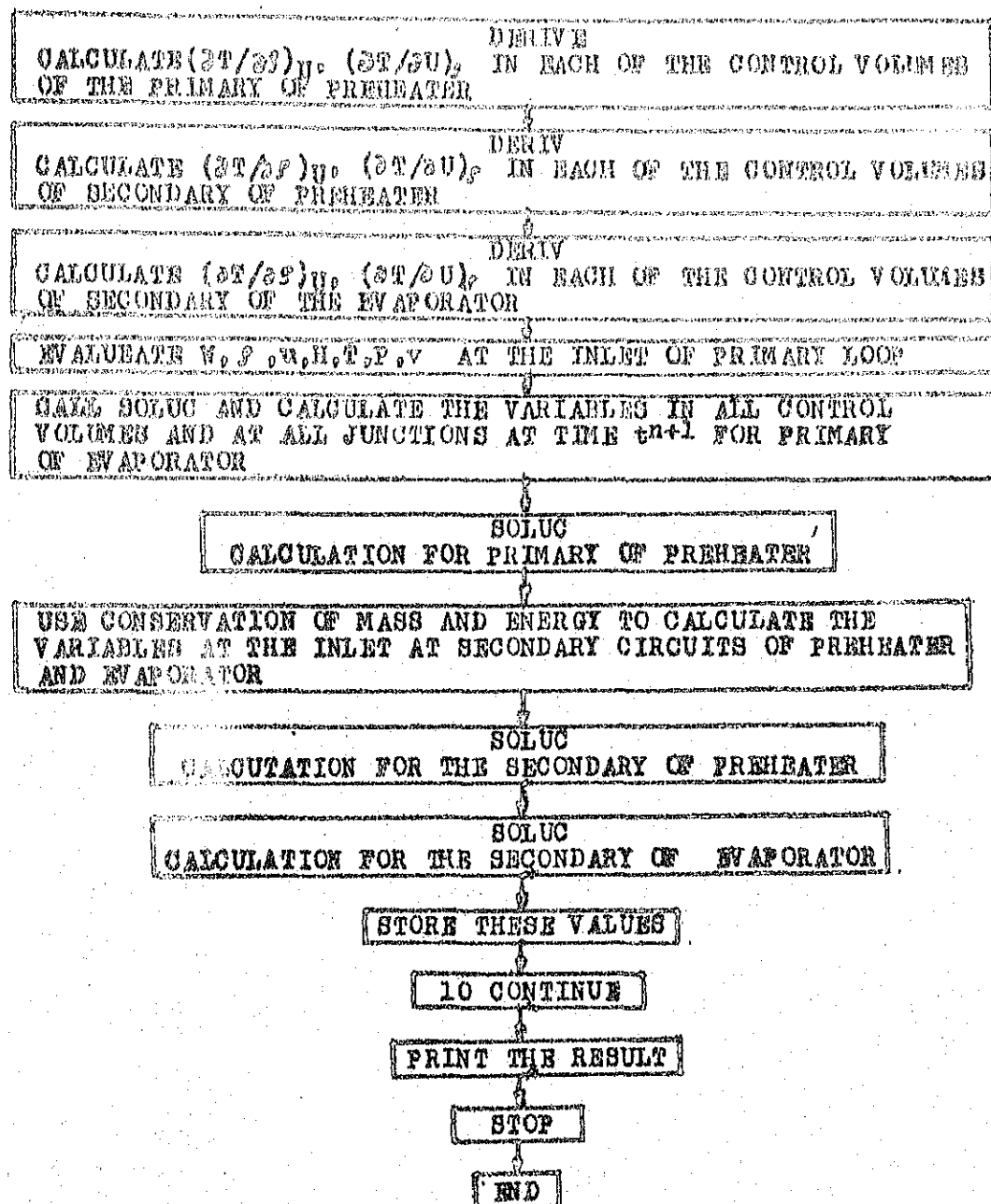
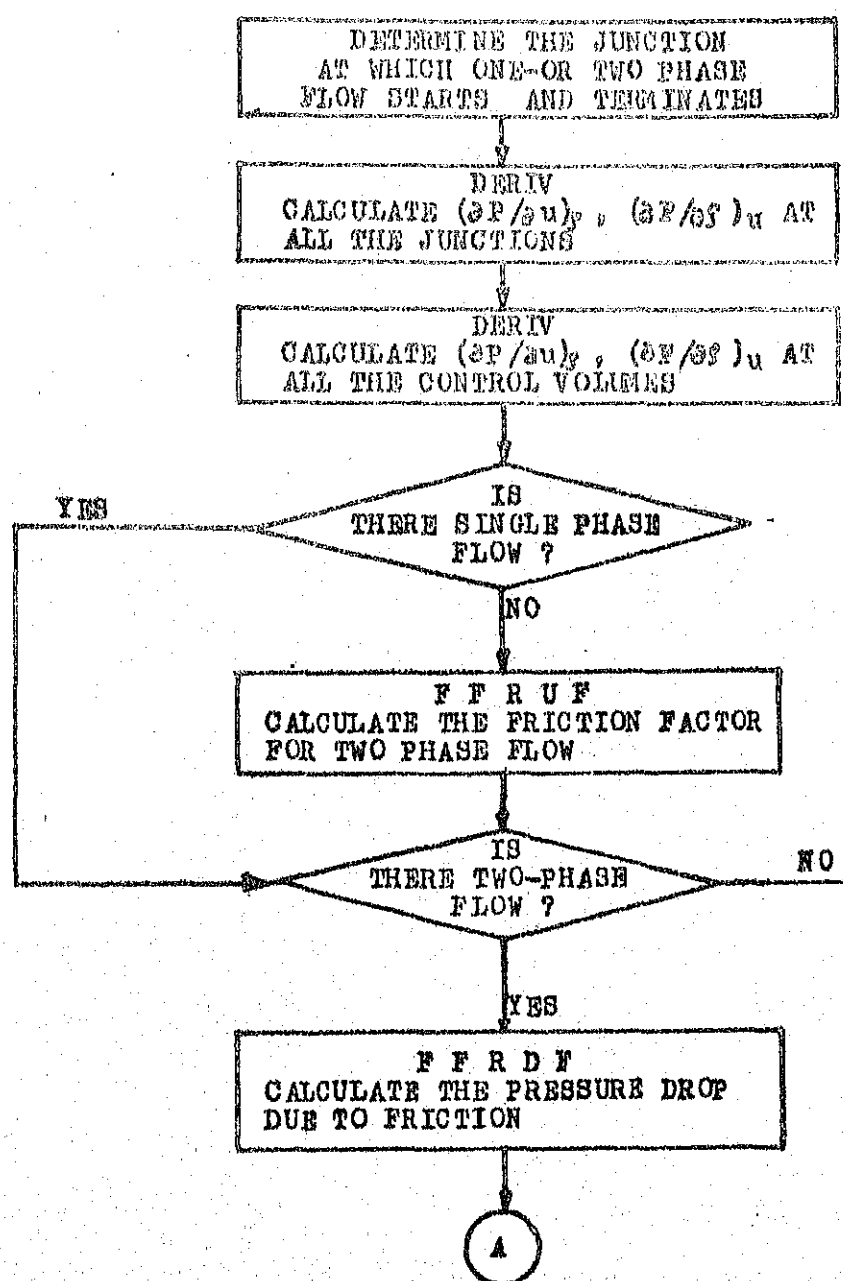


Fig. 3.2 : Flow chart of the programme simulating the transients



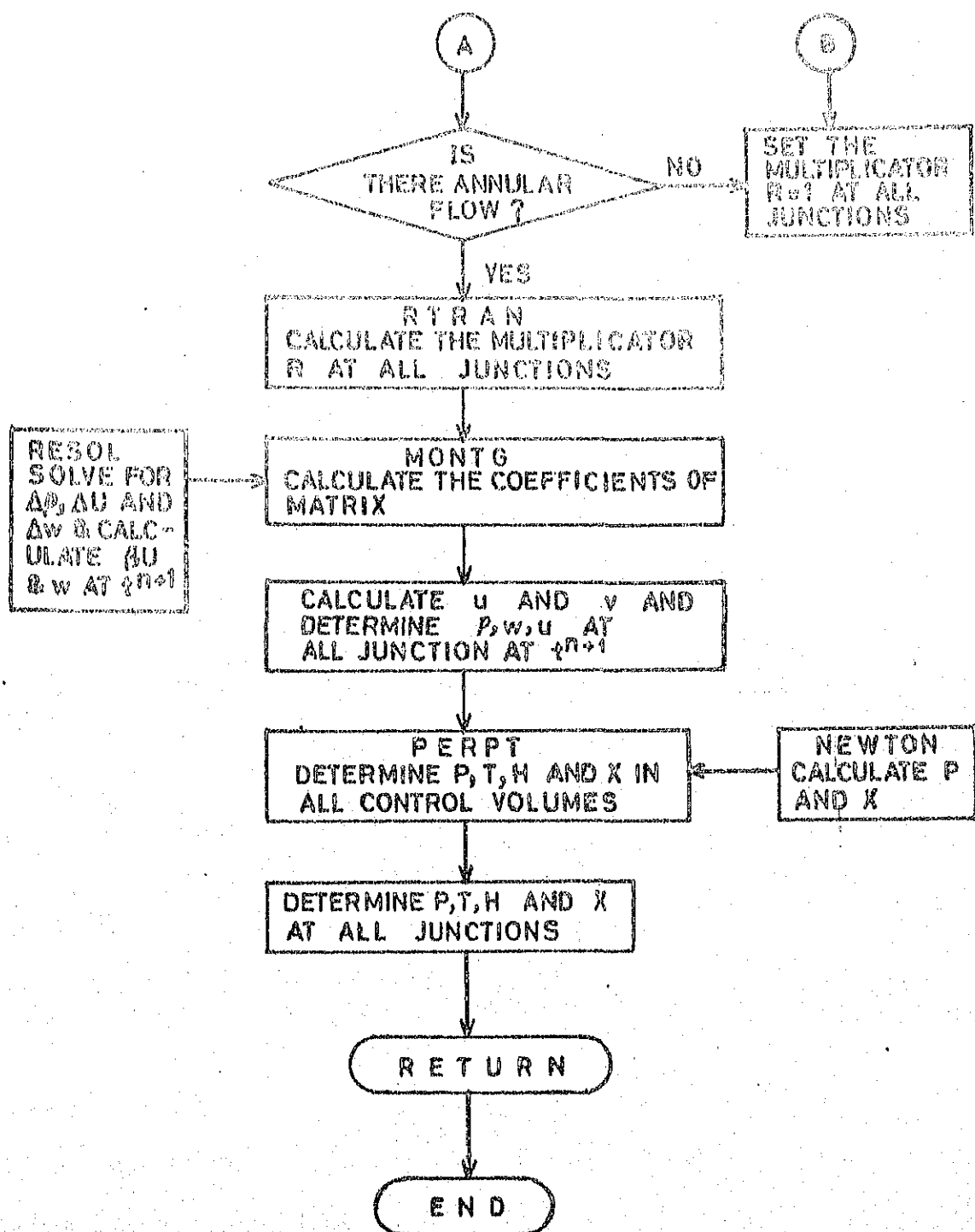


Fig.3.3 Flow chart of the subroutine SOLUC

CHAPTER IV

4.1 MODIFICATIONS MADE IN THE STEADY STATE SIMULATION

The steady state simulation developed by Pinto [6] has some limitations. There the only thing that was fixed in advance was total heat flux. The way in which simulation has been done is given in Appendix I. An assumption which was made in it is that the steam flow rate (w_s) is equal to quality (x) times the total flow rate (w_t) at the exit and is always fixed.

$$w_s = x_{exit} \cdot w_{Total} = \text{Constant}$$

So in order to match the total heat flux one can have many alternatives of total flow rate and exit quality. There can be a higher quality mixture with less flow rate and vice-versa. But this particular program is converging for only initial approximation for quality which is around 0.4. It also always converges towards the same quality which is 0.39.

As mentioned in ref. [11] a crude measure of adequacy of secondary coolant flow through the tube bundle is the "circulation ratio" which is defined as weight of water circulating in the exchanger per unit-weight of steam generated. A small circulation ratio indicates a large fraction of steam in the tube bundle and the possibility of

poor heat transfer on the shell side. In addition to this a low circulation ratio leads to flow instability. In the past, units had been designed with circulation ratios such that the steam quality at the exit of the bundles did not exceed 20 to 25 %.

A low circulation ratio can lead to flow oscillations that cause periodic uncovering of a portion of the heat exchanger surface. This 'chugging' phenomenon reduces the heat transfer efficiency, and flow oscillations of sufficient amplitude can lead to large fluctuations in the water level or steam flow rate.

Experience shows that flow stability can be achieved by keeping the steam quality in the bundle low, or equivalently by keeping the recirculation ratio high.

So it was tried to reduce the quality at the exit by assuming low qualities around 0.25 to 0.3. But the scheme did not converge. Many modifications have been tried but they failed. At last the total flow rate was made constant and the steam flow rate and quality left open to converge to their own values. By this a control over total flow rate was achieved. As expected this has worked well and quality started decreasing with the increase in flow rate and vice-versa. Finally a quality of around 0.3 has been chosen for transient simulation.

4.2 MODIFICATIONS MADE IN THE TRANSIENT SIMULATION

In earlier formulation the results exhibit some instability which produces large variation in the parameters and almost all the results are converging to abnormal limits.

As a first step the whole problem was reformulated and compared with previous formulation [1]. It was found, there is no error as far as the mathematical formulation is concerned. Though it was mentioned that the instability is purely a numerical instability, no attempts were made to pin point the problem. Some of the possibilities are :

1. There may be a big calculation mistake in the program.
2. The scheme used may not be logically correct.
3. There may be typographic errors in the program.

If everything is alright as mentioned in the previous work, it is purely a numerical instability, and a better time step will automatically eliminate the instability.

As it was mentioned that the instability could be due to large time step, the first trial that was made with the program, was to study the program with reduced size of time steps. When it was tried with time steps less than previous time step (0.001), instead of converging to better solution it started diverging. At this stage if one is very confident about the correctness of other things it can be

concluded that this method will not converge for the present problem.

In order to see the effect of the scheme two simple schemes were tried. One is Euler's method (most simple of all) and the second one is Fourth Order Runge Kutta Method (very accurate of one step methods).

The Euler's method started blowing up immediately after four to five iterations. It has given an idea that the accuracy of the method is also very important for the present problem. It was confirmed when fourth order Runge Kutta method run smoothly. But the instability persisted there. This has revealed the truth that there must be some calculation or logical mistake.

Proof reading of the program was done several times as a result of which some typographic errors were found. At two-three places the brackets were placed at wrong location. But the mistake is such that the computer can not find out the error during compilation. Ofcourse this correction did not change the solution very much.

The most crucial calculation of the program is the calculation of increment function from equation (3.20). This involves the inversion of a 3×3 matrix at all the control volumes and at all the time steps. It is very well known that the matrix inversion is so sensitive that it reacts greatly even for small fluctuation in the values of its elements.

So the accuracy of the elements of matrix A (3.20) must be ascertained. As it involves several derivatives of pressure and temperature, accurate evaluation of derivatives is needed because of the fact that the calculation of the derivatives is only possible through the interpolation of curves given in steam and water tables [13]. On verification it was found that the interpolated values of the derivatives were very erroneous. The new values of the derivatives have been interpolated and introduced in a new subroutine (DERIV) for finding derivatives, in the place of the subroutines DPREU and DPRER.

Not only the value of derivatives but also the method of expressing (finding) partial derivatives from functional relations is important. So the partial derivatives have been expressed as shown in section 3.4.

Here is an important modification which has almost nullified the instability. In the previous work there is an assumption made while finding the derivatives of \bar{U} with respect to $\bar{\rho}_i$, \bar{u}_i , \bar{W}_i . The term Q in the energy equation (3.11) is assumed constant with respect to average density $\bar{\rho}_i$ and average internal energy \bar{u}_i . The simple expansion of Q explains why this assumption is wrong.

$$Q = H_{A,i} (T_{o,i} - \bar{T}_i)$$

$H_{A,i}$ over all heat transfer coefficient between primary and secondary at control volume i.

\bar{T}_i Average temperature of the fluid in control volume i.

Here the average temperature of secondary fluid is a strong function of internal energy and to some extent density.

The elements $\frac{\partial \dot{U}_i}{\partial \bar{p}_i}$, $\frac{\partial \dot{U}_i}{\partial \bar{u}_i}$ of matrix A (eqn. 3.20)

involve the terms $(H_{A,i} \cdot \frac{\partial \bar{T}_i}{\partial \bar{p}_i})$ and $(H_{A,i} \cdot \frac{\partial \bar{T}_i}{\partial \bar{u}_i})$ which are

not negligible. Hence it can be concluded that $\frac{\partial Q}{\partial \bar{p}_i}$, $\frac{\partial Q}{\partial \bar{u}_i}$ are not only non-zero but also significant.

With the above modifications the instability has been reduced very much. Yet there is no convergence at all as far as mass flow rate is concerned. Except the mass flow rate all the other variables are converging. But the quality rises to a very high value around 0.7 to 0.8 and converges at that point. Whereas the steady state quality is around 0.4. Just by increasing the energy content of primary liquid by 5 %, it is highly impossible physically to get a quality jump from 0.39 to 0.8 an increment of about 100% for a small variation in the primary side. At the same time the flow rate

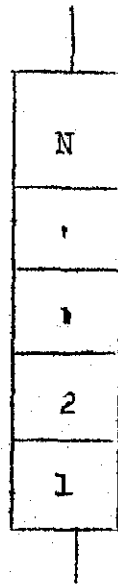
rate is highly fluctuating. This has given a clear indication that neither the mass nor the energy is conserving properly. The previous work did not bother to verify the total heat transfer rate with the time. When it was tried to get the printout of heat transfer rate, surprisingly it was reducing to very low value with the time, which was as low as 50 % less than the steady state value.

At this stage it was tried to verify the logic very carefully. During this verification some logical errors were found.

THE LOGIC USED IN THE PREVIOUS WORK IS:

After deviding the channel into N number of equal parts, the conservation equations have been solved for the increments in the first and Nth control volumes only and it was assumed that the average of these two increments can be taken as total increment from bottom to top.

Also this total increment can be distributed equally in all the control volumes. So in the previous work they did not tried to include the effect of the values of the intermediate control volumes. Also it was assumed that the distribution of various parameters along the length of the channel with time is parallel to the initial distribution (steady state distribution).



It seems that these assumptions are wrong. The first assumption is incorrect, because it involves gross error, and it has to be corrected. Though it is not the correct approach, there is no harm in considering the second assumption. The increments here are of the order of less than 0.1 % of the actual value. So it is reasonable if the increments, which were found out at different control volumes explicitly, were averaged over the length of the channel. In other words the increment at any time step is constant and is equal to average of all the individual increments.

Mathematically if $\Delta \bar{Y}_i^T$ is a small increment of a function at any control volume i , then the logic of previous work is as follows :

Find $\Delta \bar{Y}_1^T$ and $\Delta \bar{Y}_N^T$

$\Delta \bar{Y}_1^T$ - Increment in the first control volume at time T.

$\Delta \bar{Y}_N^T$ - Increment in the Nth control volume at time T.

$$\Delta \bar{Y}^T = \frac{\Delta \bar{Y}_1^T + \Delta \bar{Y}_N^T}{2N}$$

At any control volume i $\bar{Y}_i^{T+1} = \bar{Y}_i^T + \Delta \bar{Y}^T$

The correct logic that should be used:

Find $\Delta \bar{Y}_i^T$ $i = 1, 2, \dots, N$ (explicitly)

$$\bar{Y}_i^{T+1} = \bar{Y}_i^T + \Delta \bar{Y}_i^T$$

Another logic that can be used reasonably is

Find $\Delta \bar{Y}_i^T$ $i = 1, 2, \dots, N$ (explicitly)

$$\bar{Y}_i^T = \frac{\sum_{i=1}^N \Delta \bar{Y}_i^T}{N}$$

$$\bar{Y}_i^{T+1} = \bar{Y}_i^T + \bar{D}\bar{Y}^T$$

There is a semi-explicit scheme which can be derived and is very powerful for some problems.

Find $\Delta \bar{Y}_i^T$ Using the inlet values of control volume i at time $T+1$ and exit values of control volume i at time T .

$$\text{Find } \bar{Y}_i^{T+1} = \bar{Y}_i^T + \Delta \bar{Y}_i^T$$

Using the expression

$$\bar{Y}_i^{T+1} = \frac{\bar{Y}_i^{T+1} + \bar{Y}_{i+1}^{T+1}}{2}$$

$$y_{i+1}^{T+1} = \bar{y}_i^{T+1} - y_i^{T+1}$$

Knowing the values of junction 1 at time $T+1$ (y_1^{T+1}), one can go forward to get the exit values.

After this modification, another logic step was found which was unreasonable. There are some statements which state that whenever one of the variable become negative, after adding the increment, subtract back that increment and proceed with the previous value. This is definitely a suppression of error which is existing at that point. In the basic program, for which some results have been given, the removal of these statements produce results which are not correct. In other words, the program is not at all running properly. While searching for the reason for it, it was found that flow rate becomes negative after some time. So the program is becoming unstable. This is definitely an indication of error and one has to stop at this stage to search for the error, because the increment should always be within the limits. After the present modification this type of error is not reoccurring.

Coming back to the heat balance, simply speaking, the heat transfer rate is approximately equal to $W(H_1 - H_2) = W \Delta H$. Where W is the average flow rate in secondary of evaporator ΔH is Enthalpy change in secondary of evaporator.

On the other hand flow rate can be written as

$$W = Q / \Delta H$$

where, Q is the heat transfer rate calculated from the correlation of various heat transfer regimes along the length of the channel. As the flow rate is highly fluctuating it was expected it is mainly due to erroneous calculation of ΔH .

As shown in fig. (2.2) at the inlet of the secondary of evaporator a jet of recirculated water at certain conditions will mix with another jet of feed water from the preheater of the secondary side. To start with the calculation of various parameters along the length of the channel one has to know the inlet conditions. For the secondary of evaporator inlet conditions are nothing but the conditions of the mixture. Because of the lack of details about the internals of the heat exchanger, it is difficult to make a momentum balance or heat balance for finding the conditions of mixture at the inlet so it is necessary to assume approximate values for the parameters. It was assumed that the total enthalpy and specific volume of the mixture consists of their individual values in proportion to their mass flow rate, i.e.

$$H = \frac{W_1 H_1 + W_2 H_2}{W_1 + W_2}$$

w_1, w_2 - Mass flow rates of two jets

H_1, H_2 - Enthalpies of two jets respectively.

This assumption is reasonable. Before coming to this point we need to state that there is another mistake committed in the previous work while calculating liquid enthalpy of recirculated water. Here is the formula that was used

$$H_{liq} = \left(\frac{1 - x_{exit}}{1 - 2x_{exit}} \right) H_{exit}$$

If one thoroughly goes through this expression he can be convinced it is not correct.

Expanding the above expression

$$(1 - 2x_{exit}) H_{liq} = (1 - x_{exit}) H_{exit}$$

When quality at exit i.e. $x_{exit} = 1$ then $H_{liq} = 0$ which has not got any meaning at all, because when quality reaches one, recirculation flow reaches zero. So, w_{rec} will become zero but not the enthalpy content of liquid at that point.

Also if $x_{exit} = 0.5$ than $H_{liq} = \infty$ which is improper so if the quality at the exit reaches very close to 0.5 the enthalpy content of the recirculated water reaches very very high value and ultimately at 0.5 becomes infinite.

It can be reasonably assumed that the mixture is in thermodynamic equilibrium. As the mixture is at saturation state, the saturation liquid enthalpy can be taken as enthalpy of recirculated water. With this modification, proper heat balance has been achieved.. But there is no convergence as yet. Flow rate is still fluctuating.

In the previous work no assumption of perfect control of feed water was made, i.e. The feed water rate is assumed to be constant through out the transient. The disadvantage of this assumption is as follows: For instance, if all of a sudden the energy content of the primary liquid is increased and kept constant, then, the heat transfer rate from primary to secondary circuit will increase. So the quality at the exit of secondary circuit will be increased. The increase in quality will increase the steam flow rate and reduce the recirculation rate. As the total flow rate in the evaporatory is the sum of the recirculation and feed water flow rates this total flow rate is going to be reduced. Because the feed water rate is still same as steady state value. As the less amount of liquid receives the same higher amount of heat flux, quality will still increase, this inturn will improve the steam flow rate further and decreases the total flow rate in the evaporator. If this process continues there may be a possibility that the quality at the exit may become 1, and hence there will be no recirculation at all.

The feed water that is supplying will be directly converted to steam. This may lead to burnout condition also. In order to avoid this there should be some control over feed water rate. A possible elimination of this sort of trouble is by feeding more feed water. That is if it is assumed that

$$W_{\text{feed}} = X_{\text{exit}} \cdot W_{\text{total}} = W_{\text{steam}}$$

This means that the feed water rate should be adjusted such that the feed water rate can always match with the steam flow rate.

One more mistake was found at this stage. It was another wrong assumption made in the previous work, that the pressure at the inlet of the secondary of evaporator is equal to pressure at the exit of the evaporator at the previous time step, i.e. $PSJ(1)^{T+1} = PSJ(\text{EXIT})^T$. As there will be a pressure change of only about less than 1 PSI between any two time steps, it is improper to assume this. This means the pressure drop from inlet to exit is negligibly small. This will obviously affect the flow rate considerably. So it was tried by assuming the pressure at the exit of the pre-heater equal to pressure at the entrance of evaporator. This way it is giving better results. But still not very convincing. It was assumed that the pressure should be inbetween these two. By taking the average of these two

pressures still better results have been obtained.

Then the program was tested at varying time steps and for varying step changes. The effect of these variations have been discussed in the last chapter.

CHAPTER V

5.1 RESULTS AND DISCUSSION

This chapter consists of the discussion of the results obtained after making all the modifications given in chapter IV.

5.1.1 Steady State Values:

The steady state operating values which are used for transient simulation are given in Appendix III. In the computer code developed by Pinto [7] a lower total flow rate and a higher quality (0.4) have been used in the secondary side. But in the present case some what higher flow rate and lower quality (0.3) is used. By reducing the exit quality on secondary side, the region in which film boiling exists, is reduced. This is because of the fact that the film boiling is unstable compared to nucleate boiling. Besides this, the heat flow correlations are not very accurate in film boiling compared to nucleate boiling. Flow is also more stable at lesser qualities compared to higher qualities.

5.1.2 Transient Values :

The results of the transient analysis are presented in graphical forms from fig. 5.1(a) to fig. 5.4(f).

- (i) 5 % increment in internal energy at the inlet of the primary circuit : The figures 5.1(a) to fig. 5.1(f) consists of this case.

With the increase in internal energy on primary side there will be more energy available at any time in the primary liquid. This will increase the heat transfer rate from primary to secondary liquid. As it can not transfer the entire internal energy to the secondary side the internal energy at the exit of the primary side will increase. The temperature of the primary liquid at the exit will increase, as some of the extra energy available in the primary liquid can be utilized in increasing the temperature of the primary liquid itself. Coming to the secondary side the extra heat supplied can be utilized in two ways

1. It can increase vapour content of the secondary fluid and thereby increase the quality and flow rate. Here again, there can be two types of explanations for pressure variation. One, with the increase in the quality, the corresponding saturation pressure may reduce and hence the temperature. The second one, with the increase in flow rate the pressure drop has to be increased and hence the exit pressure will reduce. As the mixture is at saturation state this will reduce the corresponding temperature at the exit.
2. The extra heat can be utilized in heating the mixture to a high temperature. With this the corresponding saturation pressure will also increase. Here unless some extra vapour forms the quality will come down.

- (ii) 5 % increase in mass flow rate at the inlet of the primary circuit (figures 5.2(a) to fig. 5.2(h)) will represent this situation.

As the flow rate was increased the heat transfer coefficient from the primary fluid to wall increased, because Reynold's number increases with the increase in velocity. So the heat transfer rate from the primary to secondary liquid will increase.

On the primary side, in order to accommodate extra flow rate the pressure at the exit will decrease. As it can not transfer all the extra heat due to extra flow the temperature at the exit will increase. The flow rate at the exit is slightly increasing to above 5 % level and finally stabilising at 5 %. level in a short period.

On the secondary side, the increased heat transfer rate can produce two effects as discussed in the previous case. Here in this case, the internal energy and quality are increasing and the pressure and temperature are decreasing. This means most of the energy is utilized in improving vapour content or quality.

$$\text{Mass flow rate } W = \rho_{av} A V_{av}$$

With the increase in quality, average density will decrease as more vapour forms. At the same time average velocity will increase as vapour velocity is more compared to liquid. So the

I.I.T. KANPUR
CENTRAL LIBRARY

Acc. No. A 66825;

mass flow rate will be effected according to the dominance of one of these. If the variation in density is less predominant then the mass flow rate will increase and if the density variation is predominant mass flow rate can decrease. In the present case it can be said that density variation is not predominant as the flow rate is increasing. Also, to accomodate more pressure drop the pressure at the exit decreases.

- (iii) Internal energy was increased by 15 % at the inlet of the secondary circuit : fig. 5.3(a) to 5.3(h) will represent this situation.

This increase in energy content of secondary side will decrease the heat transfer rate from primary to secondary liquid. But due to such a high amount of extra energy on the secondary side, quality will increase at the exit. If we go through the simple heat balance.

$$\text{Heat Transfer Rate } (Q) = \text{Mass flow rate} \times \text{Enthalpy change}$$

With the increase in internal energy the enthalpy at the exit is increasing as the enthalpy at inlet is also increasing. But there is not much change in H . So the reduction in heat transfer rate will reduce the flow rate. In order to reduce the pressure drop, pressure at the exit will increase and hence the corresponding saturation temperature will increase.

Coming to the primary side, as less heat is transferring to the secondary liquid, the internal energy and temperature of the outgoing liquid will increase. This increase in temperature can slightly reduce the density. Because of the isothermal flow assumption on primary side the pressure at the exit will decrease correspondingly. This decrease in pressure will slightly increase the pressure drop and hence the flow rate. But all these changes in primary side are very small compared to the secondary side changes.

- (iv) Mass flow rate was increased by 20 % and kept constant at the entrance of secondary side (fig. 5.4(a) to 5.4(f)). will represent this situation.

As we supply a constant amount of extra cold water this reduces the quality on the secondary side. As the quality reduces, the flow rate will also reduce. This will result in a lesser pressure drop and hence the pressure at the exit of the secondary circuit will increase, increasing the corresponding saturation temperature.

5.1.3 Comparison of Results with Previous Results:

As there are no experimental results available to compare the present results, a trial was made to compare these results with those of Silva [9]. But there is a major difference between these two as far as initial values are concerned. In Silva's work the transients are studied for the steady state conditions, consisting of a total flow rate of about $2\frac{1}{2}$ times the

flow rate we are using. This means, they are considering a maximum quality of only about 0.12 i.e. at the exit of secondary of evaporator. As it is well known, the annular flow starts at a quality of about 0.2, hence the above region is much below film boiling region. So, it can be seen, that always at all the control volumes there will be only subcooled (nucleate) boiling. But the major aim of this work is to study the transient with two phase flow. So we have used a quality such that, there will be at least 40 % of the secondary of evaporator section, in which partial film boiling (annular flow) exists. So even if we compare these results with the present results we can not see a good agreement. So, even for the present work one case was studied with the same conditions as above for comparison sake and it was found that the results were in good agreement.

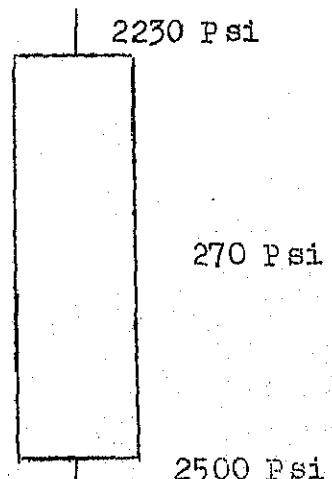
This program is not working efficiently for pressure variations. If a pressure reduction of 30 % is given at the inlet of say primary side then the flow situation can behave in two ways.

At steady state the pressures are as shown in fig. 5.1.1.

The pressure drop is around 11% of inlet. Hence if all of a sudden we reduce the pressure to such a low value, then there can be flow reversal.

But as the present program is not written to take care of the

Fig.5.1.1



flow reversals it is hard to expect any reasonable results from this program for such a high pressure fluctuations. Also at the inlet of primary side the liquid is almost at saturation point. If suddenly the pressure reduces, there will be two phase flow in the primary circuit itself. But as it was assumed that always there would be a single phase flow, so even a small reduction of about 5 to 10 % in pressure will create two phase flow in primary circuit and hence this program can not give better results for pressure fluctuations.

Coming to the secondary side, the reduction in pressure at inlet may reverse the flow in the preheater. If all of a sudden the pressure at the exit reduces, to adjust to the higher pressure drop, there can be two phase flow in preheater section. But, even here it was assumed that there would only be single phase flow in the preheater. So, it is contradicting this assumption. Hence, this program can not give accurate results for pressure fluctuations on the secondary side.

Program was run at different step increment on both primary and secondary sides. It was found that the program can not be used for higher step increments on primary side. On primary side maximum of 10 % to 12 % increment in internal energy and flow rate can be used. But on the secondary side it can give better results even for very high step increments as about 20 % in internal energy and as high as 30 % for flow rate.

5.1.4 Conclusions:

From the above discussion and from the graphs it can be concluded that the fluctuations in the primary side inlet will affect the operating conditions more compared to the fluctuations in the secondary inlet flow i.e. the feed water flow. Also, the most predominant and important parameter that can highly affect the operating conditions, is the primary internal energy. As it can be seen from graphs for 5 % step change, maximum rate of variation of exit parameters on secondary side is with the 5 % step change in primary internal energy. Next comes the mass flow rate.

On the secondary side, 5 % step change in flow rate does not affect the operating conditions much. This is true, because the feed water rate is only 30 % as compared to 70 % re-circulation. So the net effect in the secondary of evaporator is very less.

It was also found that the mixture parameters at the inlet of the secondary of evaporator are very important in finding the operating parameters in a transient case, especially, the mixture pressure which will be used as inlet pressure of secondary of evaporator. The interpolated values of derivatives also will play very important role in determining the transients.

Time Step Size : The program was run for 5 different time steps 0.01, 0.005, 0.001, 0.0005, 0.0001. It was found that the program is highly diverging for the first time step (0.01).

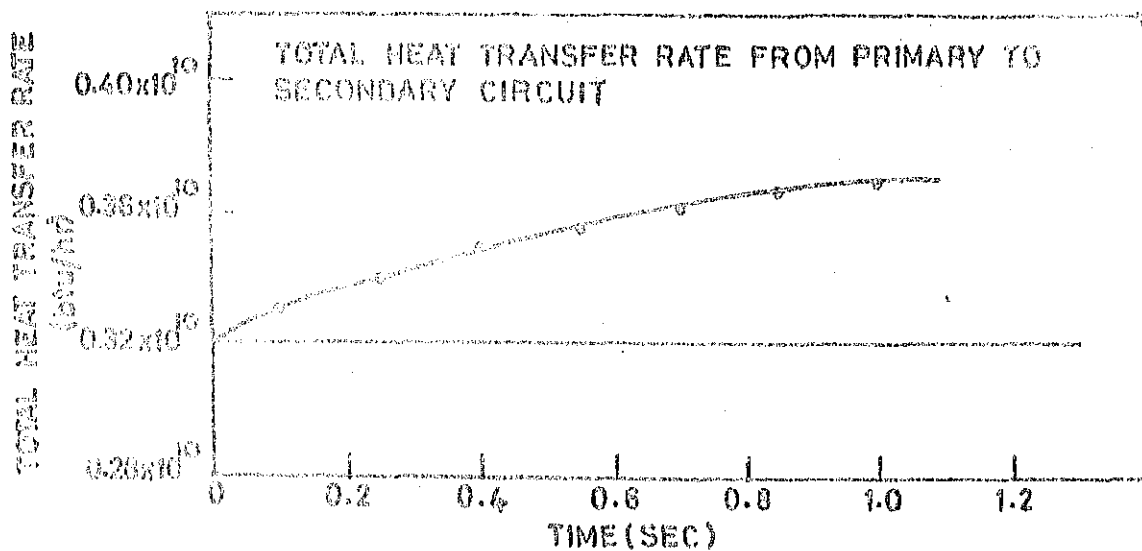


FIG.5.1(a)

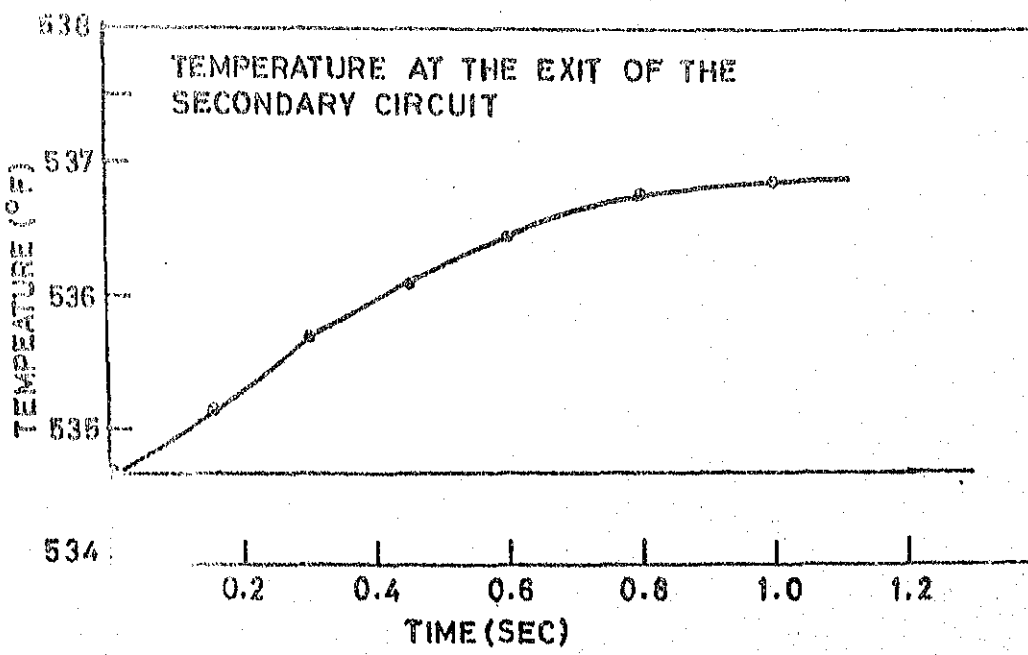
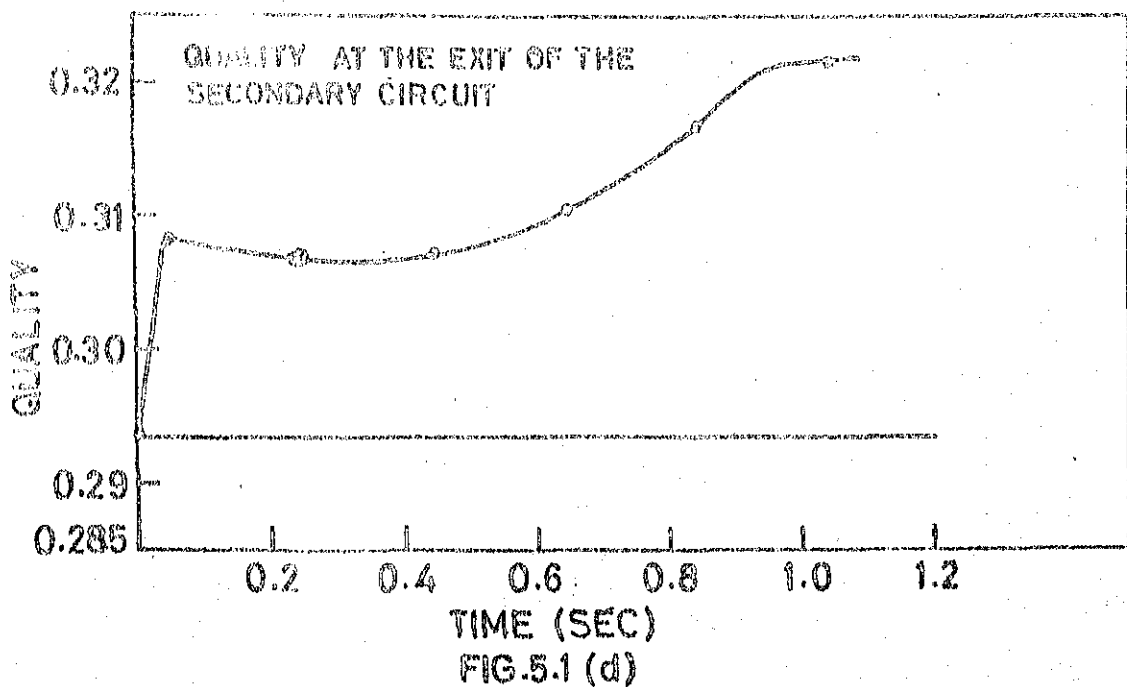
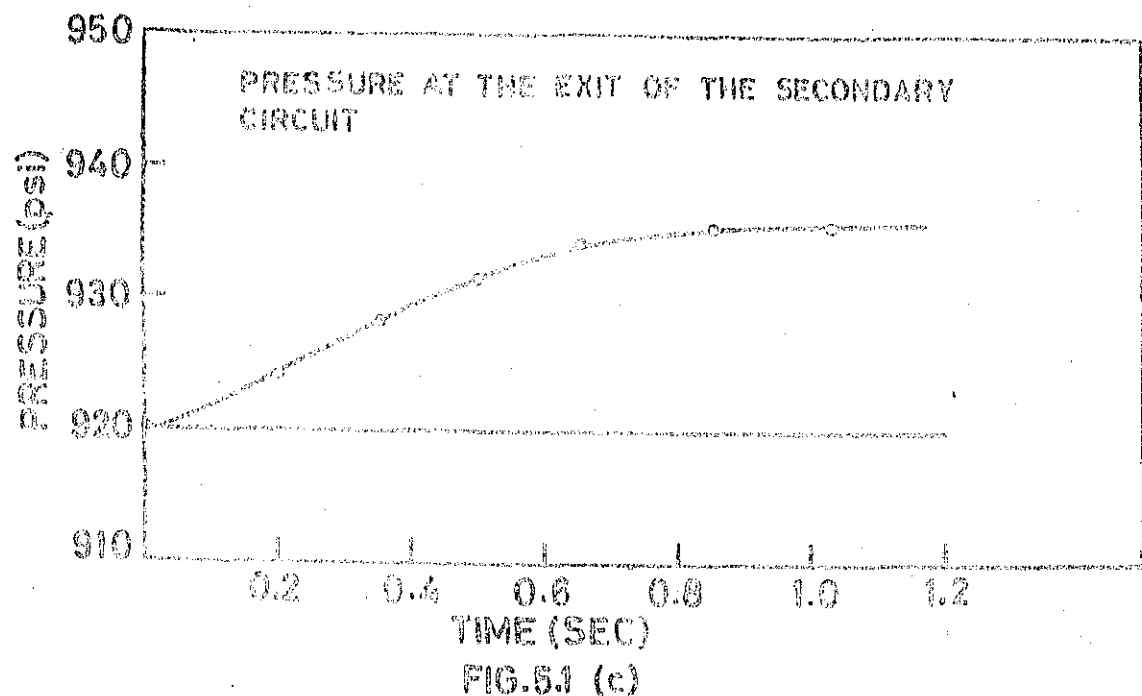
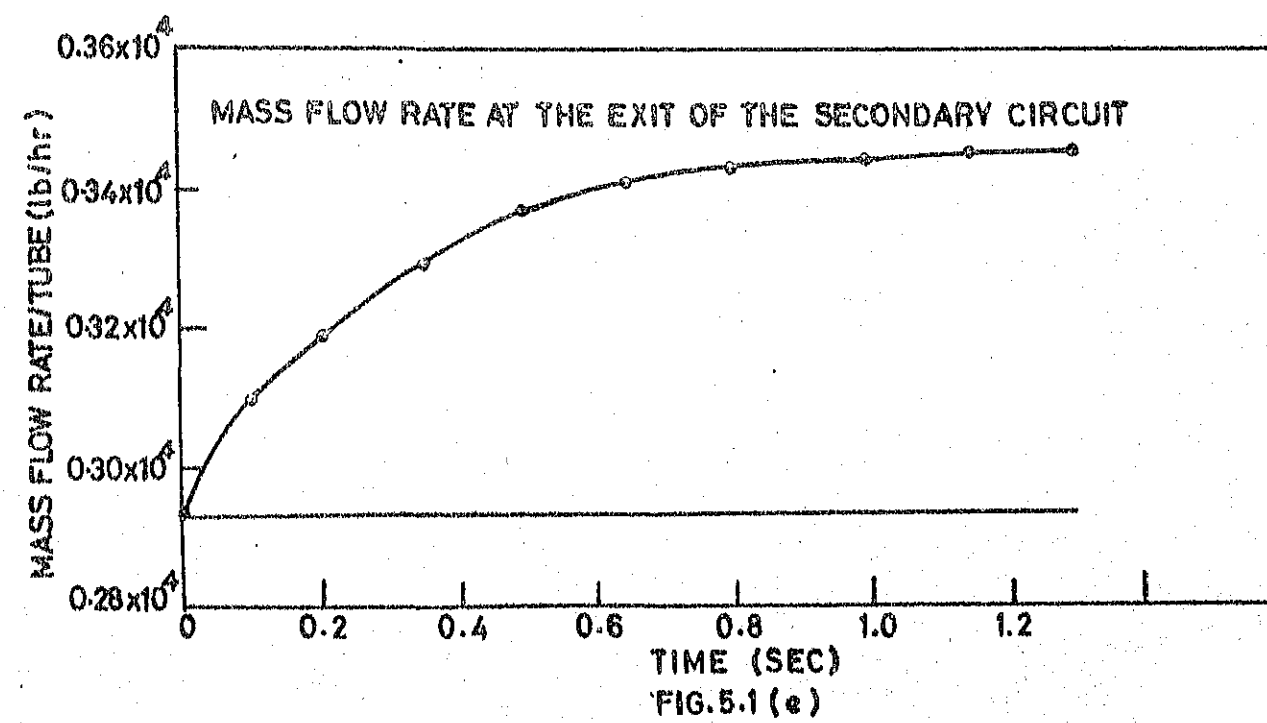
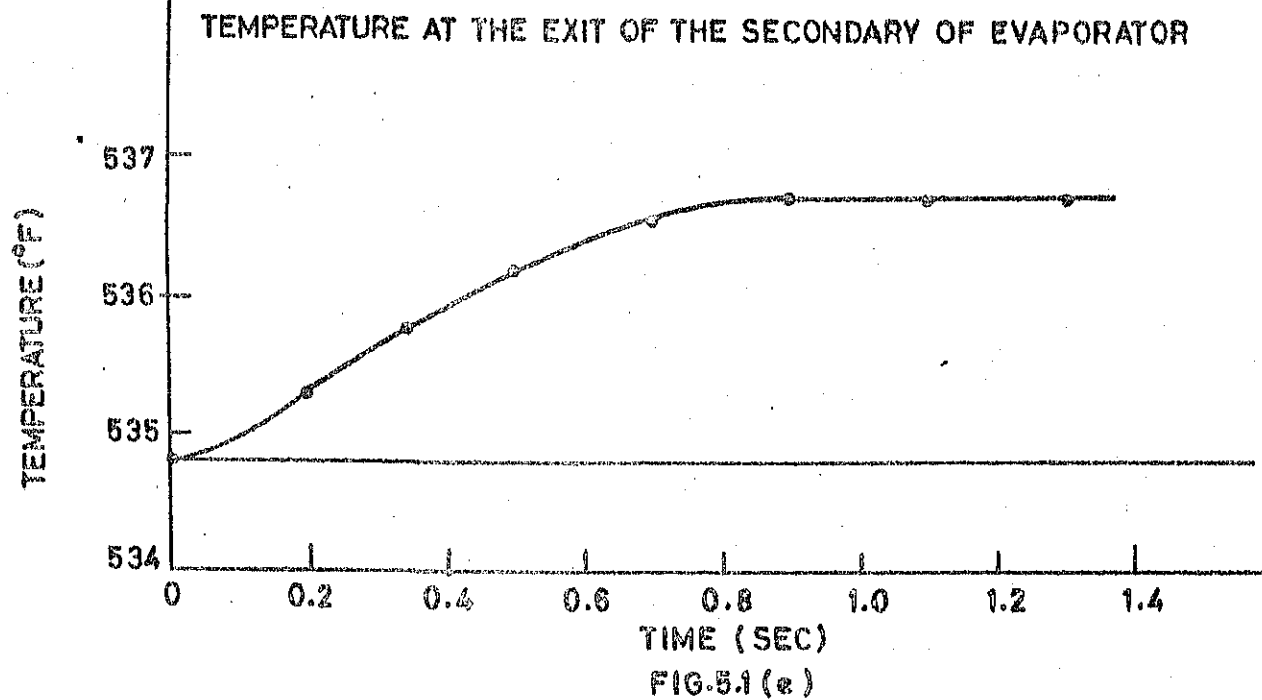


FIG.5.1(b)

INTERNAL ENERGY OF PRIMARY LIQUID WAS
INCREASED BY 5.0 % AT THE ENTRANCE OF THE
EVAPORATOR



INTERNAL ENERGY OF PRIMARY LIQUID WAS INCREASED
BY 5% AT THE INLET OF THE EVAPORATOR



INTERNAL ENERGY WAS INCREASED BY 5% AT THE
INLET OF THE PRIMARY CIRCUIT

QUALITY AT THE EXIT OF THE SECONDARY OF EVAPORATOR

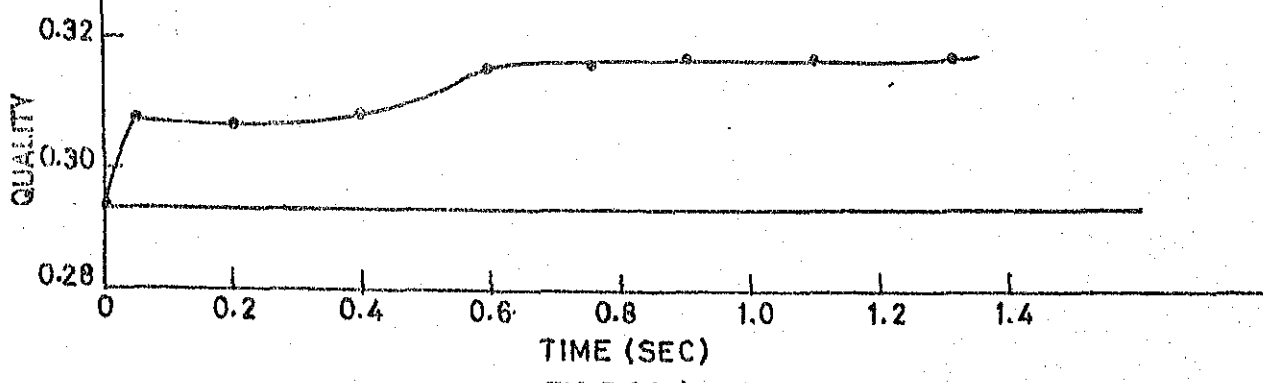


FIG.5.2 (a)

MASS FLOW RATE AT THE EXIT OF THE SECONDARY OF EVAPORATOR

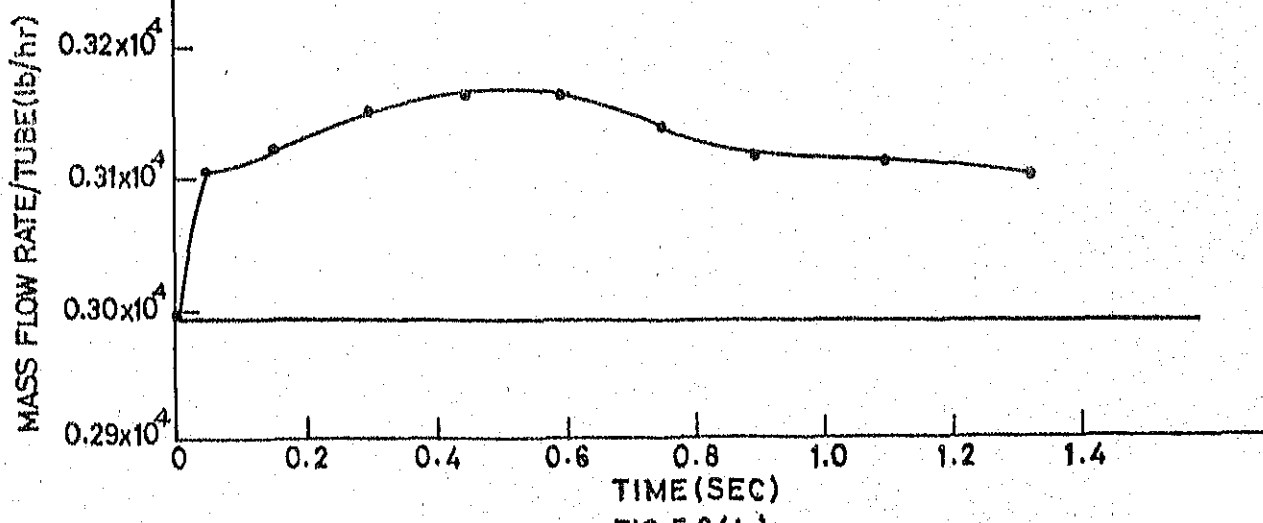
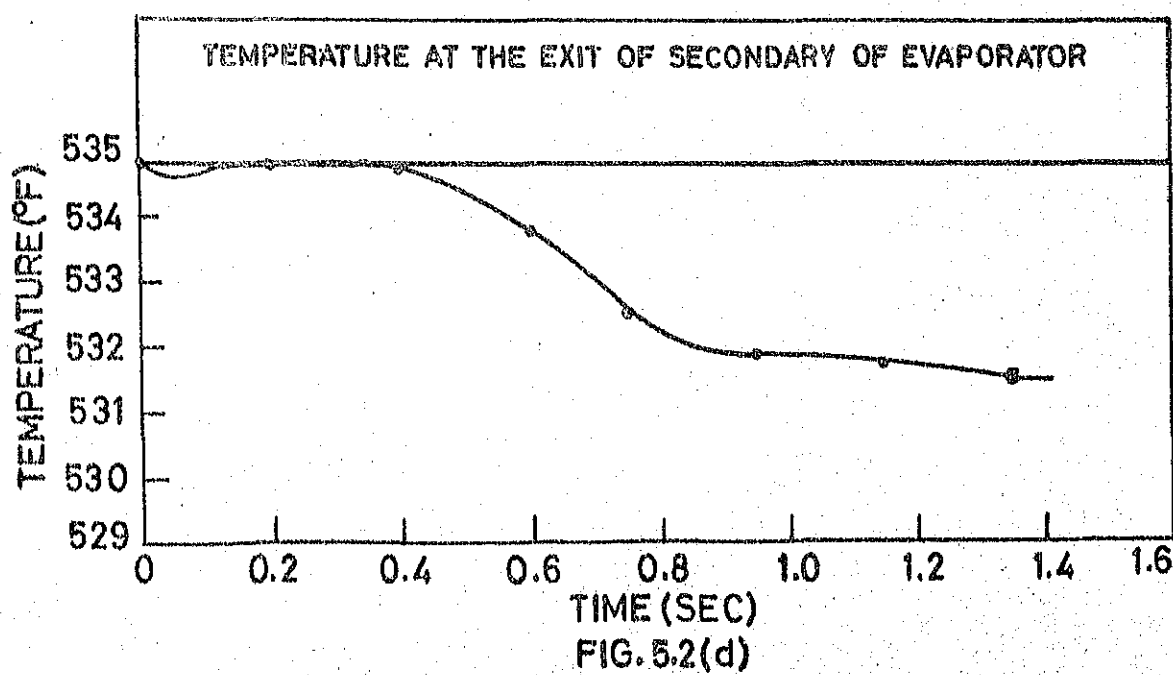
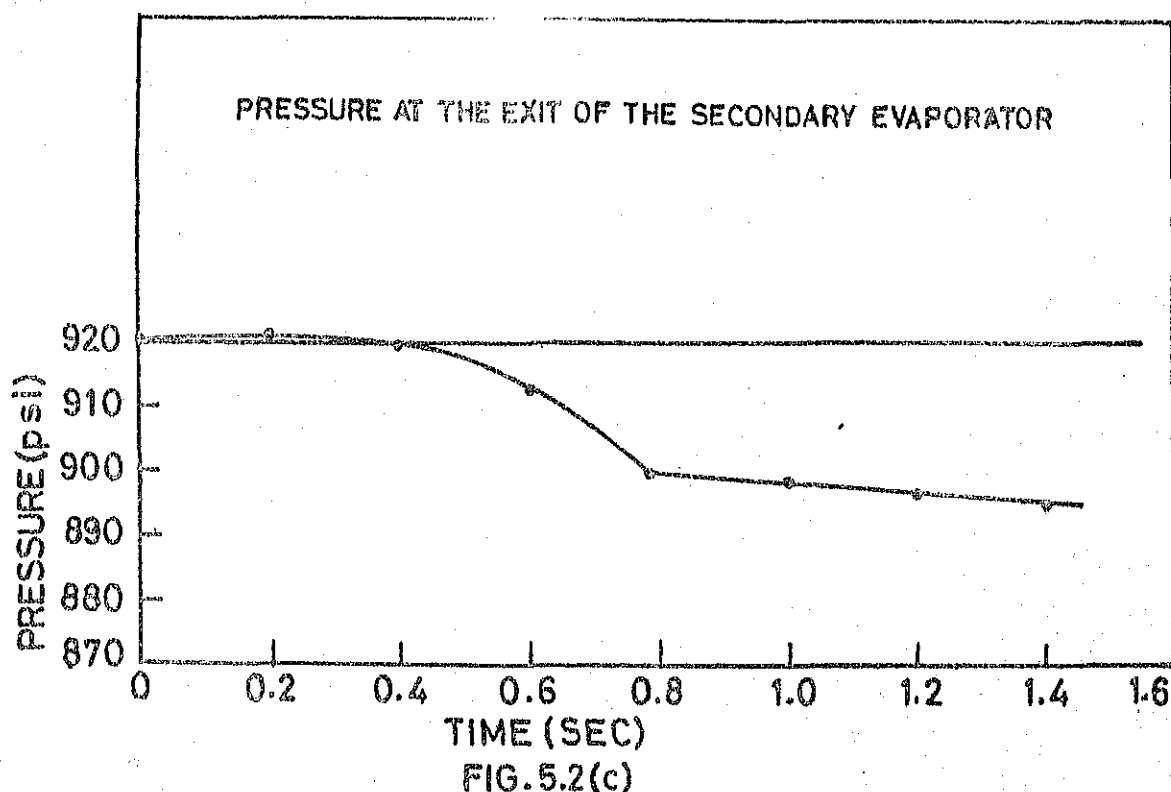


FIG.5.2 (b)

MASS FLOW RATE WAS INCREASED BY 5% AT THE
INLET OF THE PRIMARY CIRCUIT



MASS FLOW RATE AT THE INLET OF PRIMARY CIRCUIT
WAS INCREASED BY 5 %

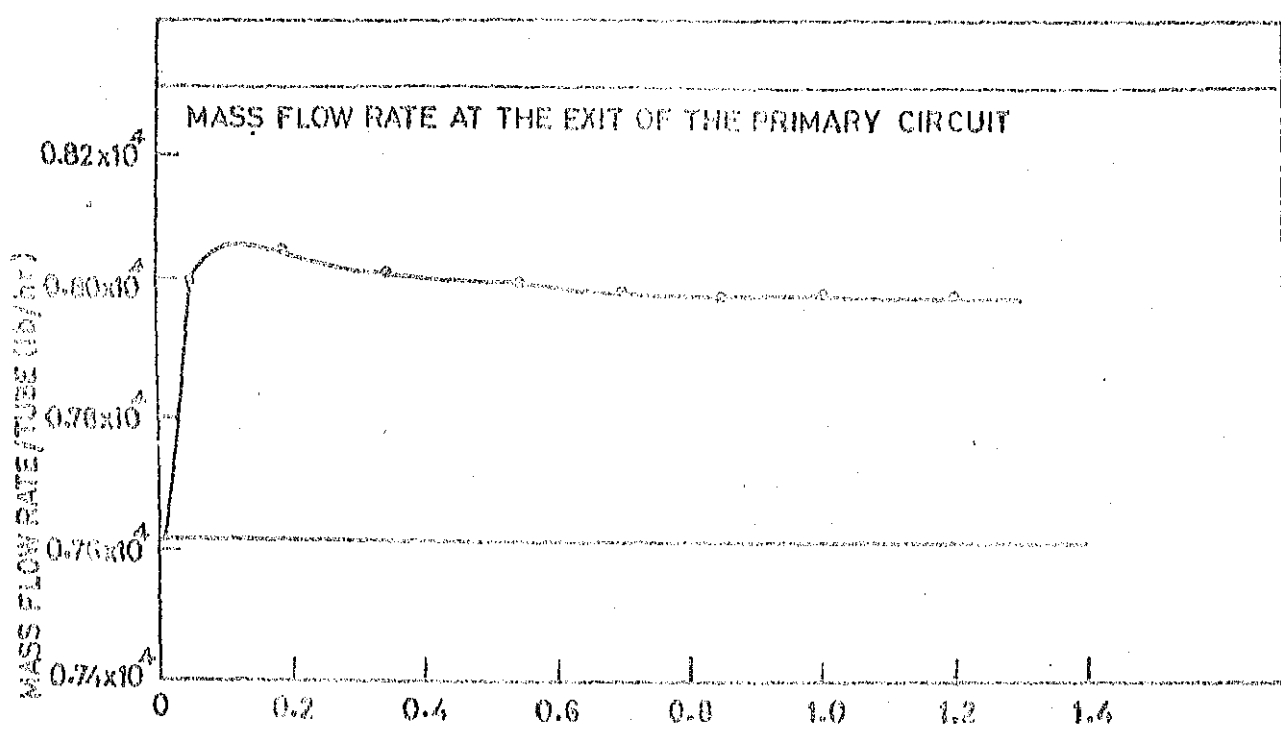


FIG.5.2 (e)

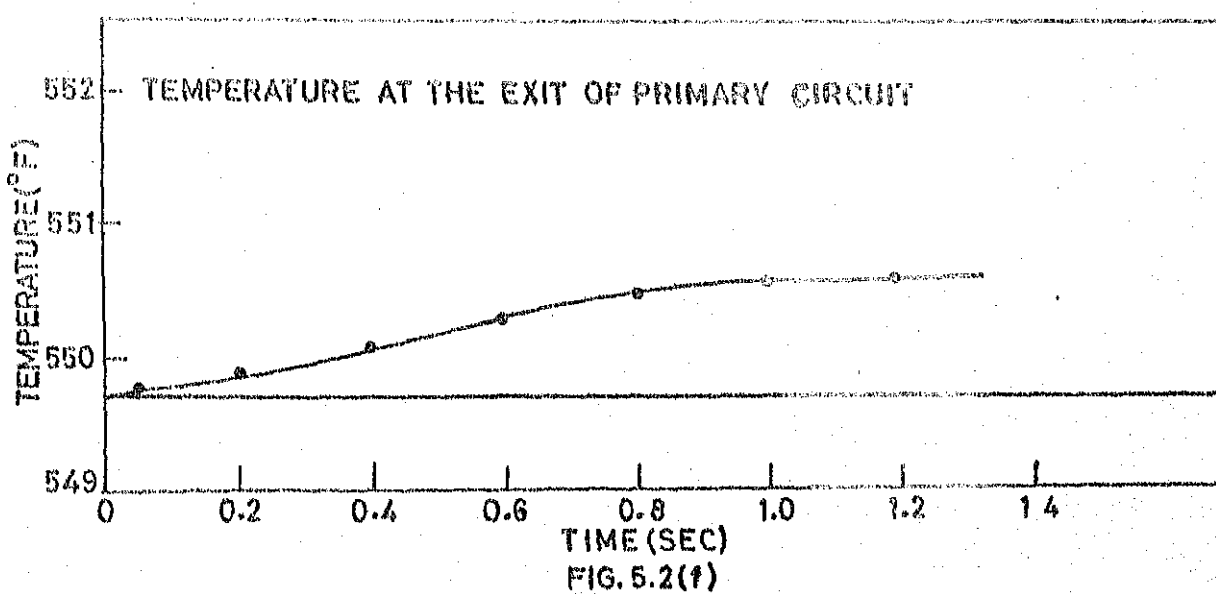
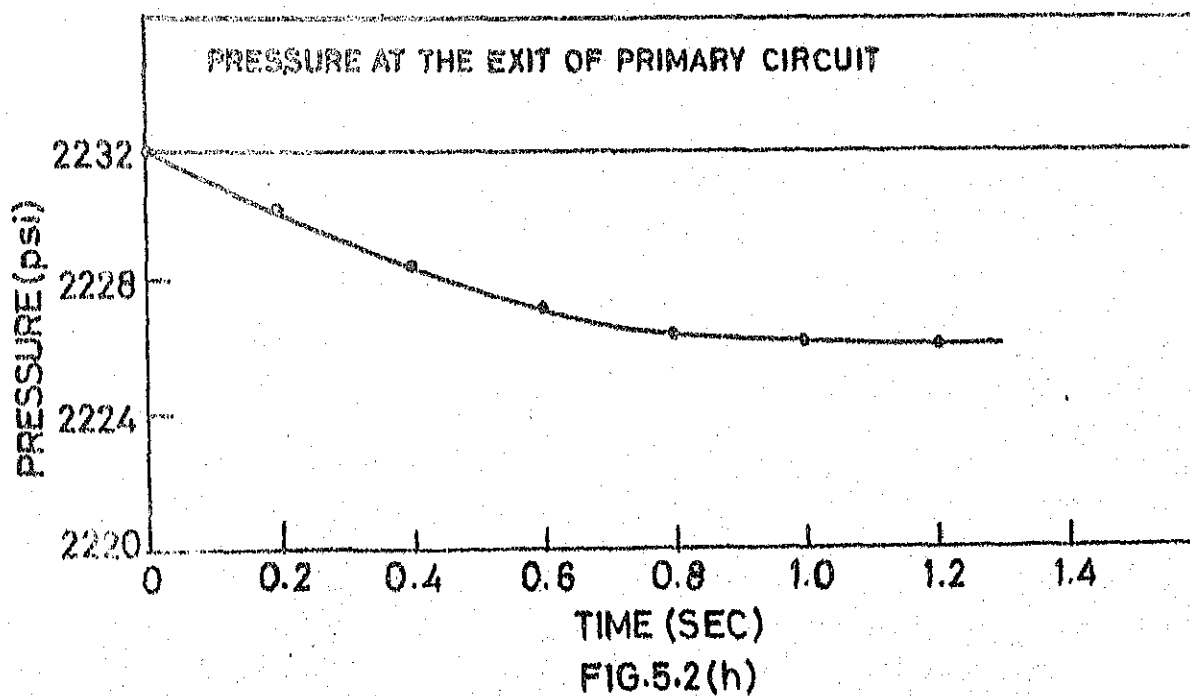
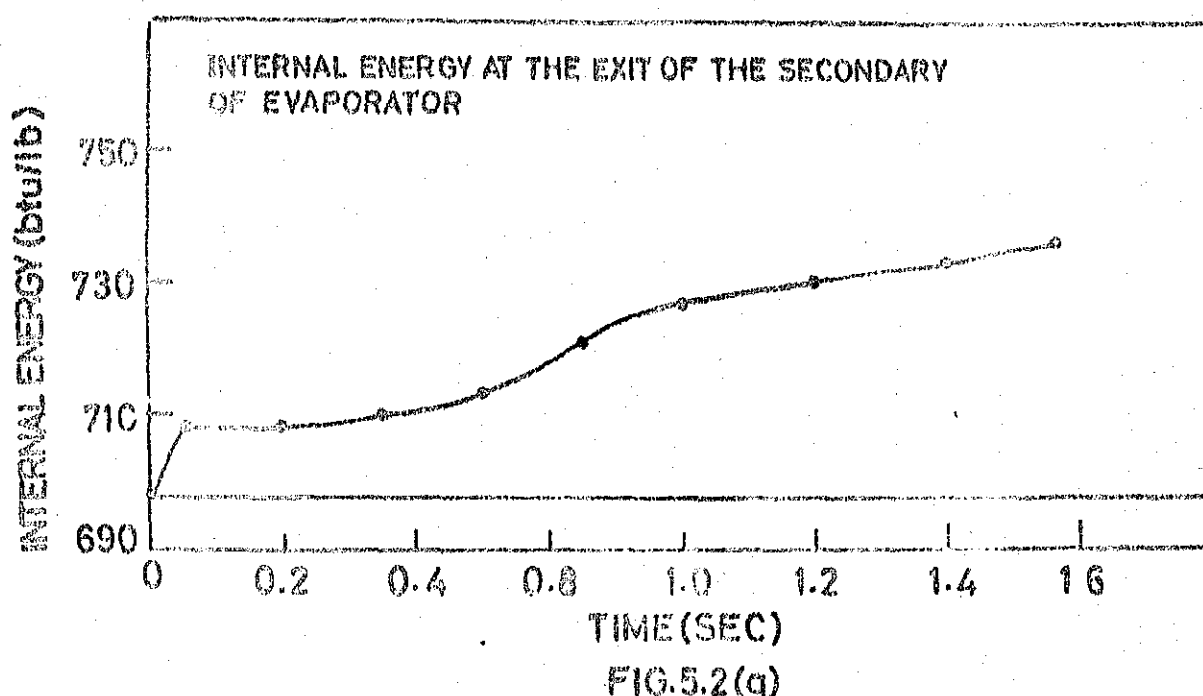
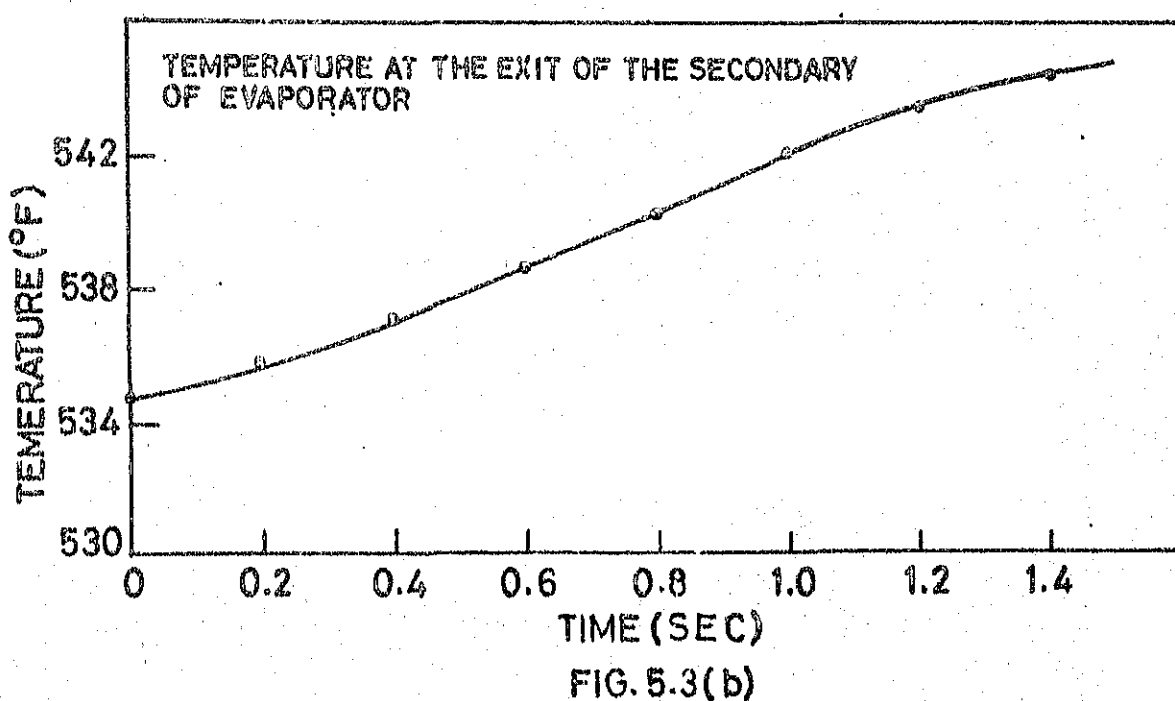
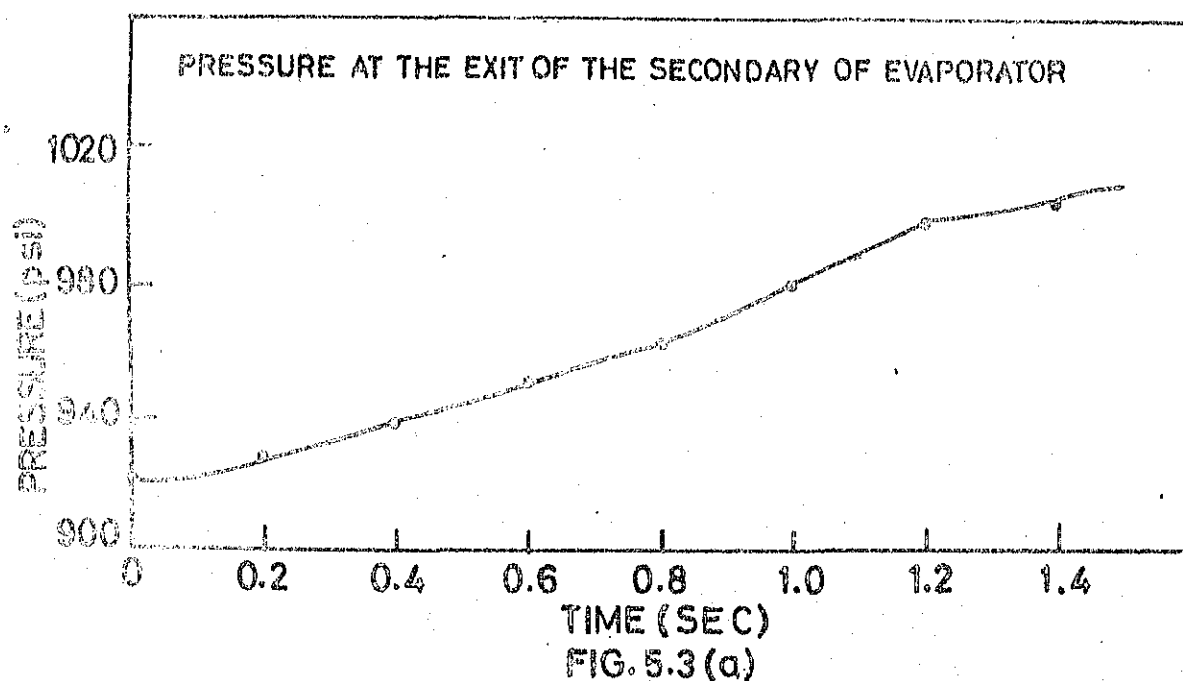


FIG.5.2(1)

MASS FLOW RATE WAS INCREASED BY 5% AT THE INLET
OF THE PRIMARY CIRCUIT



MASS FLOW RATE WAS INCREASED BY 5% AT THE INLET OF THE PRIMARY CIRCUIT



INTERNAL ENERGY WAS INCREASED BY 15 % AT THE
INLET OF THE SECONDARY CIRCUIT

QUALITY AT THE EXIT OF THE SECONDARY CH RADIATOR

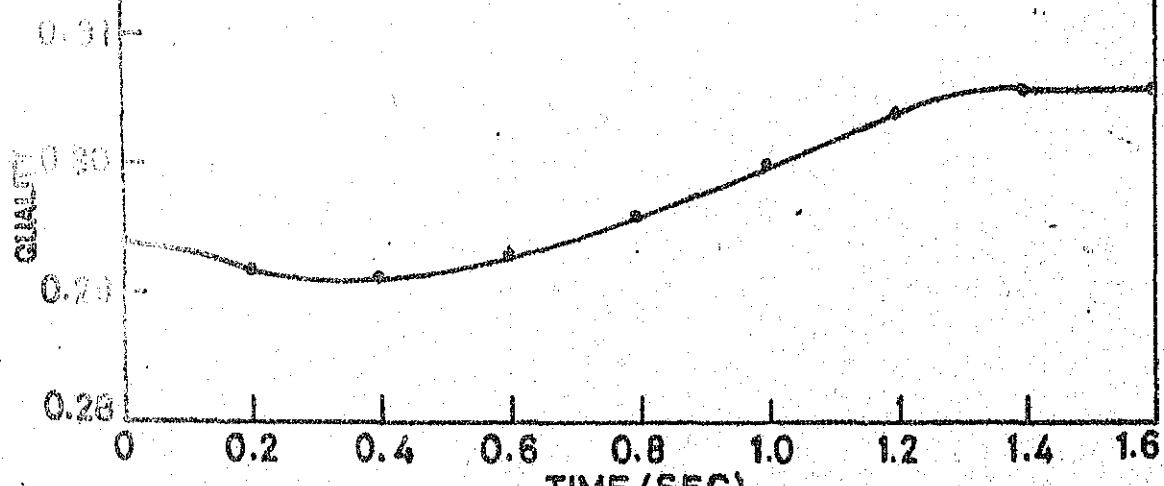


FIG.5.3(c)

INTERNAL ENERGY AT THE EXIT OF THE SECONDARY
OF EVAPORATOR

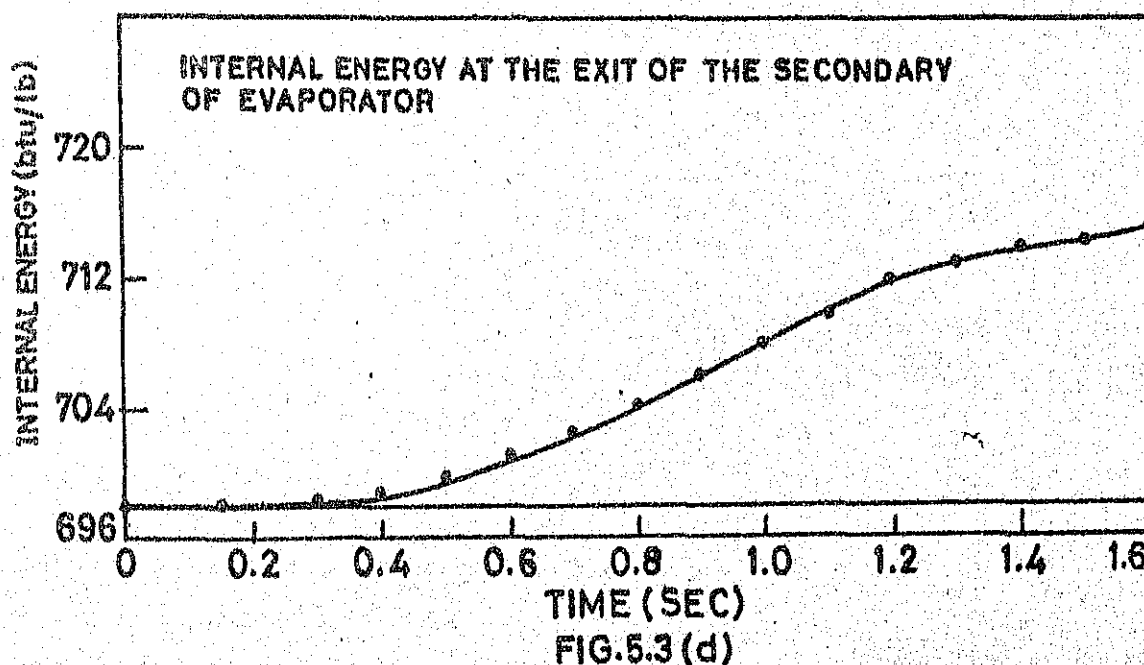
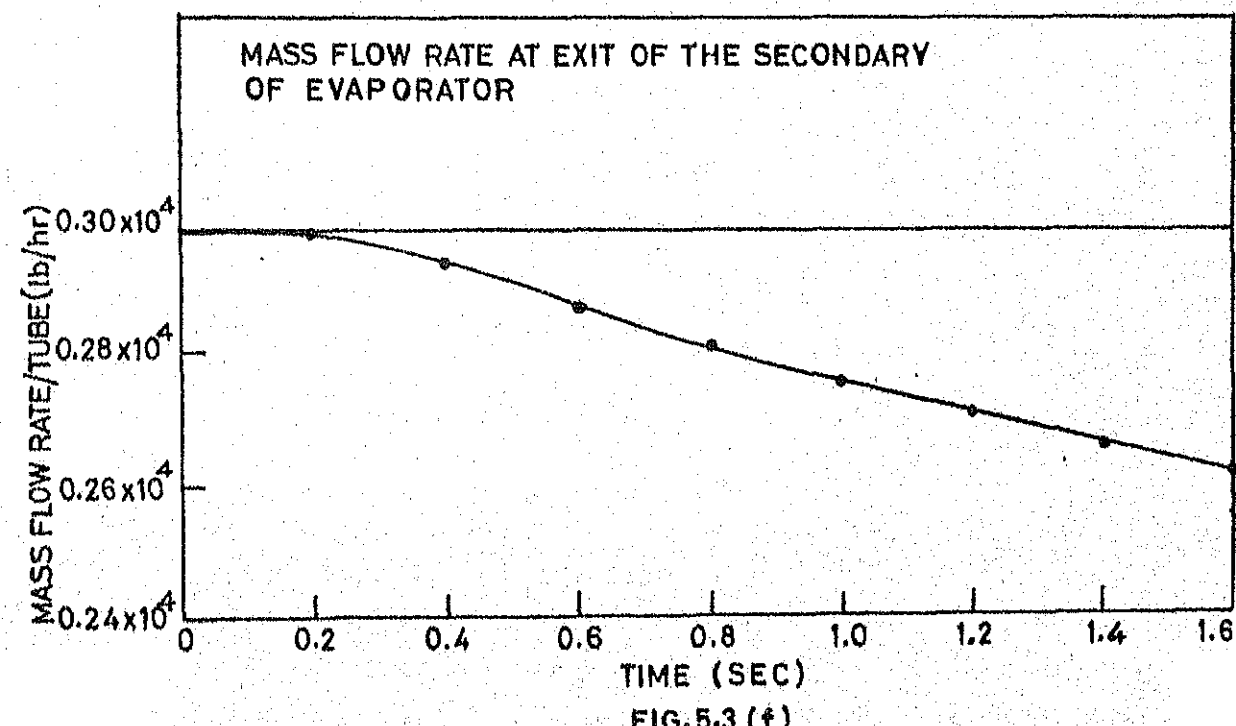
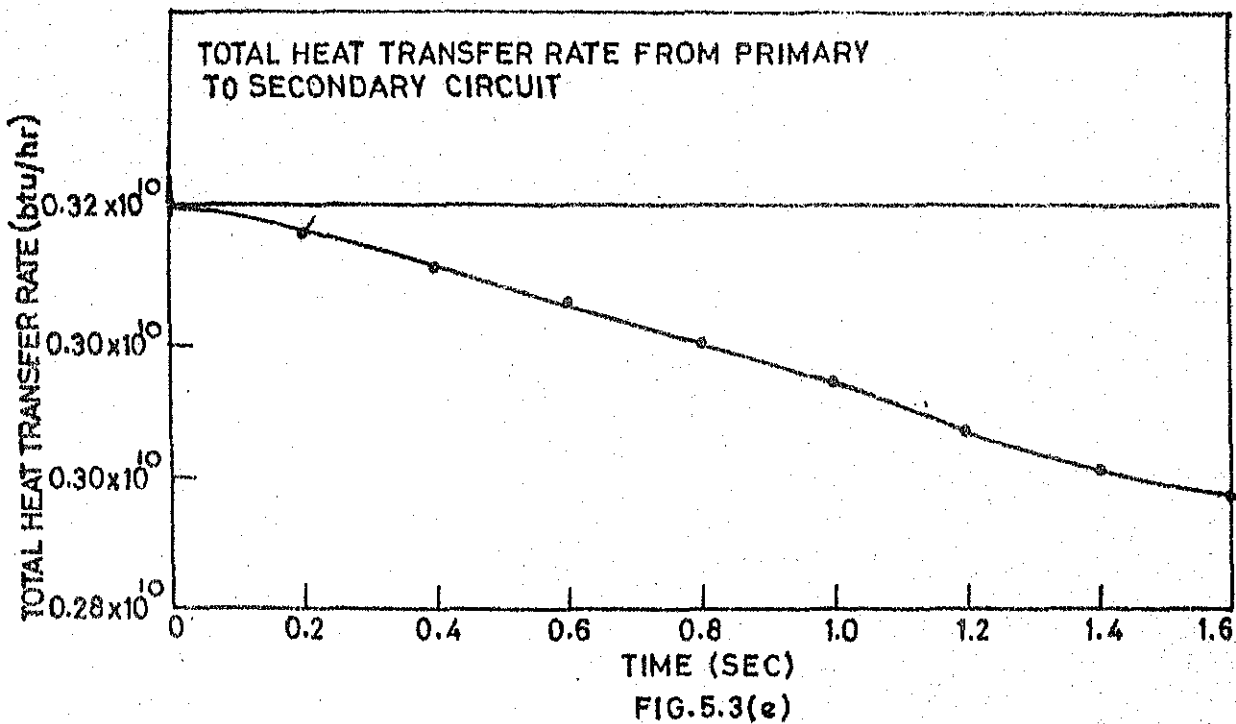
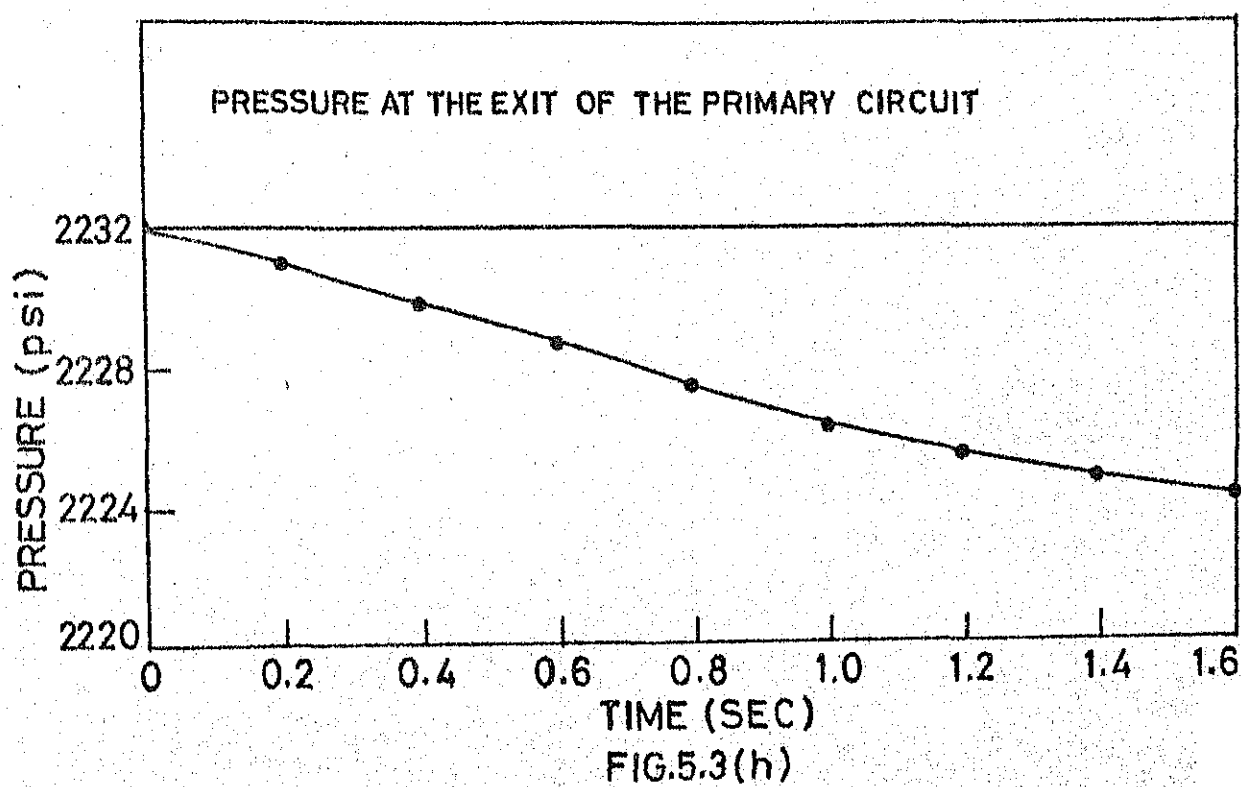
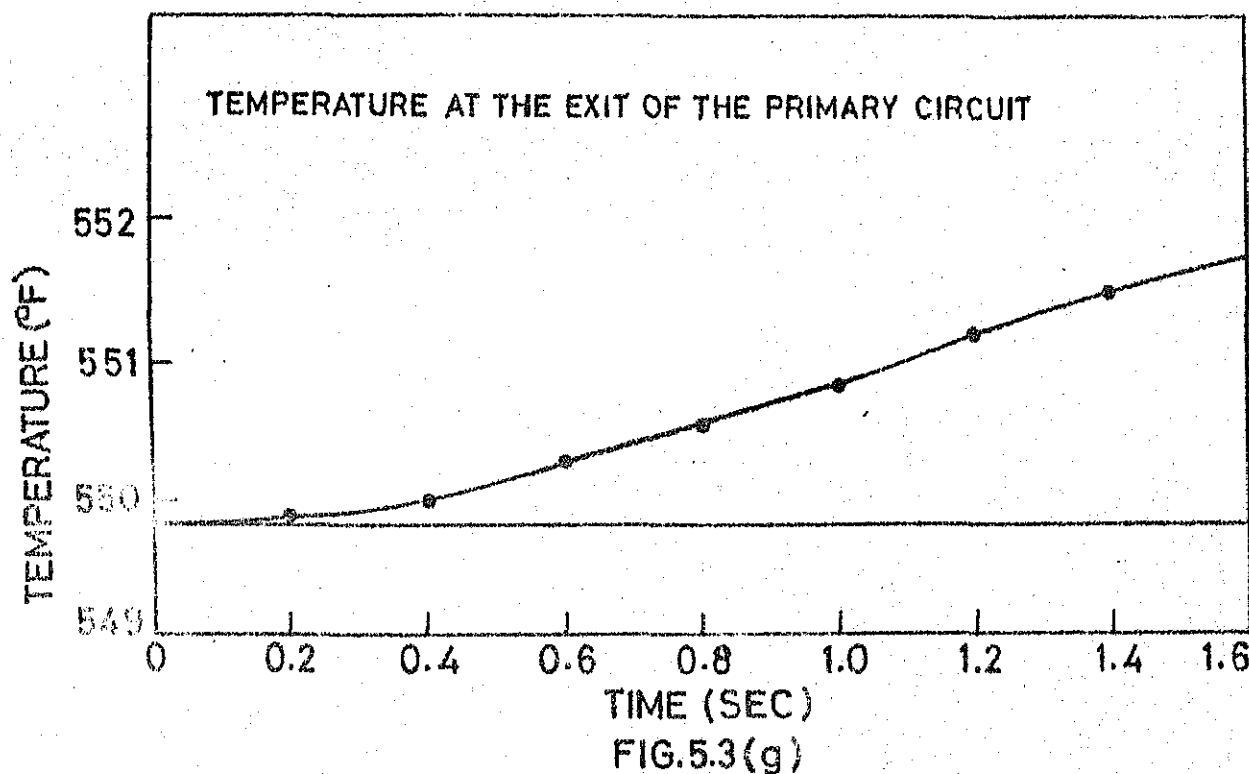


FIG.5.3(d)

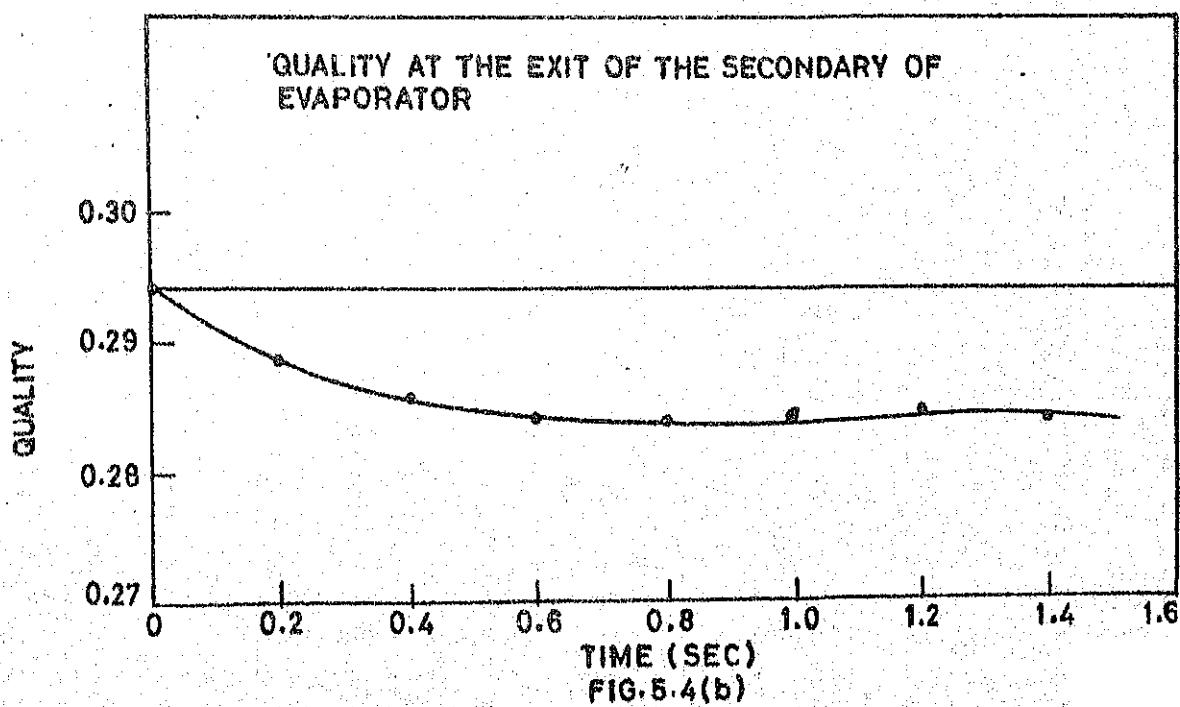
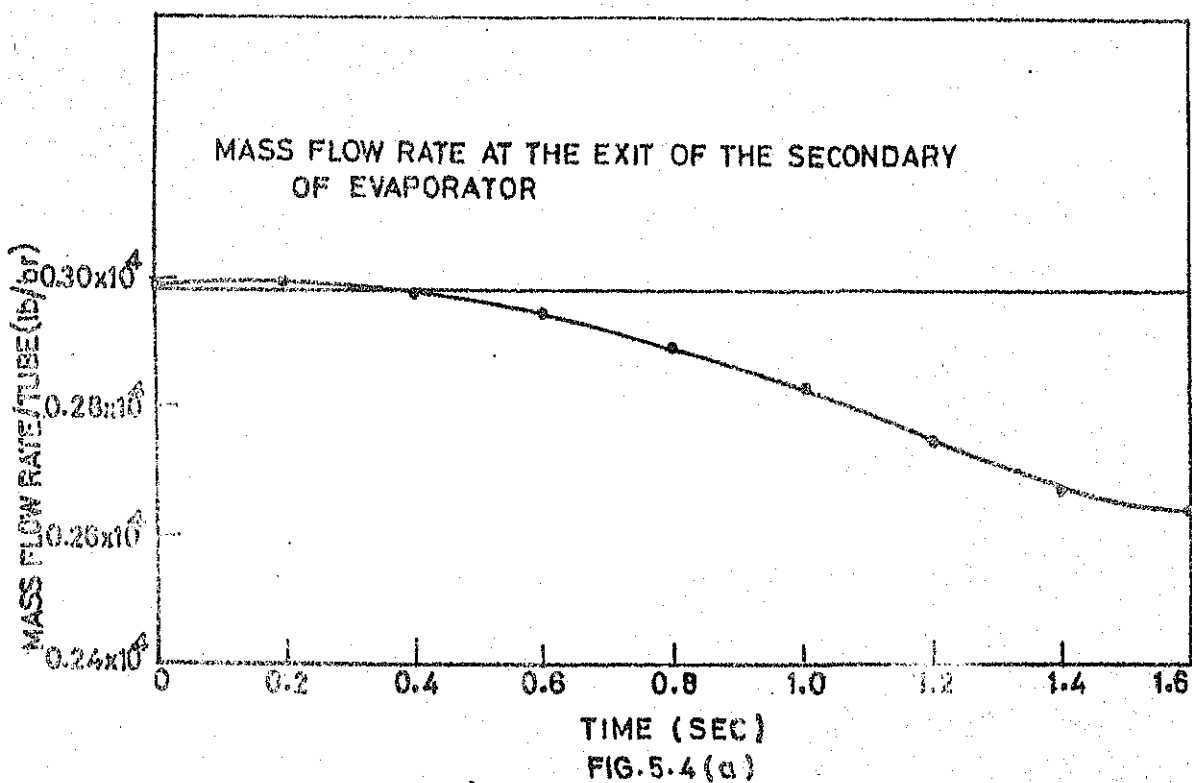
INTERNAL ENERGY AT THE INLET OF THE SECONDARY CIRCUIT
WAS INCREASED BY 15 %



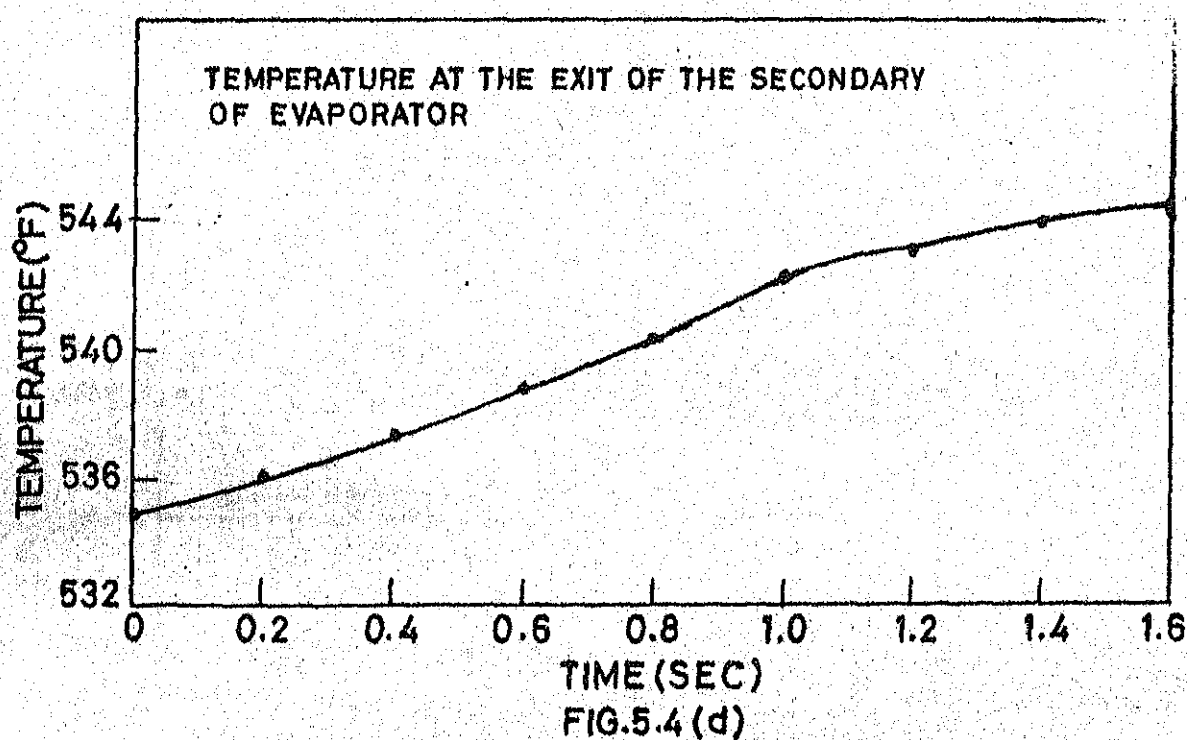
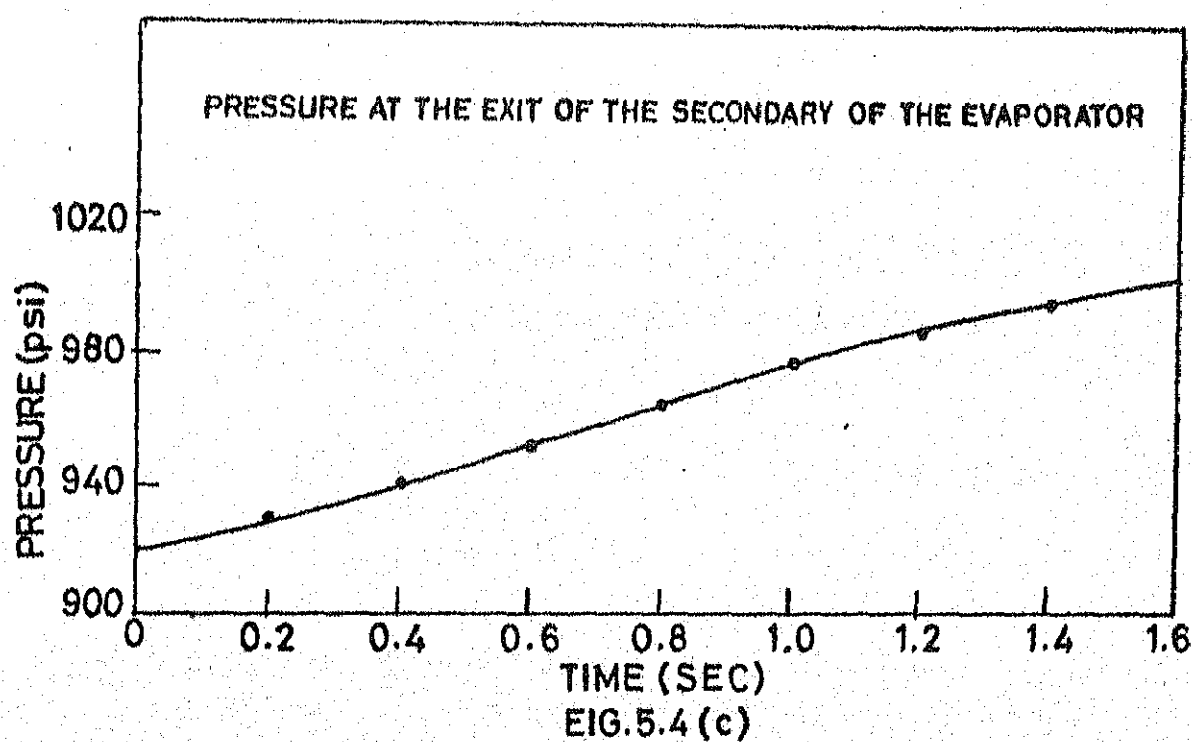
INTERNAL ENERGY WAS INCREASED BY 15% AT THE
INLET OF THE SECONDARY CIRCUIT



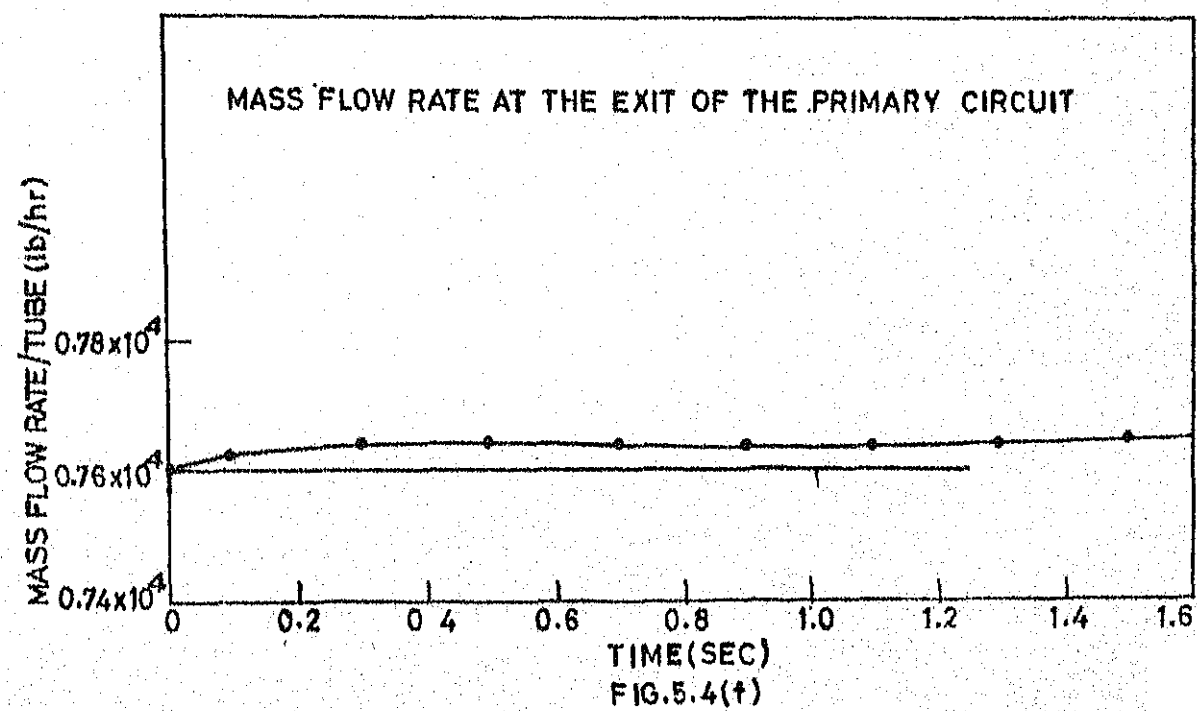
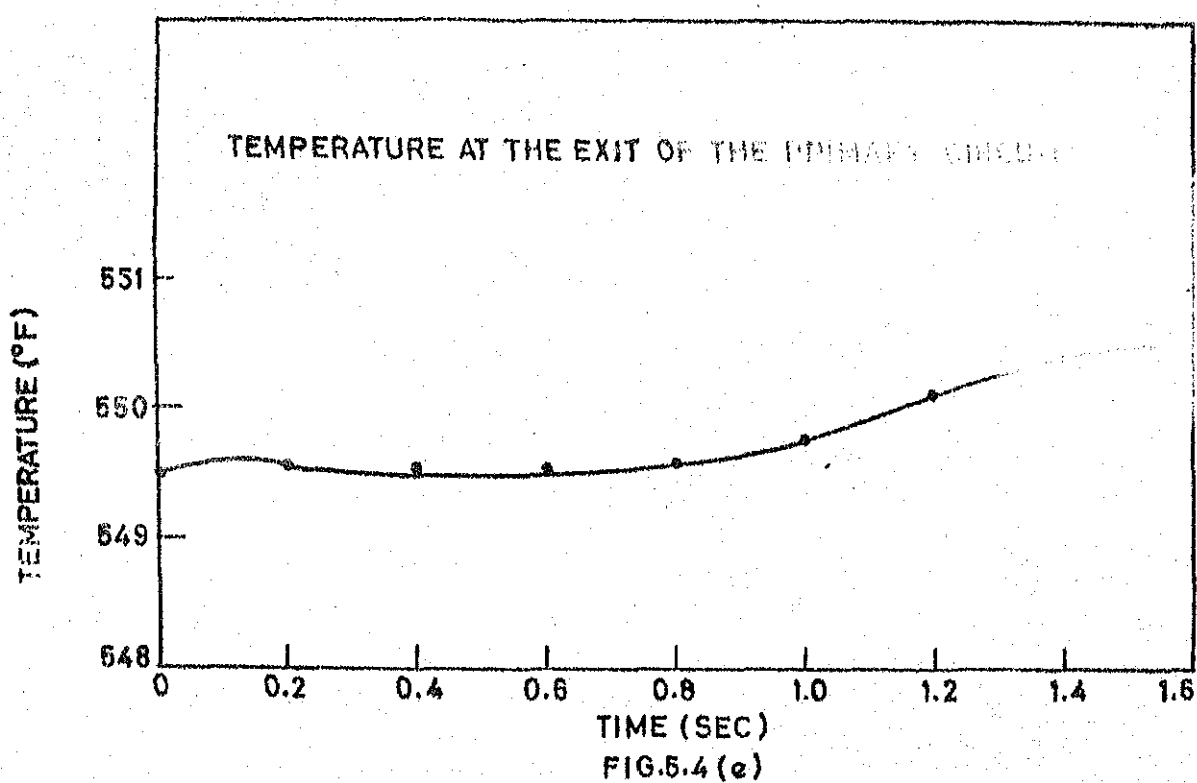
INTERNAL ENERGY WAS INCREASED BY 15% AT THE INLET
OF THE SECONDARY CIRCUIT



MASS FLOW RATE WAS INCREASED BY 20% AT THE INLET OF SECONDARY CIRCUIT



MASS FLOW RATE WAS INCREASED BY 20% AT THE INLET
OF THE SECONDARY CIRCUIT



MASS FLOW RATE WAS INCREASED BY 20% AT THE
INLET OF THE SECONDARY CIRCUIT

REFERENCES

1. Aravinda Kar, "Digital Simulation of Transients of the Steam Generator of Pressurized Water Nuclear Reactor", M.Tech. Thesis, Nuclear Engineering and Technology Programme, I.I.T., Kanpur, 1980.
2. RELAP4 - A computer code for transient thermal hydraulic Analysis, K.V. Moore and W.H. Rettig, USAEC Report, ANCR-1127 (1975).
3. FLASH - A computer code for PWR Thermal Hydraulic Analysis, J.A. Redfield and J.H. Murphy, Nucl. Appl. Technol, 6, 129 (1969).
4. D.C. Arwood and T.W. Kerlin, "A Mathematical Model for an Integral Economizer U-Tube Steam Generator", Nuclear Technology, 35, 12 (1977).
5. A. Hoeld, "A theoretical model for the calculation of large transients in nuclear natural-circulation U-tube steam generator (Digital code UTSG)", Nuclear Engineering and Design, 47, 1 (1978).
6. I.M.D. Silva, "Codigo para simulacão de transients tipo PWR", Tese de Mestrado, Instituto Militar de Engenharia, Rio de Janeiro, Brasil, 1979.
7. A. COSTA PINTO, K.S. RAM and R.K. NAIR, "A simplified model of steam generator for Digital Simulation", Annals of Nuclear Energy, Vol. 7, 381 (1980).

8. Armando Costa Pinto, "Codigo Para simulacão do gerador de vapor do reactor nuclear PWR", Tese de Mestrado, Instituto Militar de Engenharia, Rio de Janeiro, Brasil, 1978.
9. I.M.D. Silva, "Codigo para Simulacão de Transients em um gerador de vapor de Reactor Nuclear Tipo PWR", Tese de Mestrado, Instituto Militar de Engenharia, Brasil, 1979.
10. L.S. Tong, "Boiling Heat Transfer and Two-Phase Flow", John Wiley and Sons., Inc., N.Y., 1965.
11. L.S. Tong and J. Weisman, "Thermal Analysis of Pressurized Water Reactors", American Nuclear Society, NY, 1970.
12. T.A. Porschning, J.H. Murphy and J.A. Redfield, Nucl. Sci. and Eng., 43, 218 (1971).
13. J.H. Keenan and F.G. Keyes, "Thermodynamic Properties of Steam", John Wiley and Sons., Inc., NY, 1951.
14. A. Høld, "Linear Analytical One-Dimensional Model Describing the Frequency Response of Shell-And-Tube Type Counterflow Heat Exchangers with Respect to Primary and Secondary Inlet Temperature and Mass Flow Perturbations", Nuclear Engineering and Design 26 (1974), pp. 231-241.

A SIMPLIFIED MODEL OF STEAM GENERATORS FOR DIGITAL SIMULATION

A. COSTA PINTO, K. S. RAM* and R. K. NAIR

Instituto Militar de Engenharia, Rio de Janeiro, Brazil

(Received 23 August 1979; received for publication 14 November 1979)

Abstract—This paper develops a simplified model of a PWR steam generator. A computer programme for the steady state operation was developed, which will be useful for the dynamic analysis for describing accident situations. The model incorporates all the various flow regimes and heat transfer regimes that are likely to be encountered by the secondary flow of the steam generator. The primary flow is considered as single phase compressed liquid. Given the heat transfer area, pitch and the size of the tubes the computer programme matches the total power generated within five percent accuracy. Detailed pressure and temperature distributions along the length of the preheater and evaporator are also computed.

INTRODUCTION

With the present interest in the safety studies of nuclear reactor behaviour, it becomes important to simulate the behaviour of various reactor components. Steam generator forms one of the important components of a reactor system where heat is exchanged between the primary coolant of the reactor and the secondary stream of the working fluid for generating power. In the literature there are no simplified models available for simulating the steam generators excepting the complicated models of the reactor thermal hydraulic computer codes such as RELAP-4 (Moore and Rettig, 1975) and FLASH (Redfield and Murphy, 1969), etc. Recently few mathematical models were developed by Arwood and Kerlin (1977) and Höld (1978) to simulate the U-tube steam generator. However, these papers use linearized equations to predict the behaviour around a steady state operating point. In reference Arwood and Kerlin (1977) the detailed heat transfer regimes are also not considered explicitly. The present paper deals with a simplified model of the steam generator taking into account the various heat transfer regimes and the respective correlations into account. A computer programme was developed to analyse a typical steam generator utilized in a 600 MW(e) PWR reactor.

MODEL OF THE STEAM GENERATOR

The steam generator model used in the present study is shown in Fig. 1. The steam generator is repre-

sented in two sections, preheater (economizer) and an evaporator. In reality the steam generators of the PWR reactors have U-tube geometry, the present model simplifies it to parallel tube geometry but retains all the significant factors such as the total heat transfer area, total amount of heat transferred, pre-heater. Lack of detailed data about the internals of the steam generator, such as the pressure drop due to baffles, quality of steam at the outlet of the generator before the steam separators, etc. is circumvented by the pressure balance and heat balance equations as described in the later sections.

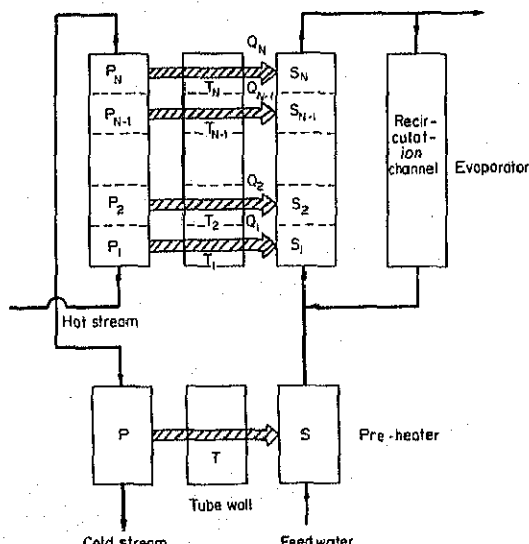


Fig. 1. Simulation model of steam generator.

* On leave of absence from: Indian Institute of Technology, Kanpur, India.

Table 1

Mode	Flow regime	Heat transfer regime	Heat transfer correlation	Reference
1. Single phase compressed liquid	Pure convection		$Nu = 0.023 Re^{0.8} Pr^{0.4}$	Dittus and Boelter (1930)
2. Single phase compressed liquid	Local boiling	$T_p \sim T_{sat} = \frac{0.072 (\dot{q})^{1/2}}{\exp(p/1260)}$		Tong and Weisman (1970)
3. Bubbly flow	Nucleate boiling			
4. Annular flow	Evaporation by forced convection		$h = S(0.00122) A + F(0.023) Re_t^{0.8} Pr_t^{0.4} \frac{K_t}{D_e}$ $A = \frac{K_t^{0.79} e_t^{0.45} \rho_t^{0.49} g_e^{0.25} \Delta T^{0.24} \Delta p^{0.75}}{\sigma^{0.5} \mu_t^{0.29} H_{fg} \rho_v^{0.20}}$	Chen (1963) <i>F and S obtained from Chen (1963)</i>
5. Annular flow	Stable film boiling	$\frac{hD_e}{K_{film}} = 0.0136 \left(Re_{film} \frac{1-x}{x} \right)^{0.853} \frac{\alpha}{1-\alpha} Pr_{film}$		Polomik <i>et al.</i> (1964)

As indicated in the figure the coolant from the reactor outlet enters the primary side of the generator as a hot stream in the evaporator section and leaves the generator from the preheater section as a cold stream to enter the reactor. The heat flow from the primary side is conducted through the tube walls of the steam generator and enters the secondary stream. The figure also indicates that the liquid in the secondary stream leaving the evaporator section of the generator along with the vapour is recirculated. The feedwater enters the preheater section and mixes with the secondary stream after the preheater.

The liquid in the primary side of the stream generator is assumed to be in the form of compressed liquid transferring heat by pure convection process. On the secondary side however the liquid enters the generator as near saturated liquid with or without local boiling. It is envisaged that the secondary liquid will encounter bubbly flow and annular flow regimes and the heat transfer regimes will be pure convection, local boiling. The various flow regimes and the heat transfer modes and the correlations used in each mode are indicated in Table 1. The logic used to determine the regime of heat transfer is shown in Fig. 2.

The computer programme developed calculates the equivalent lengths of preheater and evaporator, pressure and temperature variations along the length in both the primary and secondary loops and also the exit quality of steam and its variation on the secondary side of the steam generator. The programme requires the following input information: geometrical characteristics of the steam generator such as the pitch, the total heat transfer area, etc., the thermodynamic properties of the primary liquid entering the steam generator, the total heat received by the

primary liquid in the reactor (or indirectly the output power of the nuclear plant) and the desired vapour output and pressure.

ANALYTICAL MODEL

In the analysis it is assumed that the flow is vertical. There is no transfer of work across each control volumes indicated in Fig. 1. Further the area of flow cross section is assumed to be constant. Each control volume is bounded by two junctions, one at the inlet and the other at the outlet connecting the subsequent control volume. Thus the conservation equation of mass, momentum, energy given below representing steady state are solved for each control volume:

Mass:

$$A \frac{\partial \rho}{\partial t} = - \frac{\partial w}{\partial z} = 0,$$

Momentum:

$$A \frac{\partial(\rho V)}{\partial t} = A \frac{\partial p}{\partial z} - \frac{\partial F_k}{\partial z} - A \rho g - \frac{\partial}{\partial z} (WV) = 0,$$

Energy:

$$A \frac{\partial}{\partial t} (\rho e) = \dot{q} \frac{\partial A_T}{\partial z}, \quad \frac{\partial W_a}{\partial z} - \frac{\partial}{\partial z} (pAV) = 0,$$

where \dot{q} is the heat flux, $W = \rho AV$ is the mass flow rate, $e = u + V^2/2 + gz$ is the energy per unit mass of the fluid and F_k is the frictional force. A and A_T represent the flow cross sectional area and the heat transfer area, respectively. The above equations are cast in the form of volume average quantities and

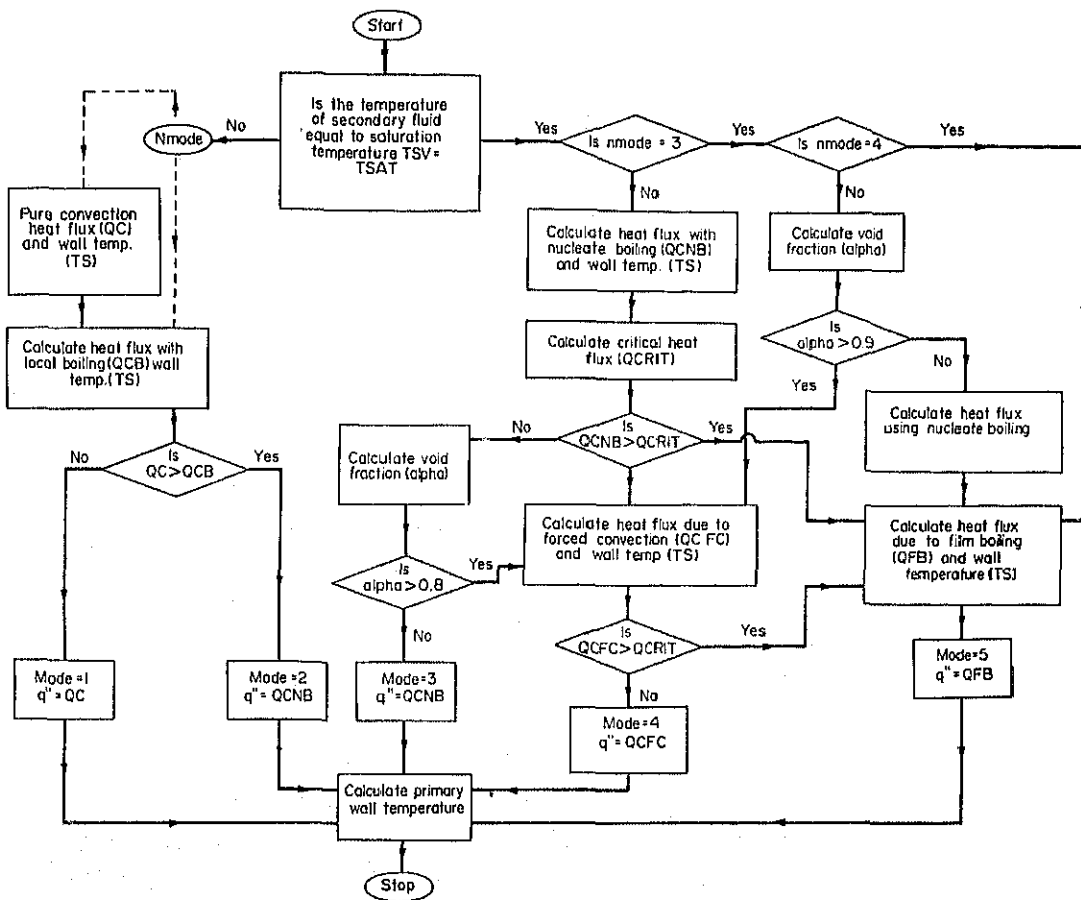


Fig. 2. Logic to determine the region of heat transfer.

the values at the junction by integrating between the functions and defining the volume averages as the arithmetic means of the function values.

The various flow regimes and the respective heat transfer correlations are indicated in Table 1. The pressure drop calculation required in the momentum equation are divided into three categories of friction, acceleration and elevation. In reality there are baffles placed in the flow of the secondary fluid and thus increases the pressure drop due to friction. However, since the details were not available, it is proposed to use the pressure drop due to friction in the control volume n , Δp_n , in the form

$$\Delta p_n = (\bar{f} + \bar{K}) \frac{G^2 v_n}{2g_e} \cdot \frac{\Delta z}{D_e}, \quad (2)$$

where f_n is the friction factor and K is a form factor to account for baffles, change of cross sectional flow

area, etc., ΔZ is the height of the control volume and D_e is the hydraulic diameter. The above equation is valid only for single phase flow. Since the secondary fluid will encounter two phases, this equation has to be corrected. In this work empirical correlation of Baroczy (1966) was used to account for the two-phase flow. The work of Baroczy is considered to be continuation of Martinelli and Nelson. The empirical factor ϕ^2 defined as,

$$\phi^2 = \frac{(\Delta p / \Delta L) \text{ two phases}}{(\Delta p / \Delta L) \text{ single phase}}, \quad (3)$$

was obtained by polynomial curve fitting to the graphs around a mass flux of $10^6 \text{ lb/ft}^2 \text{ h}$ ($4.89 \times 10^6 \text{ kg/m}^2 \text{ h}$). Thus the friction factor in equation (2) will be modified as,

$$(\bar{f}_n) \text{ two phase} = \phi^2(\bar{f}) \text{ single phase.} \quad (4)$$

The pressure drop due to acceleration was considered by the following equation,

$$\Delta P_{\text{acc}} = \frac{G^2}{g_c} (\bar{V}_{n+1} - \bar{V}_n). \quad (5)$$

This pressure drop is experienced in going from control volumes $n - 1$ to junction n . The above equation is applicable for the single phase flow. However, in two-phase flow slip ratio comes into play. Normally the correction factors are dependent on the quality x and void fraction α . For annular flow the correction factor r is computed as

$$r = \left[\frac{(1-x)^2}{(1-\alpha)} + \frac{x^2}{\alpha} \left(\frac{\rho_l}{\rho_v} \right) \right] / \left[(1-x) + X \left(\frac{\rho_l}{\rho_v} \right) \right]. \quad (6)$$

The above equation (5) is modified as

$$\Delta p_{\text{acc}} = \frac{G^2}{g_c} (r_{n+1} \bar{v}_{n+1} - r_n \bar{v}_n). \quad (7)$$

The void fractions are calculated in the case of evaporation by forced convection and annular flow using Thom's (10) correlation,

$$\alpha = \frac{\gamma x}{1 + X(\gamma - 1)}, \quad (8)$$

where γ is an empirical constant tabulated as a function of pressure. Similarly in the case of stable film boiling and annular flow Polomik *et al.*'s (1964) correlation is used:

$$\frac{1}{\alpha} = 1 + \left(\frac{1-x}{x} \right) \left(\frac{\rho_v}{\rho_l} \right)^{2/3}. \quad (9)$$

The elevation pressure drop is simply calculated at each junction as

$$\Delta P_{\text{elevation}} = \rho_n g \Delta z. \quad (10)$$

Conduction across the primary tube is calculated using the following equation,

$$\dot{q} = K \frac{(T_{pi} - T_{pe})}{r_e \ln(r_e/r_i)}$$

where subscripts i and e stand for internal and external while pi and pe stand for primary inlet and exit conditions. K_p is the thermal conductivity of the wall material.

METHOD OF COMPUTATION

Essentially the computer code used in this model solves the three basic conservation equations of mass,

momentum and energy in each volume of the primary and the secondary side. Conservation of mass can be written as $W = \text{constant}$. The conservation of energy equation can be rewritten as

$$H_{n+1} = H_n + \frac{Q_n}{W} - \frac{G^2}{2g'_c J} (V_{n+1}^2 - V_n^2) \\ - \frac{g \cdot 1}{g'_c J} \cdot \Delta z,$$

where \bar{Q}_n is the average amount of heat transferred in control volume n , whose boundaries are described by the junctions n and $n + 1$. Also, $H = U + p/\rho$ and $G = W/A$ relationships are utilized in the above equation.

Similarly the momentum equation can be simplified assuming that in each control volume an average value of friction, based on the average flow properties, can be calculated. The average liquid properties in each control volume are assumed to be the same at the interface junction of the subsequent control volume. Based on these assumptions the momentum equation can be written as

$$\bar{P}_n = \bar{P}_{n-1} - \frac{1}{2A} (\bar{F}_{k,n-1} + \bar{F}_{k,n}) \\ - \frac{G}{144g'_c} (V_n - \bar{V}_{n-1}) - \frac{g}{144g'_c} (\bar{V}_n - V_n) \\ - \frac{g}{144g'_c} \frac{\Delta z}{v_n}.$$

The above equation can be rewritten in terms of pressure drops due to friction, acceleration and elevation as,

$$\bar{P}_n = \bar{P}_{n-1} - \frac{1}{2} [(\bar{\Delta P})_{n-1} - (\bar{\Delta p})_n]_{\text{friction}} \\ - [(\bar{\Delta p})_{n-1} - (\bar{\Delta p})_n]_{\text{acceleration}} \\ - \bar{\Delta p}_{\text{elevation}}.$$

The overscores indicate average values and those that do not have an overscore indicate the junction values.

With the known primary inlet conditions and an initial guess at the quality at the outlet of the evaporator the recirculation rate and an approximate linear pressure profile is established. With these one can march in the forward direction to determine the secondary outlet conditions. If the secondary outlet conditions do not match the operating conditions furnished, the quality is adjusted and calculations repeated until the specified number of iterations are exceeded or the total heat transfer and the secondary outlet conditions converge within desired limits.

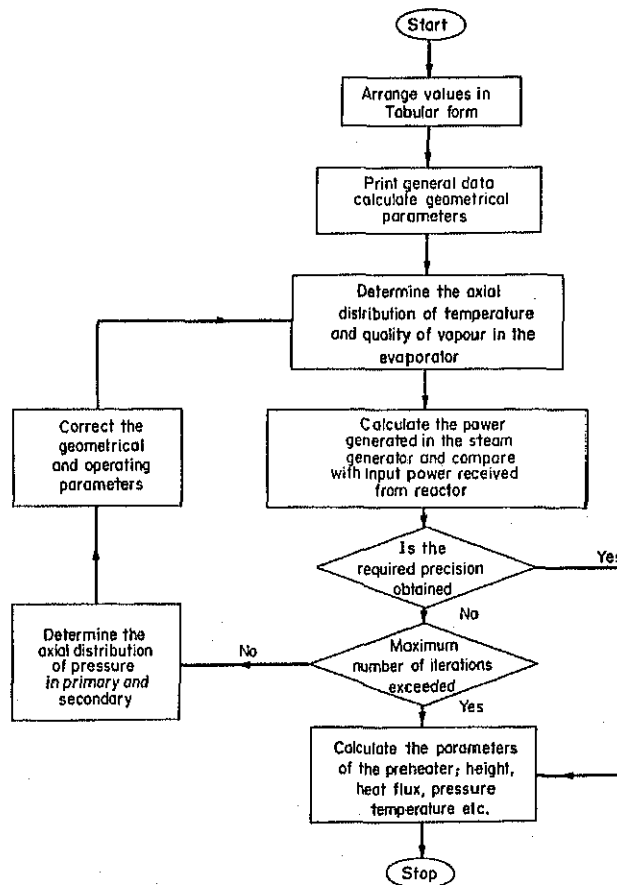


Fig. 3. Flow chart of the computer programme simulating the steam generator.

The major problem in evolving a computer programme is to have the thermodynamic properties of water and steam in the various regimes that are likely to be encountered in the programme. The present programme contains various subroutines in the form of polynomials obtained by least square fit to the tabulated properties. Similarly some of the two phase pressure drop calculations which were available in graphical form were also written as subroutines in the form of polynomials obtained by curve fitting. The flow chart of the computer programme is given in Fig. 3.

The computer programme needs the initial values for computation details of which are given below. The evaporator height is taken as a fraction of the total generator height

$$L_{ev} = K \frac{\text{area of heat transfer}}{\text{number of tubes} \times \text{perimeter of each tube}} \quad (11)$$

$K = 0.7$ has given quick convergence for most of the results and it is used throughout this work.

The quality at the exit is taken as 90% of the maximum expected value.

$$X_{e,ev} = 0.9 X_{\max} \quad (12)$$

When once quality is fixed the secondary flow rate is calculated using

$$W_{s,ev} = W_{make up} + W_{recirculation} = \frac{W_{vapour}}{X_{e,ev}} \quad (13)$$

The recirculation water and feedwater are assumed to mix at the entrance of the evaporator at the same pressure and temperature. Initial value of pressure drop is calculated by making the following assumptions.

1. Thermodynamic properties are calculated based on the exit pressure of the evaporator,

2. An average specific volume is taken as

$$v_{s, ev} = \left(\frac{v_e + v_i}{2} \right)_{s, ev} = \left(\frac{v_e + v_{l,e}}{2} \right)_{s, ev}. \quad (14)$$

3. The vapour quality is assumed to vary linearly along the generator as

$$X_{s, ev} = \left(\frac{X_e}{2} \right)_{s, ev}. \quad (15)$$

Pressure drop in the secondary flow is calculated by knowing the flow rates

$$P_{s, ev} = \frac{1}{144} \frac{G_{s, ev}^2}{g_c} \left(\bar{f} \frac{\bar{v}L}{2D_c} + v_e - v_i \right). \quad (16)$$

Initially an approximate value is used for $P_{s, ev}$ but subsequently it is corrected by using the \bar{f} value along with the corrected thermodynamic properties of water at the average pressure in the evaporator, viz.

$$\bar{P}_{s, ev} = (P_e + \frac{1}{2}\Delta p)_{s, ev}. \quad (17)$$

Assuming adiabatic compression, it is possible to calculate the enthalpies with which the recirculation flow and make up water are mixed at the entrance,

$$(h_{l,s})_{ev} = (h_{e,s})_{PA} = (h_{l,e} + v_{l,e}\Delta p)_{s, ev}. \quad (18)$$

The amount of heat transferred in the preheater and evaporator are calculated using energy conservation equations.

$$Q_{PA} = [W(h_e - h_l)]_{s, PA}, \quad (19)$$

$$Q_{ev} = \left[W(h_e - h_l) + \frac{W^3}{2A^2} (v_e^2 - v_i^2) \frac{1}{Jg_c} \right]_{s, ev} \quad (20)$$

and

$$Q_{total} = Q_{PA} + Q_{ev}. \quad (21)$$

If the total amount of heat transfer differs from the desired value, repeat the calculations by changing X_e , the quality of the vapour at the exit according to the equation

$$\begin{aligned} \frac{\Delta X_e}{X_e} \\ = - \left(\frac{X_e v_{l,e}^2 + (X_e - 2)v_{l,e}^2 - 2(X_e - 1)v_{l,e}v_{v,e}}{X_e v_{v,e}^2 + (X_e - 4)v_{v,e}^2 - 2(X_e - 2)v_{l,e}v_{v,e}} \right)_{s, ev} \\ \times \frac{\Delta Q_{total}}{Q_{total} - Q_{PA} - W_{vapour}(h_{l,e} - h_{l,s})_{s, ev}}. \end{aligned}$$

The process is repeated till either the desired accuracy is achieved or total number of iterations are exceeded.

READJUSTMENT OF THE CALCULATED VALUES (ITERATION)

After each step the total heat transferred in the evaporator is compared with the desired value. If difference exists beyond the desired accuracy then the following adjustments are made.

(a) Height of the evaporator

The amount of heat transferred is directly proportional to the heat transfer area and hence to the length of the tube of a fixed diameter. Hence the length is corrected as follows:

$$(L_{ev})_{corrected} = L_{ev} \frac{Q_{total} - Q_{PA}}{(Q_{total})_{calculated} - Q_{PA}}.$$

(b) Quality of the vapour at the exit of the evaporator

The total heat transferred is calculated using the expression

$$\begin{aligned} Q_{total} &= \left\{ W \left[h_e - h_l + \frac{W^2}{2A^2} (v_e^2 - v_i^2) \frac{1}{Jg_c'} \right] \right\}_{s, ev} \\ &+ W_{vapour}(h_e - h_l)_{s, PA}. \end{aligned} \quad (24)$$

To express Q as a function of quality X , use is made of the conservation equation of momentum:

$$\begin{aligned} \frac{W^2_{vapour}}{2A^2 X_e^2} \left[(v_e - v_i) \frac{1}{Jg_c'} \right]_{s, ev} \\ \simeq \frac{1}{2J} (\Delta p - \Delta p_{friction})_{s, ev}. \end{aligned} \quad (25)$$

It is also assumed that

$$\begin{aligned} (h_{l,s})_{s, preheater} &= (h_{l,e})_{s, evaporator}, \\ (v_{l,s})_{s, preheater} &= (v_{l,e})_{s, evaporator}. \end{aligned}$$

Then the change in total heat flux dQ is set equal to zero to obtain

$$\begin{aligned} \frac{\Delta X_{exit}}{X_{exit}} \\ = - \left\{ \frac{\frac{\Delta p_{friction}}{2} \left(v_{l,e} + \frac{2 - X_e}{X_e} v_{l,v} \right) \frac{\Delta L}{L}}{\frac{\Delta p}{X_e} v_{l,e} + \Delta p_{friction} \left(\frac{X_e - 3}{X_e} v_{l,e} - v_{l,v} \right)} \right\}_{s, ev} \end{aligned} \quad (26)$$

(c) Pressure, temperature and enthalpy of the liquid entering the evaporator

Pressure drop in the evaporator is the sum of the pressure drops in each control volume (calculated by

Table 2. Characteristics of the U-tube steam generator

Number of tubes	4674
External diameter of the tube	0.75 in. (1.905 cm)
Nominal thickness of the tube	0.043 in. (0.109 cm)
Total area of heat transfer	48,300 ft ² (4487 m ²)
Tube spacing	1.0675 in. (2.711 cm)
Pitch	Square
Heat transferred	$3.211 \times 10^9 \text{ Btu h}^{-1}$ ($0.941 \times 10^9 \text{ W}$)
PRIMARY	
Pressure at entrance	2250 psi (155.27 kgf cm ⁻²)
Inlet temperature	620°F (326.7°C)
Coolant flow rate	$3.55 \times 10^7 \text{ lbm h}^{-1}$ ($1.61 \times 10^7 \text{ kg h}^{-1}$)
SECONDARY	
Make up water pressure	1121 psi (77.36 kgf cm ⁻²)
Make up water temperature	430°F (221.1°C)
Vapour pressure	920 psi (63.49 kgf cm ⁻²)
Vapour flow rate	$4.08 \times 10^6 \text{ lbm h}^{-1}$ ($1.85 \times 10^6 \text{ kg h}^{-1}$)

the programme). Using this pressure drop the enthalpy of the liquid entering the evaporator can be calculated. Knowing the pressure and enthalpy the temperature is calculated.

(d) Heat transferred in the preheater

Knowing the new value of the enthalpy of the liquid at the entrance of the evaporator the amount of heat transferred in the preheater is recalculated using equation (19).

(e) Secondary flow in the evaporator

Knowing the corrected quality, the flow rate of the secondary steam in the evaporator can be calculated using equation (13).

The above corrections are repeated till the desired accuracy is achieved in the calculation of the total heat transferred.

RESULTS

The above programme is utilized for analysing the steam generator of a typical PWR plant whose data is given in Table 2.

Results of the computation are given in Table 3 and the resulting errors of the various parameters are listed in Table 4. From the table it is clear that the programme calculates most of the design parameters with less than 10% error. The error in the total heat flux is less than 1% and the length and hence the heat transfer area are reproduced within 6% error. Also it should be pointed out that in most of the cases convergence was achieved in less than eight iterations. A typical run took less than 1 min on an IBM 370/145

Table 3. Steam generator of ANGRA 1 nuclear reactor

Geometric data	No. of tubes 4674	d_{ex} 0.75	d_{in} 0.664	A_T 48,300	\bar{L}_{total} 52.629	Spacing d 1.0675	Pitch Square	
							P_i	H_i
Operational data	2250	620	640.46	3.555			1121	430
Initial value	x_c	L_{ev}	L_{P_A}	L_{tot}	$\Delta P_{s,w}$	$Q_{tot} \times 10^{-9}$	$Q_{vap} \times 10^{-9}$	A_T
1	0.20	52.629	16.174	34.149	50.323	3.87	0.49843	2.7308
2	0.25	52.629	16.216	35.711	51.927	3.90	0.49843	2.7392
3	0.30	52.629	16.189	37.009	53.198	3.87	0.49843	2.7337
4	0.20	44.735	16.186	33.777	49.963	17.7	0.49843	2.7332
5	0.25	44.736	16.241	34.949	51.190	18.3	0.49843	2.7445
6	0.30	44.735	16.211	36.005	52.217	18.7	0.49843	2.7384
7	0.20	36.841	16.194	33.709	49.903	17.7	0.49844	2.7348
8	0.25	36.841	16.186	33.890	50.076	17.8	0.49843	2.7332
9	0.30	36.841	16.224	34.866	51.090	18.3	0.49843	2.7411
10	0.35	36.841	16.175	35.537	51.712	18.4	0.49843	2.7310

Table 4. Comparison of the results of steam generator simulation

Parameter	Expected	Value			Maximum percentage deviation	Expected value	Average value
		Average	Minimum	Maximum			
L_{PA}	—	16.200	16.174	16.241	—	—	0.25
L_{ev}	—	34.960	33.709	37.009	—	—	5.86
Δp_p	—	18.25	17.70	19.10	—	—	4.66
$\Delta p_{S,ev}$	—	3.95	3.87	4.30	—	—	8.86
$Q_{PA} \times 10^{-9}$	—	0.49843	0.49843	0.49843	—	—	0.002
$Q_{ev} \times 10^{-9}$	—	2.7401	2.7308	2.7445	—	—	0.34
$Q_{tot} \times 10^{-9}$	3.2115	3.2318	3.2992	3.2429	0.98	0.34	0.34
A_T	48.300	46.951	45.798	48.821	5.18	3.98	3.98
$W_V \times 10^{-9}$	4.085	4.1141	4.1062	4.1268	1.02	0.31	0.31
x_e	—	0.2908	0.1979	0.3834	—	—	32.00

computer. Several test runs were made by varying the pitch and spacing and the above trend persisted in all the runs.

The interaction of the primary and secondary circuits will be crucial in transients when the steam generator will be operating outside the range of steady state design. This programme is being extended in order to study the transients in the primary circuit, such as reduced mass flow rates and temperature perturbations of a PWR type nuclear power plant.

Chen J. (1963) A correlation for boiling heat transfer to saturated fluids in convective flow. *ASME 63-HT-34*.

Dittus F. W. and Boelter L. M. K. (1930) *Heat Transfer in Automobile Radiators of Tubular Type*, p. 443. Publications in Engineering, University of California, Berkeley.

Höld A. (1978) A theoretical model for the calculation of large transients in nuclear natural-circulation U-tube steam generators (digital Code UTSG). *Nucl. Engng Design* 47, 1.

Moore K. V. and Rettig W. H. (1975) RELAP 4—A computer code for transient thermal hydraulic analysis. *USAEC Rep. ANCR-1127*.

Polomik E. E., Levy S. and Sawochka S. G. (1964) Film boiling of steam water mixtures in annular flow at 800, 1100 and 1400 psi. *J. Heat Transfer* 86C, 81.

Redfield J. A. and Murphy J. H. (1969) FLASH—A computer code for PWR thermal hydraulic analysis. *Nucl. appl. Technol.* 6, 129.

Thom J. R. S. (1964) Prediction of pressure drop during forced circulation boiling of water. *Int. J. Heat Mass Transfer* 7, 709.

Tong L. S. and Weisman J. (1970) Thermal analysis of pressurized water reactors. *ANS Monogr.*

REFERENCES

- Arwood D. C. and Kerlin T. W. (1977) A mathematical model for an integral economizer U-tube steam generator. *Nucl. Technol.* 35, 12.
 Baroczy C. J. (1966) A systematic correlation of two phase pressure drop. *Chem. Engng Prog. Ser.* 64, 62, 232.

APPENDIX II

This consists of description of some important subroutines used for transient simulation.

- (1) CPAGC : It calculates specific heat C_p of compressed water at constant pressure as a function of temperature ($^{\circ}\text{F}$) at various pressure ranges. The unit of specific heat is Btu/lb- $^{\circ}\text{F}$.

$$C_p = A \cdot T^2 + B \cdot T + C$$

Values of A,B,C for various pressure ranges are tabulated in Table 1.

- (2) CPAGS : It calculates specific heat C_p of saturated water as a function of temperature T ($^{\circ}\text{F}$)

$$C_p = A \cdot T^2 + B \cdot T + C$$

The values of constants A,B,C for various temperature ranges are tabulated in Table 2.

- (3) CTAGC : It calculates the conductivity (K) of compressed water in Btu/hr-ft- $^{\circ}\text{F}$ as a function of pressure (Psi) and temperature ($^{\circ}\text{F}$)

$$K = A \cdot T^2 + B \cdot T + C$$

The values of constants A,B,C for various pressure ranges are tabulated in Table 3.

- (4) CTAGS : It calculates the conductivity (K) of saturated water as a function of temperature T ($^{\circ}$ F)

$$K = A \cdot T^2 + B \cdot T + C$$

The values of constants A, B, C for various temperature ranges are tabulated in Table 4.

- (5) CTMTP : It calculates the conductivity of the material of the tube. The material chosen in this problem is Inconel-718.

$$K = 57.78 (-1.98 \times 10^{-6} T^2 + 8.91 \times 10^{-4} + 0.151)$$

where K is in Btu/hr-ft- $^{\circ}$ F and T in $^{\circ}$ C.

- (6) FTMDf : It calculates the multiplication factor needed to evaluate two-phase frictional pressure drop. For this Baroczy's plot [11] is used. The x axis of this log-log plot is divided into 6 regions and the segments in each region is assumed linear such that

$$\phi_{L0}^2 = \text{Exp}(A + B \ln I)$$

where A, B are constants

$$I = (\mu_1 / \mu_v)^{0.2} (\rho_1 / \rho_v)$$

Region I : 0.0001 I 0.001

Region II : 0.001 I 0.003

Region III	:	0.003	I	0.007
Region IV	:	0.007	I	0.03
Region V	:	0.03	I	0.1
Region VI	:	0.1	I	1.0

- (7) QFOCV : In calculates F, S, and σ to be used in Chen's correlation

$$F = \text{Exp} [a + b \cdot \ln (X_{tt}^{-1})]$$

Values of a, b for different ranges of X_{tt}^{-1} are tabulated in Table 5(a).

$$S = c \cdot B^2 + d \cdot B + e$$

$$\text{where, } B = Re_1 \cdot F^{1.25}$$

Values of c, d, e for different ranges of B are tabulated in Table 5(b).

$$\sigma = a \cdot P^2 + b \cdot P + c$$

Values of constants a, b, c are tabulated in Table 5(c).

- (8) TLSUB : It determines the temperature of compressed water for a given pressure (P, Psi) and specific enthalpy (H, Btu/lbm).

$$H = A \cdot P^2 + B \cdot P + C$$

Values of the constants A, B, C for different temperatures are tabulated in Table 6.

- (9) VIAGC : It determines the viscosity (μ) of compressed water in lbm/hr-ft as a function of pressure (P, psi) and temperature (T, $^{\circ}$ F)

$$\mu = A T^3 + B T^2 + C T + D$$

Values of constants A, B, C, and D for different pressure and temperature ranges are tabulated in Table 7.

- (10) VIAGS : It determines the viscosity of saturated wafer (μ) in lb/hr-ft as a function of temperature (T)

$$\mu = A T^3 + B T^2 + C T + D$$

Values of constants A, B, C and D for different temperature ranges are tabulated in Table 8.

- (11) VIVAS : It determines the viscosity of saturated vapour in lbm/hr-ft as a function of pressure (psi)

$$\mu = 1.15826(-0.24353 \cdot 10^{-8} P^2 + 0.13778 \cdot 10^{-4} P + 0.029109)$$

- (12) DERIV : This subroutine evaluates the various derivatives of pressure and temperature with respect to internal energy and density at constant density and internal energy respectively. These interpolated values are tabulated in two tables which are Table 8(a) and Table 8(b).

TABLE I

Specific heat of compressed water as a function of
pressure and temperature.

PRESSURE RANGE (PSI)	TEMPERATURE RANGE (°F)	A	B	C	D
0 - 1500	0 - 1493.15	-0.00000000	-0.149315	-1.0 - 0.00000000	-0.0241
1500 - 2500	0 - 1907.24916	-0.00000000	-0.190724916	-1.0 - 0.00000000	-0.00349
2500 - 3500	0 - 2455.93813	-0.00000000	-0.245593813	-1.0 - 0.00000000	-0.0028
3500 - PST	0 - 3194.4512	-0.00000000	-0.31944512	-1.0 - 0.00000000	-0.0051
PST - ABSV	0 - 4707.23613	-0.00000000	-0.470723613	-1.0 - 0.00000000	-0.0072
ABSV - 300	0 - 10377.813	-0.00000000	-0.10377813	-1.0 - 0.00000000	-0.01375
300 - 500	0 - 1320.716	-0.00000000	-0.1320716	-1.0 - 0.00000000	-0.0028
500 - 600	0 - 69.772	-0.00000000	-0.069772	-1.0 - 0.00000000	-0.0051
600 - 690	0 - 132.970	-0.00000000	-0.0132970	-1.0 - 0.00000000	-0.0072
690 - 700	0 - 0.00000000	-0.00000000	-0.00000000	-1.0 - 0.00000000	-0.0000

TABLE II

SPECIFIC HEAT OF SATURATED WATER AS A FUNCTION OF TEMPERATURE.

T	C = A + T ² + B ³ + T ⁴
0	1.00000000
10	0.99999999
20	0.99999998
30	0.99999997
40	0.99999996
50	0.99999995
60	0.99999994
70	0.99999993
80	0.99999992
90	0.99999991
100	0.99999990
110	0.99999989
120	0.99999988
130	0.99999987
140	0.99999986
150	0.99999985
160	0.99999984
170	0.99999983
180	0.99999982
190	0.99999981
200	0.99999980
210	0.99999979
220	0.99999978
230	0.99999977
240	0.99999976
250	0.99999975
260	0.99999974
270	0.99999973
280	0.99999972
290	0.99999971
300	0.99999970
310	0.99999969
320	0.99999968
330	0.99999967
340	0.99999966
350	0.99999965
360	0.99999964
370	0.99999963
380	0.99999962
390	0.99999961
400	0.99999960
410	0.99999959
420	0.99999958
430	0.99999957
440	0.99999956
450	0.99999955
460	0.99999954
470	0.99999953
480	0.99999952
490	0.99999951
500	0.99999950
510	0.99999949
520	0.99999948
530	0.99999947
540	0.99999946
550	0.99999945
560	0.99999944
570	0.99999943
580	0.99999942
590	0.99999941
600	0.99999940
610	0.99999939
620	0.99999938
630	0.99999937
640	0.99999936
650	0.99999935
660	0.99999934
670	0.99999933
680	0.99999932
690	0.99999931
700	0.99999930

TABLE 3

CONDUCTIVITY OF COMPRESSED WATER AS A FUNCTION OF
PRESSURE(PSI) AND TEMPERATURE(°C)

$$K = A \cdot T^2 + B \cdot T + C$$

PRESSURE RANGE	A	B	C
0 - 1500 PSI	-0.11315E+5	0.64326E-3	0.30963
1500 - 2500 PSI	-0.11259E+5	0.63854E-3	0.31182
2500 - 3500 PSI	-0.11495E+5	0.67117E-3	0.31050

TABLE 4

CONDUCTIVITY OF SATURATED WATER AS A FUNCTION OF
TEMPERATURE:

$$K = A \cdot T^2 + B \cdot T + C$$

TEMPERATURE RANGE	A	B	C
0 - 100	-0.24173E-5	0.99835E-3	0.28852
100 - 400	-0.10409E-5	0.56280E-3	0.32132
ABOVE 400	-0.20081E-5	0.15749E-2	0.66240

TABLE 5(a)

* E * OF CHEN'S CORRELATION

$$E = \text{EXPL} \cdot a + b \cdot \ln(x_{ff}^{\frac{1}{2}})$$

X	a	b
0.1 - 0.2	0.60358	0.01681
0.2 - 0.6	0.94034	0.42604
0.6 - 2.0	1.0359	0.61316
2.0 - 100	0.96332	0.71791

TABLE 5(b)

* S * OF CHEN'S CORRELATION

$$S = C \cdot B^2 + d \cdot B + e$$

B	C	d	e
14990-100000	0.43321E-10	-0.10254E-4	0.97877
100000-300000	0.54595E-11	-0.33653E-5	0.65916
300000-500000	0.10265E-11	-0.99733E-6	0.34334
500000-700000	0.11075E-12	-0.18338E-6	0.16405
ABOVE 700000	0.0000000E00	0.0000000E00	0.00000

TABLE 5(c)

OF CHEN'S CORRELATION

$$= A \cdot P^2 + B \cdot P + C$$

RANGE OF PRESSURE P(PSI)	A	B	C
0 - 1000	0.157E-8	0.36872E-5	0.0033944
1000 - 3000	0.2023E-9	0.14020E-5	0.0024308

TABLE 6

TEMPERATURE OF COMPRESSED WATER AS A FUNCTION
OF PRESSURE (P) AND ENTHALPY (H)

	H = A + P ² + B + P + C	A	B	C
*	*	*	*	*
*	TEMPERATURE	A	B	C
*	*	*	*	*
*	100	0.0000000	0.26127E-2	68.0349
*	200	0.0000000	0.22714E-2	157.946
*	300	0.0000000	0.188834E-2	259.445
*	400	0.49075E-7	0.105060E-2	374.708
*	500	0.10528E-6	-0.560720E-3	498.122
*	600	0.81068E-6	-0.845050E-2	628.158
*	620	0.43558E-5	-0.13685E-1	656.845
*	640	0.18528E-5	-0.20086E-1	711.776
*	660	0.63821E-5	-0.46992E-1	794.942
*	680	0.75397E-5	-0.72980E-1	896.170
*	690	0.19416E-4	-0.16793E+0	1104.600
*	700	0.24845E-4	-0.22748E+0	1274.500
*	*	*	*	*

TABLE 7(a)

VISCOSITY OF COMPRESSED WATER AS A FUNCTION
OF PRESSURE AND TEMPERATURE:

PRESSURE (PSI) (F)	TEMPERATURE (°F)	A	B	C	D
0 - 1500	0 - 110	* 0.00000	* .3705E-3	* -0.87235	* 6.5531
0 - 1500	110 - 400	* -0.56532E-7	* 0.66982E-4	* -0.2374E-1	* 3.3519
0 - 1500	ABOVE 400	* 0.00000	* 0.44575E-5	* -0.20341	* 0.90965
1500 - 2500	0 - 110	* 0.00000	* 0.36425E-1	* -0.89631E-1	* 5.55907
1500 - 2500	110 - 400	* -0.65878E-7	* 0.66302E-4	* -0.2354E-1	* 3.3435
1500 - 2500	ABOVE 400	* 0.00000	* 0.11304E-5	* -0.1735E-2	* 0.84579
2500 - 3500	0 - 110	* 0.00000	* 0.35894E-3	* -0.8472E-1	* 5.525
2500 - 3500	110 - 400	* -0.65076E-7	* -0.65502E-1	* -0.23315E-1	* 3.3325
2500 - 3500	ABOVE 400	* 0.00000	* 0.52496E-5	* -0.41356E-2	* 0.70403

TABLE 7(b)

VISCOSITY OF SATURATED WATER AS A FUNCTION OF TEMPERATURE

TEMPERATURE (°F)	A	B	C	D
0 - 110	* 0.00000	* 0.37564E-3	* -0.68541E-1	* 5.7181
110 - 400	* -0.57639E-7	* 0.68025E-4	* -0.24029E-1	* 3.8665
ABOVE 400	* 0.00000	* 0.29905	* -0.67608E-3	* 0.62286

CHECKING THE PROGRAM

INPUT SPECIFICATIONS OF THE STEAM GENERATOR

-NUMBER OF CONTROL VOLUMES 10

-PRECISION REQUIRED 0.10000E-06

-MAXIMUM NO. OF ITERATIONS 25

-ACCELERATION DUE TO GRAVITY 0.31174E+02

PRINT OPTION 0

CHARACTERISTICS OF THE STEAM GENERATOR

NUMBER OF TUBES 4674

EXT. DIAMETER 0.75000E+00

INT. DIAMETER 0.66400E+00

TOTAL HEAT TRANSFER AREA 0.48300E+05

FORM COEFF. 0.27144E+01

SPACING 0.10675E+01

RECTANGULAR TUBES

PRIMARY CIRCUIT

PRESSURE AT ENTRY 0.22500E+04

TEMP. AT ENTRY 0.61830E+03

ENTHALPY AT ENTRY 0.64040E+03

FLOW RATE 0.35550E+08

ESTIMATED STEAM PRESSURE 0.22300E+04
SECONDARY CIRCUIT

PRESSURE 0.11210E+04

TEMPERATURE 0.42895E+03

ENTHALPY 0.40780E+03

VAPOUR PRESSURE 0.92000E+03

QUALITY 0.31900E+00

VAPOUR FLOW RATE 0.40850E+07

RATE OF HEAT TRANSFER 0.32115E+10

TABLE 8(a)

SPECIFIC INTERNAL ENERGY (U)	DERIVATIVE OF PRESSURE (dP/dS)	DERIVATIVE OF PRESSURE (dT/dS)
68.04	5577.95	1.89075
168.04	5748.97	4.44731
269.52	5186.20	6.70073
347.27	4230.15	8.61391
428.60	3656.88	8.37016
485.10	2955.79	10.02420
508.50	2712.02	10.021480
532.60	2466.91	10.5520280
557.40	2178.00	10.56390
583.10	1949.84	10.81580
609.90	1667.01	10.71360
638.30	1428.93	10.88470
668.70	1201.41	11.02110
702.30	972.17	11.08470
741.70	999.50	13.66450

TABLE 8(b)

$$dp/d\mu = A + B \cdot U$$

$$dp/d\mu = C + D \cdot U$$

DENSITY (S)	A	B	C	D
61.9963	81.1512	0.125973	0.978586	7.998475
60.11178	175.7350	0.167236	0.941878	7.998475
57.3132	295.9620	0.460533	0.987133	6.670533
53.6538	517.0680	0.915354	0.271761	9.984417
51.4589	593.3869	0.993442	0.535391	4.440911
48.9476	549.54932	0.284503	0.286995	1.130133
47.8240	720.99120	0.1124449	0.148570	1.885714
46.6200	653.34110	0.352303	0.374650	4.400900
45.3104	152.7980	0.477300	0.572264	3.997333
42.3191	339.2240	0.710325	0.383808	1.519644
40.5681	70.2542	0.249500	0.223570	0.0294845
38.5654	767.6040	0.014860	0.878320	0.0000000
36.1402	74.7736	0.000000	0.221.677739	*
32.9815	79.1472	0.000000	*	*

NUMBER OF ITERATIONS 21

PRECISION OBTAINED 0.75287E-07

EQUIVALENT LENGTH OF PREHEATER 0.15984E+02

TOTAL EQUIVALENT LENGTH OF EVAPORATOR 0.34786E+02

TOTAL EQUIVALENT LENGTH 0.50770E+02

TOTAL HEAT TRANSFER AREA IN SQ.FT. 0.46593E+05

DISTRIBUTION OF PRESSURE AND TEMPERATURE IN THE PRIMARY CIRCUIT

	PRESSURE (PSI)	FLUID TEMP. (DEGREE F)	WALL TEMP. (DEGREE F)	ENTHALPY (BTU/LB)	FLUX (BTU/SQ.FT/HR)
VOLUME 1	0.22500E+04	0.61830E+03		0.64040E+03	
	0.22492E+04	0.61389E+03	0.58949E+03	0.63383E+03	0.14625E+06
VOLUME 2	0.22485E+04	0.60948E+03		0.62727E+03	
	0.22477E+04	0.60557E+03	0.58389E+03	0.62146E+03	0.12923E+06
VOLUME 3	0.22470E+04	0.60165E+03		0.61566E+03	
	0.22462E+04	0.59776E+03	0.57858E+03	0.61058E+03	0.11324E+06
VOLUME 4	0.22455E+04	0.59387E+03		0.60549E+03	
	0.22447E+04	0.59035E+03	0.57358E+03	0.60107E+03	0.98412E+05
VOLUME 5	0.22440E+04	0.58664E+03		0.59665E+03	
	0.22432E+04	0.58379E+03	0.56915E+03	0.59282E+03	0.85479E+05
VOLUME 6	0.22425E+04	0.58073E+03		0.58898E+03	
	0.22418E+04	0.57808E+03	0.56529E+03	0.58564E+03	0.74415E+05
VOLUME 7	0.22411E+04	0.57542E+03		0.58230E+03	
	0.22403E+04	0.57321E+03	0.56247E+03	0.57951E+03	0.61947E+05
VOLUME 8	0.22396E+04	0.57100E+03		0.57673E+03	
	0.22389E+04	0.56910E+03	0.55988E+03	0.57435E+03	0.53182E+05
VOLUME 9	0.22382E+04	0.56720E+03		0.57196E+03	
	0.22375E+04	0.56553E+03	0.55746E+03	0.56987E+03	0.46578E+05
VOLUME 10	0.22368E+04	0.56387E+03		0.56777E+03	
	0.22360E+04	0.56239E+03	0.55522E+03	0.56592E+03	0.41359E+05
PREHEATER	0.22353E+04	0.56092E+03		0.56406E+03	
	0.22337E+04	0.55535E+03	0.54952E+03	0.55706E+03	0.33924E+05
	0.22321E+04	0.54979E+03		0.55006E+03	

ME-1981-M-RAO-DIG